LASER HEATING OF A
STATIONARY PLASMA

L.C. Steinhauer, 1970

Published on demand by
UNIVERSITY MICROFILMS
University Microfilms Limited, High Wycomb, England
A Xerox Company, Ann Arbor, Michigan, U.S.A.

LASER HEATING OF A STATIONARY PLASMA

by

LOREN CLIFFORD STEINHAUER

A dissertation submitted in partial fulfillment

of the requirements for the degree of

DOCTOR OF PHILOSOPHY

UNIVERSITY OF WASHINGTON

1970

Approved by Hobart R. Clauser

Department Aeronautics and Astronautics

Date November 24, 1970

UNIVERSITY OF WASHINGTON

Date: October 26, 1970

We have carefully read the dissertation entitled
"Laser Heating of a Stationary Plasma"
submitted by
Loren C. Steinhauer in partial fulfillment of
the requirements of the degree of Doctor of Philosophy
and recommend its acceptance. In support of this recommendation we present the following joint statement of evaluation to be filed with the dissertation.

This is an outstanding thesis which makes a number of original contributions to the general theory of laser heating of plasmas. In addition there is an original contribution to the mathematics of diffusion waves in the coherent limit.

The first portion of the thesis is the treatment of the stationary heating of a one-dimensional plasma with a laser pulse. The general one fluid two temperature equations of a plasma are used. Through appropriate nondimensionalization and limit analysis the equations are reduced to a tractable form and the method of singular perturbations is used to obtain analytic solutions. Of particular interest was the fact that these solutions demonstrated the plasma laser heating wave.

The second portion of the thesis is a treatment of the refraction problem. Geometrical optics is used to find ray path solutions which show the seriousness of this effect in propagating and absorbing a laser beam in a long magnetically confined plasma. Solutions are also found where the refraction effects are favorable. These solutions resulted in infinite intensities. These regions were examined using wave mechanics and the infinities due to caustics were removed but the infinity due to focusing on the axis must be removed by a nonlinear effect in the equations which has not yet been identified.

Finally the laser plasma heating wave was recognized to be an example of a more general problem, the bleaching wave. The mathematics of the bleaching wave is discussed in general and two more physical examples are presented with their solutions. It is also shown that the bleaching wave and the thermal wave which has been studied previously are actually the same phenomena in different limits. This results in the unified treatment of bleaching and thermal waves as diffusion waves.

DISSERTATION READING COMMITTEE: Victor D. Adler

Abraham Hertzberg

J. Kevorkian

In presenting this thesis in partial fulfillment of the requirements for an advanced degree at the University of Washington I agree that the library shall make it freely available for inspection. I further agree that permission for extensive copying of this thesis for scholarly purposes may be granted by my major professor, or, in his absence, by the Director of Libraries. It is understood that any copying or publication of this thesis for financial gain shall not be allowed without my written permission.

Signature Joan C. Steinauer

Date November 24, 1970

CONTENTS

LIST OF FIGURES

ACKNOWLEDGEMENTS

The author wishes to gratefully acknowledge the valuable suggestions and critical evaluations of Professor H. G. Ahlstrom in the preparation of this entire work. Of special value was the manner in which he directed the author toward the really important problems and away from those that are tempting but irrelevant.

The comments of Professor J. Kevorkian on the mathematical developments, and Professors A. Hertzberg and G. C. Vlases on the physics were useful. In addition, Dr. J. D. Cole of the University of California at Los Angeles provided some important references and suggestions used in chapter IV.

The author also wishes to acknowledge the support of the National Aeronautics and Space Administration through the Space Sciences fellowship for three years. Additional support was received from the Department of Aeronautics and Astronautics, NASA Grant No. NGR 48-002-044, and NSF Grant No. GK 20708.

Chapter One

INTRODUCTION TO LASER PLASMA HEATING

In recent years the need has become apparent for a new source of power generation. The conventional sources of power are either being depleted (coal, petroleum) or else require careful disposal of dangerous waste products (nuclear). If controlled thermonuclear reactions can be generated and made economically competitive, then there should be no dangerous waste products. The fuel is deuterium (D) and tritium (T), isotopes of hydrogen. Deuterium is found in water in a concentration of one part in six thousand and thus is available in limitless quantity. Tritium is not actually found in nature but can be produced by using the neutrons generated in the D-T reaction to bombard Li^6.[1,2]

The products of D-T and D-D reactions are clean. Energetic neutrons are produced but these need not lead to radioactive wastes if the proper shielding substance is used. One of the products of the reaction is a large amount of energy, in the million electron volt range. Then even if only a few reactions are produced, a large amount of energy can be released.

The difficulty in producing a thermonuclear reaction is the coulomb force barrier that surrounds any charged particle. Coulomb forces are very strong so that the two reactants must hit each other at very high speed and pretty close to dead center to cause the fusion reaction. Thus very high atomic velocities--and hence temperatures--must be present

before a significant reaction takes place. For a D-T plasma, the temperature must be in the KeV range before significant thermonuclear energy is released. For a D-D plasma, the requirement is higher by a factor of three.

There are two examples of power producing thermonuclear reactions that have been observed. One is the hydrogen bomb, where the necessary temperatures are achieved by a triggering nuclear fission reaction. This is an uncontrolled thermonuclear reaction and is not likely as a good source of commercial power. The other example is the sun (or any star) which is an astronomical thermonuclear reaction. It is in a sense controlled since it persists continuously. The goal is to produce a small "sun" in a controlled manner so that the released thermonuclear energy can be harvested and used for other needs.

In conventional energy release, such as fire, it is a simple matter to maintain a continuous reaction. This is highly unlikely with a thermonuclear reactor. The containment of a continuous reaction at 10 KeV temperatures and huge pressures is a frightening thought. For this reason, most studies have been directed toward producing a pulsed type reactor where each pulse is short enough so that containment is possible. A very simple requirement has been calculated stating the conditions necessary to achieve gain in a pulsed thermonuclear reactor. This is called Lawson's criterion.[3] Its simplest expression is that the temperature of the reactants must exceed 10 KeV, and the product of the number

density and the confinement time must exceed 10^{14} sec/cm^3. This criterion is based upon the principle that more energy must be reaped from the reaction than is required to prepare the next reaction. Thus the problem at hand is to heat a D-T plasma to a very high temperature, and to maintain it for a certain length of time.

Significant efforts have been made in several countries for more than a decade to achieve a controlled thermonuclear reaction. This length of time spent proves the difficulty in achieving the very difficult conditions of Lawson's criterion. A number of devices using various principles and geometries have been suggested and tried in search of the goal. Most of these devices have two things in common; very strong electric currents and magnetic fields which are used to heat and contain the plasma. Significant progress has been made in this direction--especially in the Soviet Union with the Tokamak device.[4] Yet, even this, the most successful device to date falls one to two orders of magnitude short of both requirements of Lawson's criterion. The Tokamak has not been fully exploited yet, but it is still wise to find other approaches that may be better. One attractive approach that has come to the front in the last three or four years is the use of lasers to heat the reactants.[5,6,7]

Ten years ago, the thought of using a laser to heat anything would have seemed unrealistic since laser power outputs were typically very low, on the order of milliwatts. But since then, laser technology has advanced at an incredible

rate and powerful lasers have become available. Of most interest to fusion is the development of the so called giant pulse, and mode-locked lasers. Giant pulse lasers produce a burst of light of microsecond to nanosecond duration. As much as 500 to 1000 Joules have been produced in this kind of a pulse. Mode-locked lasers produce pulse lengths on the order of picoseconds. As much as 80 Joules have been released in this kind of a pulse. Thus, the laser is an excellent way to rapidly deliver energy. This is essential or else the heated plasma will expand and cool before all the energy is delivered.

Another advantage of the laser is its ability to get energy into a magnetic container. Magnetic pressures have long been suggested as a means of containing a thermonuclear plasma. Some approaches have used the MHD system (including both currents and magnetic fields) to both heat and contain the plasma. This requires a great deal of versatility of the magnetic field and the currents. However, now the heating may be left up to the laser so the magnetic field can concentrate on the containment.

A thermonuclear plasma may also be confined inertially, i.e., within a jacket of very heavy atoms. The large mass of the atoms would restrict the expansion of the plasma. This approach is essentially a small explosion and the products must be contained which may be difficult in that the size of the explosion may be significant for a positive yield.

Several difficulties have been previously found in the laser heating of a plasma. The first difficulty is due to

the limited confining ability of a magnetic field. This puts a limit on the density that can be contained. But lower densities lead to very long absorption lengths--some even as high as many miles. This difficulty has been reduced with the advent of powerful gas lasers which are characterized by long wave lengths. The long wave lengths lead to shorter absorption lengths.

Another difficulty is that typical estimates of energies required to satisfy the Lawson criterion are 10^5 to 10^9 Joules per pulse. This is two or more orders of magnitude greater than present lasers.

A third difficulty arises out of the nature of inverse bremsstrahlung absorption. Inverse bremsstrahlung is a three body collision between an ion, an electron and a photon whereby the electron gains the energy of the photon. Thus only the electrons are heated directly. The deuterium and tritium ions must be heated by collisions with the hot electrons. This equilibration process may well be painfully slow-especially for lower densities, and may not even occur before the dynamics dissipates the plasma.

The purpose of this work is to examine in detail some of the phenomena in laser heating to thermonuclear temperatures. Much of the work in this field has been confined to estimates. Most previous solutions have relied on complex numerical calculations which typically leave a dearth in understanding of the physical process that produced the results. This study seeks simple analytic solutions wherever possible and avoids the computer code approach.

Standard procedures of analysis begin with the simple and once the simple is understood, the more complex is attacked. Accordingly, the first study is of a strictly one-dimensional plasma heated by a laser. Only stationary heating is considered since maximum temperatures are produced if the plasma remains stationary throughout the laser pulse. Assuming the two temperature continuum equations, analytic solutions have been found for all stationary regimes for a plasma with arbitrary density profile.

One among several heating regimes may appear. One is the stationary-frozen-nonconducting regime (where conduction will always refer to thermal conduction unless otherwise noted). The heating is sufficiently rapid that the ions remain frozen at their initial temperature and little thermal conduction occurs. This regime is characterized by two parts. For optically thin plasmas, the entire irradiated part of the plasma is heated simultaneously, producing a highly nonuniform temperature distribution. An extreme hot spot appears at the point of farthest penetration of the radiation (the critical density point). For optically thick plasmas, the plasma is opaque so that the radiation bores its way into the plasma. This phenomena is called a bleaching wave since the plasma behind the wave is made transparent by the heating. Consequently, the temperature profiles present a wave like character, the heated region advancing deeper into the plasma with time.

The stationary-frozen-conducting regime arises for less thick plasmas. In this regime, thermal conduction is very strong so that the temperature is nearly uniform. Even the plasma

beyond the light reflection point (critical density) may be heated in this case--by thermal conduction.

The equilibrium counterparts of these two regimes will arise for the lower laser energy inputs and for the longer pulse lengths. In these regimes, the electrons and ions remain in equilibrium during the heating. The solutions in these regimes are essentially the same as those for their "frozen" counterparts.

Of critical importance is the dynamics that follow the stationary heating. This process appears primarily in two regimes. The frozen-conducting regime is characterized by cold ions and isothermal plasma motion. This regime is unacceptable in that the ions never are heated to thermonuclear temperatures before the motion dissipates the plasma. The equilibrium-nonconducting regime is characterized by electron-ion equilibrium and no thermal conduction. This is the desired regime for the achievement of a thermonuclear reaction.

The classical threshold for the achievement of gain in a thermonuclear reactor is the Lawson criterion. Lawson's criterion requires the containment of the plasma for a certain length of time at a temperature of 10 KeV. Attaining this requires fairly large energy depositions, more than is available today, but probably in reach of future lasers. Also required are fairly long plasma lengths unless some means of enhancement of the confinement time is found.

Following the initial step of understanding a simple geometry comes the analysis of a more complex one. A geometry

which seems appropriate for a magnetically confined, laser heated plasma is a long cylindrical shape, the laser being fired into the end of the column. The one dimensional results would apply to this shape if conditions across the column were uniform. This of course will never happen. In fact the density variation across the cylinder will cause gradients in the index of refraction, so that the beam will be refracted.

Refraction is a major problem as demonstrated by failures in attempts to propagate a laser beam down a plasma column.[8] The reason is that the usual density profile in a magnetically confined plasma (maximum density in the center) is unfavorable --the beam is refracted out of the plasma column. Calculations are made of the refraction of the beam in a plasma column with a typical density profile. It is found that the beam is essentially refracted out of the column after moving only a few column diameters. Appropriate focusing of the beam helps by roughly a factor of three.

However, if it is possible to generate a plasma column with a favorable density profile (a density minimum in the center), then the picture is the reverse: the beam is trapped perfectly. Not only that, but the effective absorption length is enhanced due to the peculiar refractive effects. Some unusual features arise in this case. The ray paths are sinusoidal functions, oscillating back and forth across the column. Caustics are formed from the locus of points where the rays "reflect" back toward the axis.

The theoretical results on refraction in a favorable density profile are useless if it is impossible to create the

favorable profile. This type of profile can be created--and in several different ways. One way is to catch the plasma in its formation stage. Characteristic of the formation of pinch devices are collapsing and reflecting shock waves. These shock waves generate--for very short times--density profiles that are favorable.

Another approach is to change an unfavorable density profile to a favorable one by selective heating. This technique is called "density tailoring". A laser (called the pre-laser) is used for the density tailoring. It is usually advantageous to have a shorter wave length for the pre-laser than for the main laser pulse. Analysis of the lateral dynamics of a plasma column reveals that the motion will fall into one of two regimes. There is the conducting regime which is dominated by thermal conduction and the nonconducting regime. Several density tailoring techniques are suggested and studied. Most of them can be used in either regime, but in the conducting regime the favorable profiles produced will disappear rapidly when the pre-laser pulse ends.

Oftentimes in the analysis of a particular physical problem, the solution is seen to resemble solutions to other physical problems. This is a clue to mathematical similarities in the governing equations. Occasionally however, the resemblance is not due simply to chance mathematical resemblance, but rather to a principle of physics in which both problems are rooted. An apparent chance resemblance is seen between the bleaching wave and nonlinear thermal conduction phenomena (thermal waves). Further examination reveals that these two

phenomena are actually the same but in opposite limits. Both belong to a large class of nonlinear diffusion phenomena that demonstrate wave like characteristics. The bleaching wave is diffusion in the "coherent" limit, and the thermal wave is diffusion in the "equilibrium" limit. Two other physical phenomena are identified as diffusion in the coherent limit: laser irradiation of a two level substance, and the laser induced breakdown wave. Numerous examples are presented of diffusion in both limits.

Understanding wave diffusion suggests the possibility of laser heating of a very dense plasma by thermal waves. A plasma at solid density may have laser energy added at its edge by anomalous absorption, and the overdense portion would be heated by a thermal wave. Such high densities would require inertial confinement, but the problems of electron-ion equilibration may be overcome by those high densities. Also, the high density may permit heating by absorption of α-particles from the thermonuclear reaction.

Chapter Two

LASER HEATING OF A ONE-DIMENSIONAL STATIONARY PLASMA

An important limitation on the maximum temperature that can be created in a laser heated plasma arises from the plasma motion. During the laser pulse the plasma may begin to expand and much of the thermal energy would be converted to directed kinetic energy of the plasma motion, as was first noted by Basov[5] and Dawson.[6] However, the recent development of powerful sub-nanosecond Q-switched lasers and mode-locked picosecond lasers makes it possible to overcome the problem of expansion during the heating process. For appropriately short laser pulses, the plasma can be heated to thermonuclear temperatures before significant macroscopic fluid motion begins. The irradiation of a plasma by these short laser pulses then becomes a stationary heating problem.

A study has been made of the stationary heating of a one-dimensional plasma with an arbitrary density profile. The purpose of the study was to determine the fine details of the heating process as well as the overall features. The spatial distribution of temperature is one detail of interest which will hold the key to the plasma motion that will follow the heating process. Another detail of interest is the fraction of laser energy that is lost by reflection from the nonuniform plasma.

Several theoretical investigations of laser plasma heating have been made; but most models have neglected the fine details and concentrated on over-all results, e.g., the tem-

perature achieved. Previous investigations have also used time scales in which plasma motion is significant.

A study by Fader[9] considered the expansion of a spherically symmetric plasma subject to Q-switched laser radiation. The expansion of the plasma was found to be a major limitation on the temperatures achieved according to both numerical and analytical calculation. This study assumed spatially uniform absorption throughout the plasma.

A study by Kidder[10] also considered the motion of a spherically symmetric plasma but with irradiation by a radially convergent light pulse. His numerical study also showed the limitation of expansion on the temperatures achieved.

Dawson, et.al.,[11] studied the over-all absorption characteristics of a one-dimensional nonuniform overdense plasma. Without studying the details of absorption, they found the length of plasma necessary to adequately absorb the radiation. The critical density is the plasma density at which electromagnetic waves cannot propagate, i.e., the plasma frequency. Underdense and overdense refer to densities less than and greater than the critical density.

This study also considers a one-dimensional nonuniform plasma and examines the heating process for time scales sufficiently short that plasma motion can be neglected. The results indicate that for a thick underdense region, a bleaching wave propagates into the plasma, heating it in the process. For a thin underdense region, the heating is simultaneous--with an extreme hot spot appearing at the critical

density. For a very thin underdense region, thermal conduction dominates the heating so that nearly uniform temperatures appear in the underdense region and thermal conduction carries energy to the overdense region of the plasma by means of a thermal wave. The thermal wave phenomena has been mentioned by several writers (see chapter IV). The bleaching wave was seen to appear in the numerical studies of Kidder,[10] and the analytical studies of Rehm.[12]

Another result is that maximum temperatures or other optimizing conditions can be achieved by proper tailoring of the initial density profile and plasma size. The idea of tailoring the plasma to optimize the results was first suggested by Daiber, et. al.,[7] and later in another scheme by Lubin.[13]

A. EQUATIONS AND PARAMETERS

1. Model

The plasma is taken to be a one-dimensional nonuniform fully ionized gas being irradiated by a laser of wave length λ_o at normal incidence. Figure 1 is a diagram of the configuration. The initial density and temperature profiles are arbitrary to the extent that a fully ionized gas is a valid assumption. The plasma is assumed to be a dense ideal gas mixture of electrons and ions such that there is charge neutrality at every point for all times.

The one-dimensional two-temperature continuum equations will be used with the addition of terms accounting for radiative energy addition. The electromagnetic force will be neglected since its effect is small compared with the effect of thermal forces for regimes of interest. The effect of electromagnetic forces is studied in the first appendix to this chapter. Also, a form of the radiative transfer equation is added which neglects line, free-bound, and bremsstrahlung radiation. The radiative transfer equation is simplified to account only for the laser radiation entering the plasma (+ x direction) and does not take into account the reflection of radiation that would occur if the plasma is overdense. If the laser radiation does penetrate to the critical density then appropriate calculations must be made to account for the reflected light. The absorption coefficient used is that of inverse bremsstrahlung.

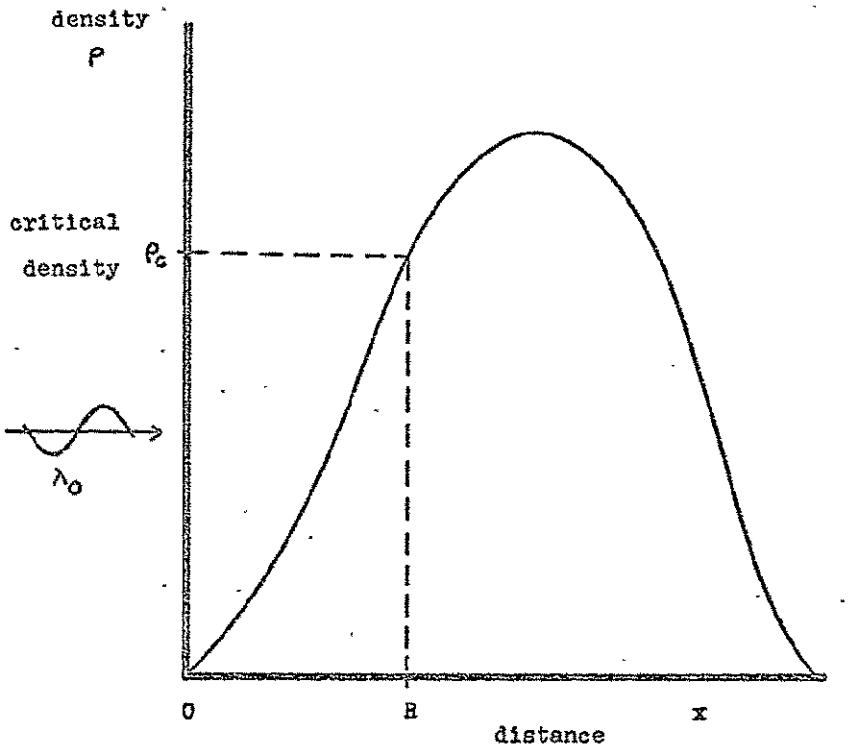

Figure 1. Plasma configuration

a. Nondimensionalization Scheme

The length scale used is R. If the plasma is overdense, then $x = R$ will define the point at which the critical density ρ_c occurs. If the plasma is not overdense at any point, then $x = R$ gives the rear edge of the plasma. The time scale is the laser pulse length t_p since only the heating process is considered in this study. Hence, the independent variables, dimensionless distance and time, will always be of order one or less. The temperature scale used for both electron and ion temperature is T_o and is defined as the temperature change that would arise if all the energy in the laser pulse were added uniformly to a critical density plasma of thickness R. Then,

$$T_o = \frac{J_o / A}{\frac{3}{2} k n_{ec} R} \tag{2-1}$$

where J_o/A is the energy contained in the laser pulse per unit area of plasma, k is the Boltzmann constant, and n_{ec} is the critical electron number density given by

$$n_{ec} = \frac{4\pi^2 \epsilon_o m_e c_o^2}{\lambda_o^2 e^2}$$

where ϵ_o is the permittivity in a vacuum, m_e is the mass of an electron, c_o is the speed of light in a vacuum, and e is the charge on an electron. The scaling factor for the density is the critical density which is related to the critical electron number density by $\rho_c = m_i n_{ec}/Z$. m_i is the

mass of the ion, and Z is the charge on the ion. The pressure scale p_o is the pressure that would arise in a perfect gas at temperature T_o and density ρ_c. The velocity scale is the acoustic speed for a perfect gas at p_o and ρ_c, i.e., $a_o^2 = 5p_o/3\rho_c$. The electron and ion entropies are scaled using the constant volume specific heat. The radiation intensity scale is the average laser intensity during the pulse, $I_o = J_o/At_p$. The absorption coefficient, electron-ion equilibration time, and the electron thermal conduction coefficient are taken from Spitzer.[14] These are based upon a scale using a density ρ_c and a temperature T_o

$$\kappa_o = 1.13 \times 10^{-19} n_{ec}/T_o^{3/2} = 6.81 \times 10^{13} Z\rho_c/WT_o^{3/2} \quad m^{-1},$$

$$t_{eq_o} = 3.17 \times 10^{7} T_o^{3/2} W/n_{ec} Z(1+Z) = 5.26 \times 10^{-26} T_o^{3/2} W^2/\rho_c Z^2 (1+Z) \quad \text{sec},$$

$$K_{e_o} = 7.40 \times 10^{3}\, T_o^{5/2}/Z \quad \text{Joule/sec-m-eV}.$$

for $n_{ec} \sim \text{cm}^{-3}$. Otherwise, MKS-eV units are used everywhere. The Columbic logarithm, $\ln\Lambda = 10$ everywhere. Henceforth, the ionic charge Z, and the atomic weight W are taken as one and two respectively as for deuterium. The radiation intensity scale is the average laser intensity during the pulse, $I_o = J_o/At_p$.

The dimensionless variables are: distance, $y = x/R$; time, $\tau = t/t_p$; density, $\zeta = \rho/\rho_c$; pressure, $\Pi = p/p_o$; electron temperature, $\theta_e = T_e/T_o$; ion temperature, $\theta_i = T_i/T_o$; absorption coefficient, $K = \kappa/\kappa_o$; fluid velocity, $U = u/a_o$; electron entropy, $\sigma_e = s_e/C_v$; ion Entropy, $\sigma_i = s_i/C_v$; and intensity, $i = I/I_o$.

b. Parameters

Using the nondimensionalization scheme described, five

parameters arise which control the plasma behavior. The first is

$$\epsilon = a_o t_p / R \qquad (2\text{-}2)$$

where ϵ is the ratio of the laser pulse time to the time for an electron acoustic wave to traverse the underdense region. It is called the dynamics paramter. If $\epsilon \ll 1$, then the pulse length is so short that essentially no plasma motion occurs. If $\epsilon \geq O(1)$, then significant motion occurs before the pulse ends.

$$\alpha = \kappa_o R . \qquad (2\text{-}3)$$

α is the ratio of the thickness of the underdense region to the absorption length scale. It is called the thickness parameter since it is a measure of the optical thickness of the irradiated plasma. The absorption length is the reciprocal of the absorption coefficient. If $\alpha \ll 1$, then the plasma is nearly transparent to the radiation. If the plasma is overdense, then the radiation will be reflected and the reflected beam will be negligibly reduce in intensity. The result will be to effectively double the absorption coefficient. If $\alpha \gg 1$, then the plasma is nearly opaque to the radiation.

$$\lambda = t_p / t_{eq_o} .$$

λ is the ratio of the pulse time to the electron-ion equilibration time and is called the equilibration parameter. If $\lambda \ll 1$, then the electrons will tend to be heated by inverse bremsstrahlung; but the ions will remain nearly frozen during

the laser pulse. If $\lambda \gg 1$, then the electron and ion temperatures will be the same.

$$\eta_{e,i} = K_{eo}/\rho_c C_v R^2 \tag{2-5}$$

where η_e is the time for significant thermal conduction to traverse the underdense region. It is called the thermal conduction parameter. Then, for example, if $\eta_e \ll 1$, there will be very little thermal conduction by the electrons during the laser pulse. If $\eta_e \gg 1$, the thermal conduction will be strong, tending to equalize the temperature of the plasma.

c. Equations

The governing equations in dimensionless form are:

$$\frac{\partial \zeta}{\partial \tau} + \epsilon \frac{\partial \zeta U}{\partial y} = 0 \tag{2-6}$$

$$\frac{\partial U}{\partial \tau} + \epsilon \left[U \frac{\partial U}{\partial y} + \frac{3}{5} \frac{1}{\zeta} \frac{\partial \Pi}{\partial y} \right] = 0 \tag{2-7}$$

$$\frac{\partial \sigma e}{\partial \tau} + \epsilon U \frac{\partial \sigma e}{\partial y} = \alpha K \frac{i}{\zeta \theta_e} - \lambda \frac{\zeta}{\theta_e^{3/2}} \frac{\theta_e - \theta_i}{\theta_e} + \eta_e \frac{2/7}{\zeta \theta_e} \frac{\partial^2 \theta_e^{7/2}}{\partial y^2}, \tag{2-8}$$

$$\frac{\partial \sigma i}{\partial \tau} + \epsilon U \frac{\partial \sigma i}{\partial y} = \lambda \frac{\zeta}{\theta_e^{3/2}} \frac{\theta_e - \theta_i}{\theta_i} + \eta_i \frac{2/7}{\zeta \theta_i} \frac{\partial^2 \theta_i^{7/2}}{\partial y^2} \tag{2-9}$$

$$\frac{\partial i}{\partial y} + \alpha K i = 0 \tag{2-10}$$

$$K = \frac{\zeta^2}{\theta_e^{3/2} (1-\zeta)^{1/2}} \tag{2-11}$$

$$\Pi = \zeta(\theta_e + \frac{1}{Z}\theta_i). \tag{2-12}$$

$$\theta_e = \zeta^{2/3}\exp(\sigma_e) \tag{2-13}$$

$$\theta_i = \zeta^{2/3}\exp(\sigma_i) \tag{2-14}$$

The equation for the absorption coefficient (2-11) breaks down for densities very near the critical density ($\zeta = 1$) . There is actually an extremely high value of the absorption coefficient at that point, but not an infinity. Hence, solutions that are found will probably have a singularity at that point and thus cannot be trusted for ζ very near one. This singularity will turn out to be integrable so that integrations with respect to y over the singularity will describe the actual case fairly accurately.

The initial conditions will be an initial temperature and an initial density profile. The boundary conditions will be on the intensity; the intensity entering the plasma will be $d\Phi/d\tau$ where Φ is the fraction of the laser energy delivered up to time τ ;

$$\Phi = \frac{1}{J_o/A}\int_0^t I(t)dt$$

so that $\Phi = 0$ at $\tau = 0$ and $\Phi = 1$ at $\tau = 1$ (the end of the pulse).

2. Preliminary Study of Parameters

The size of the parameters ϵ , λ , $\eta_{e,i}$ will determine the character of the plasma heating and the important parts of the governing equations. One of the factors determining these parameters is the size and density of the plasma. For this discussion, the plasma is assumed to be overdense (i.e, the plasma frequency at the point of highest density is greater than the laser frequency). Furthermore, to simulate a typical nonuniform plasma, the density is assumed to rise linearly from zero at the edge of the plasma and remain linear at least to the critical density point.

a. Dynamics Parameter

From (2-2), $\epsilon = a_o t_p/R$. R depends on both the electron density gradient and the critical density (which depends on the laser frequency).

$$R = \frac{n_{ec}}{\nabla n_e} = \left[\frac{4\pi^2 \epsilon_o m_e c_o^2}{e^2} \right] \frac{1}{\lambda_o^2 \nabla n_e} \qquad (2\text{-}15)$$

The acoustic speed scale a_o depends in the usual way on the temperature scale T_o . A deuterium plasma is assumed in calculating the acoustic speed. Applying (2-15) T_o becomes,

$$T_o = \frac{\lambda_o^4 \nabla n_e (J_o/A)}{\frac{3}{2} k \left[\frac{4\pi^2 \epsilon_o m_e c_o^2}{e^2} \right]^2}$$

Then, ϵ can be written,

$$\epsilon = 1.04 \times 10^{-4} \quad (J_o/A)^{1/2} \lambda_o^4 (\nabla n_e)^{3/2} t_p$$

with J_o/A in Joules per square meter, λ_o in microns, ∇n_e in electrons per meter to the fourth, and t_p in seconds.

b. Equilibration Parameter

Using Spitzer's electron-ion equilibration time,[14] with (2-4)

$$\lambda = 5.78 \times 10^{66} (J_o/A)^{3/2} (\nabla n_e)^{-3/2} \lambda_o^{-8} t_p .$$

c. Thermal Concuction Parameter

Using Spitzer's[14] electron thermal conduction coefficient, the conduction parameter (2-5) becomes

$$\eta_e = 4.55 \times 10^{-148} (J_o/A)^{5/2} (\nabla n_e)^{9/2} \lambda_o^{16} t_p .$$

Then, the pulse time t_p, laser energy per unit area J_o/A, laser wave length λ_o, and electron density gradient ∇n_e arise as the key parameters of the problem. With a particular laser pulse length t_p and wave length λ_o the various regimes can be shown graphically as a function of J_o/A and ∇n_e. Figures 2, 3, 4, and 5 show when ϵ, λ, and η_e are large or small for the cases $t_p = 10^{-9}$, 10^{-12} sec for $\lambda_o = 1.06\mu$ and $t_p = 10^{-6}$, 10^{-9} sec for $\lambda_o = 10.6\mu$.

The various lines in figures 2-5 separate the different regimes from each other. Each regime is characterized by a specific combination of large and/or small parameters. Where these regimes are distinct, they have been labeled with the

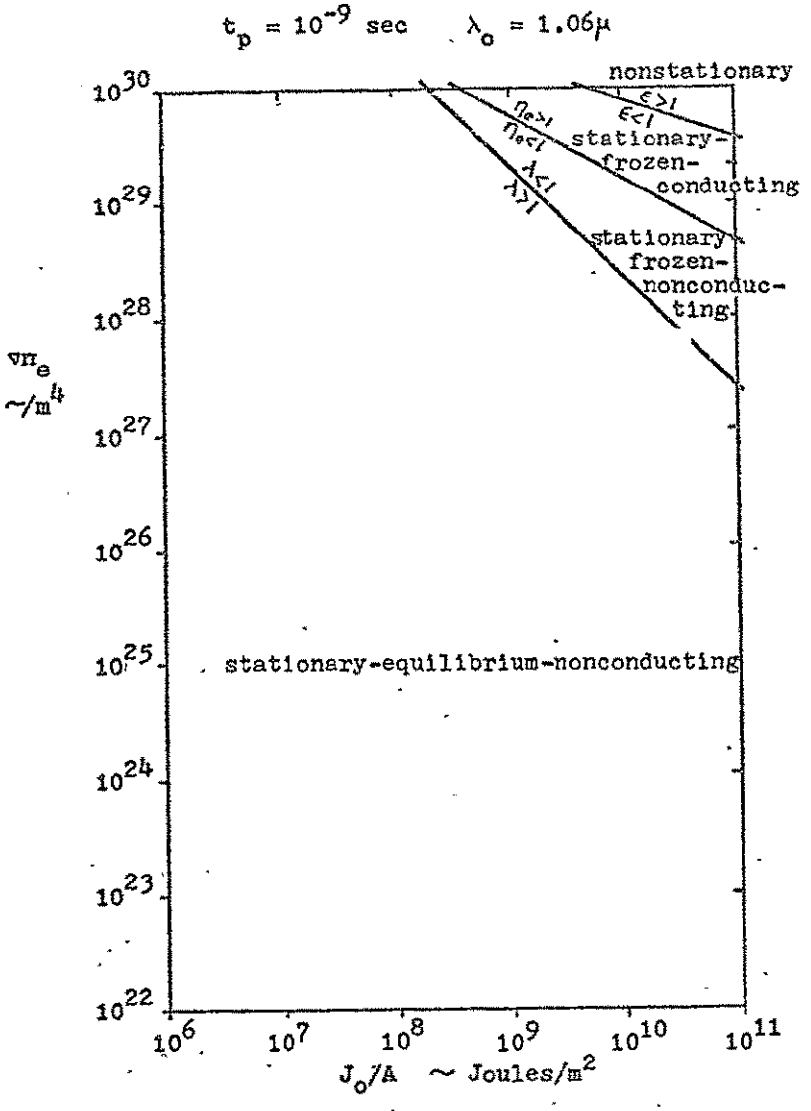

Figure 2. Heating regimes for a nanosecond pulse from a Nd$^+$ glass laser

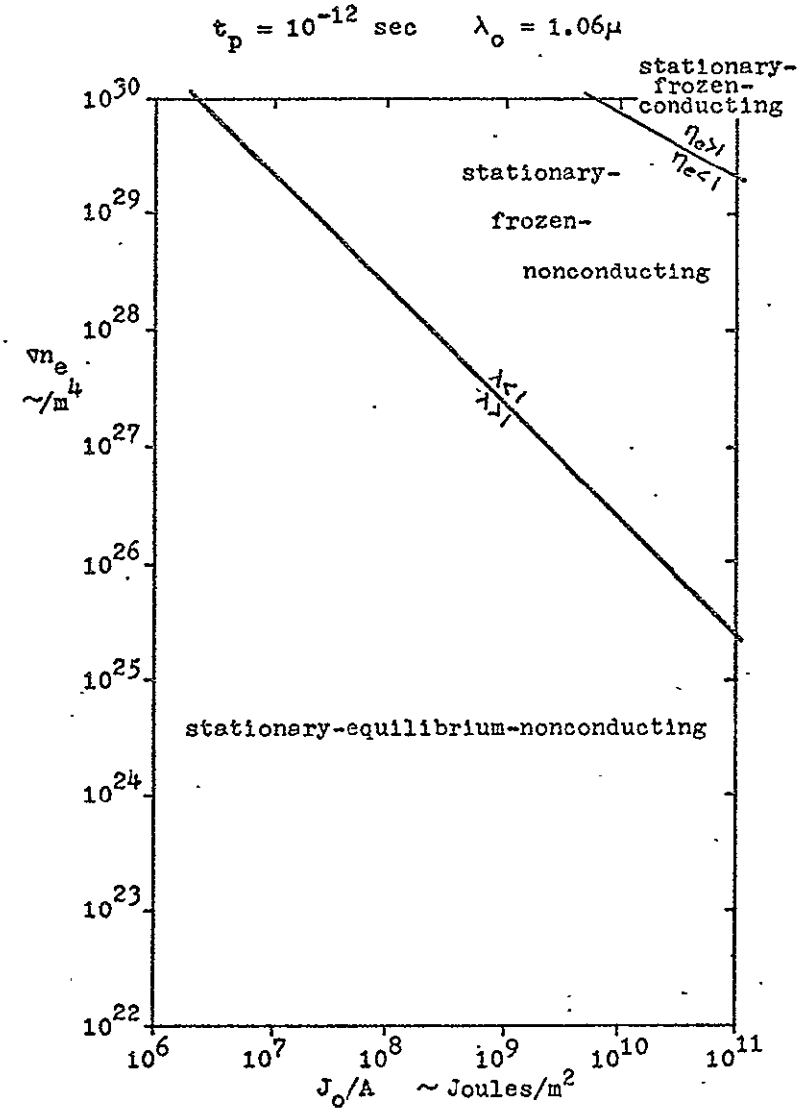

Figure 3. Heating regimes for a picosecond pulse from a Nd^+ glass laser

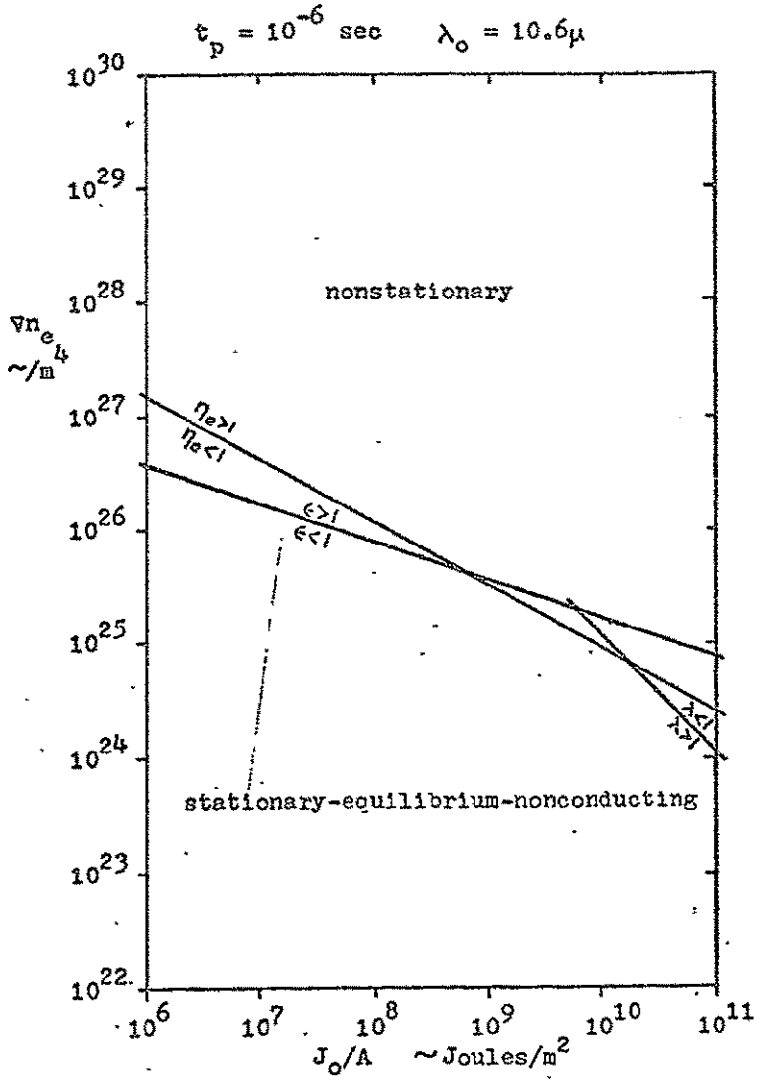

Figure 4. Heating regimes for a microsecond pulse from a CO_2 gas laser

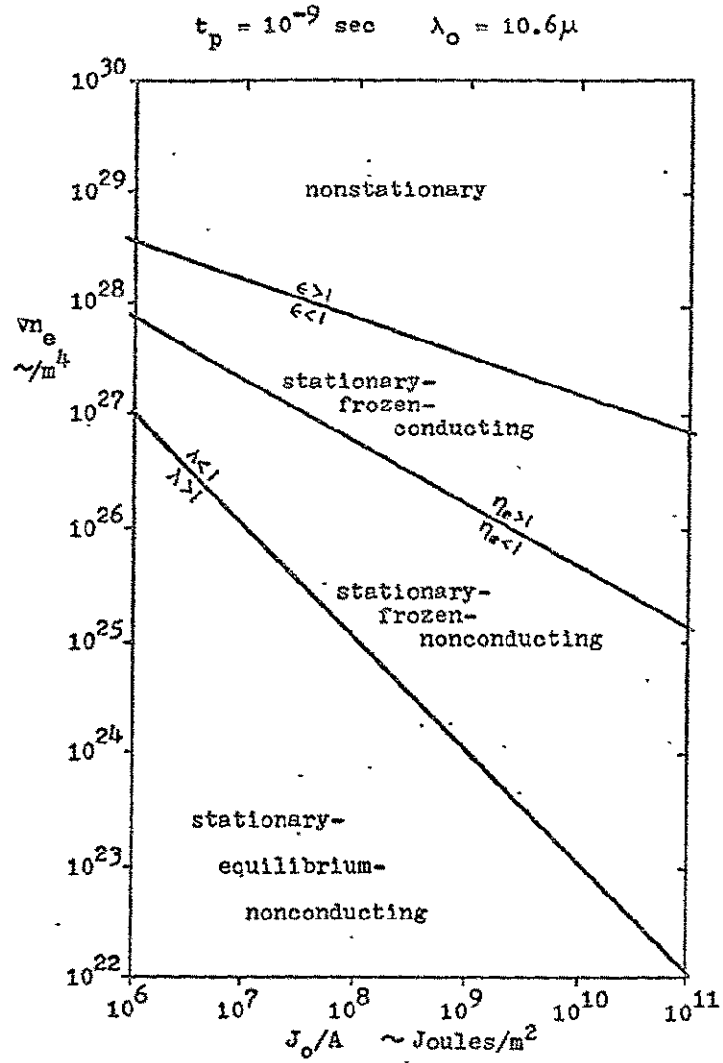

Figure 5. Heating regimes for a nanosecond pulse from a CO_2 gas laser

names, "stationary-equilibrium-nonconducting", "stationary-frozen-nonconducting", "stationary-frozen-conducting", and nonstationary. Conduction will always refer to thermal conduction unless otherwise noted. Since the purpose of this chapter is to study stationary heating, the nonstationary regime is not divided into specific regimes relating to conduction or equilibrium.

Supposedly in a particular regime, each effect is either present or not at all. For example in the stationary-frozen-nonconducting regime, one expects that there is no thermal conduction, no plasma motion, no ion heating, and only the electrons are heated by the laser. Thus in a particular regime, the neglect of certain effects requires that the appropriate parameters be much less than one (or much greater as the case may be) rather than just less than one (or greater than one). Hence the approximate solution found will probably fail near the lines bounding the various regions in figures 2-5.

It is not always enough for the parameters to be small. The frozen ion condition may break down while λ is small. If the electron temperature is much greater than the ion temperature, then $\lambda\theta_e/\theta_i$ (which appears in (2-9)) is not necessarily small even though λ may be small. Also, if the nondimensional temperature at some local point has a first or second derivative not of order one, then the solution may not be valid at that local point. For example, in the stationary-frozen nonconducting solution, there may be a large temperature gradient in some regions of the plasma. Significant thermal conduction may occur at those points even though

the remainder of the plasma is nonconducting.

d. Thickness Parameter

At this point it is of interest to calculate the thickness parameter α. The solution may take on a widely differing character for different values of α. From (2-3),

$$\alpha = 2.35 \times 10^{88} \left(J_o/A\right)^{3/2} \left(\nabla n_e\right)^{5/2} \lambda_o^{-10}$$

In considering the three stationary regimes, assumptions will be made--neglecting certain terms depending on the regime. However, terms in α will never be neglected so that α will appear in every stationary solution. Thus, in a sense α is a free parameter governing the solution, a parameter that may be large or small.

Once having solved for a particular regime, it will be necessary to re-examine the various regimes of validity. This is to be expected since the temperature depends on α, and thus its order of magnitude may be large or small compared to one.

B. STATIONARY-FROZEN-NONCONDUCTING PLASMAS

1. Equations

For very rapid energy addition, the plasma may absorb a large amount of energy before the random thermal energy begins to change to ordered fluid motion. The heating may be rapid enough so that the diffusing effect of thermal conductivity will be negligible. Also, with very rapid heating, the equilibration processes whereby the heated electrons transfer their energy to the ions will not have proceeded to any significant extent.

The problem studied here is the case where all of these conditions appear simultaneously. Then, the heating is essentially a stationary, nonconducting process whereby energy is transferred from a beam of light to the electrons in the plasma. No energy is transferred between electrons by thermal conduction, and no energy is transferred to the ions, either by electron-ion equilibration or by ordered plasma motion.

The requirement for a stationary plasma is that the dynamics parameter $\epsilon \ll 1$. For a nonconducting plasma the requirement is that the thermal conduction parameter $\eta_{e,i} \ll 1$. Also, for a plasma in which the electron and ion temperatures are uncoupled, the equilibration parameter $\lambda \ll 1$; and, if the electron temperature is large compared with the ion temperature, then $\lambda\theta_e/\theta_i \ll 1$ is required.

For the limit ϵ , λ , $\lambda\theta_e/\theta_i$, $\eta_{e,i} \to 0$, the governing equations simplify considerably. The continuity equation (2-6) becomes $\partial\zeta/\partial\tau = 0$ so that the density profile remains

stationary $\zeta = \zeta(y)$. The momentum equation (2-7) becomes $\partial U/\partial \tau = 0$ so that the velocity remains zero throughout the process. The electron entropy equation (2-8) becomes

$$\frac{\partial \sigma_e}{\partial \tau} = \frac{\alpha K}{\zeta} \frac{i}{\theta_e} \tag{2-16}$$

The radiative transfer equation (2-10) remains the same, as does the absorption coefficient (2-11) and all three equations of state (2-12, 13, 14). The electron entropy equation (2-16) plus the radiative transfer equation (2-10), the absorption coefficient (2-11), and one equation of state (2-13) form a complete set of four equations in four unknowns.

These can be reduced to a single equation for electron temperature. Solving (2-13) for σ_e , taking the time derivative and eliminating $\partial \sigma_e/\partial \tau$ using (2-16) yields

$$\frac{\partial \theta e}{\partial \tau} = \frac{\alpha K}{\zeta} i \tag{2-17}$$

Then solving for i and using (2-11),

$$i = \frac{2}{5} \frac{(1-\zeta)^{1/2}}{\alpha \zeta} \frac{\partial \theta_e^{5/2}}{\partial \tau} \tag{2-18}$$

Differentiating with respect to y ,

$$\frac{\partial i}{\partial y} = \frac{2}{5} \frac{(1-\zeta)^{1/2}}{\alpha \zeta} \frac{\partial^2 \theta_e^{5/2}}{\partial y \partial \tau} - \frac{2}{5} \frac{1 - \frac{1}{2}\zeta}{\alpha \zeta^2 (1-\zeta)^{1/2}} \frac{d\zeta}{dy} \frac{\partial \theta_e^{5/2}}{\partial \tau}$$

Combining this equation with (2-18) using (2-10) to eliminate i and (2-11) to eliminate K yields

$$0 = \frac{2}{5}\frac{\partial^2 \theta_e^{5/2}}{\partial y \partial \tau} - \frac{2}{5}\frac{1-\frac{1}{2}\zeta}{\zeta(1-\zeta)}\frac{d\zeta}{dy}\frac{\partial \theta_e^{5/2}}{\partial \tau} + \frac{\alpha\zeta^2}{(1-\zeta)^{1/2}}\frac{\partial \theta_e}{\partial \tau} \qquad (2\text{-}19)$$

which can immediately be integrated once on τ to give

$$\frac{2}{5}\frac{\partial \theta_e^{5/2}}{\partial y} - \frac{2}{5}\frac{1-\frac{1}{2}\zeta}{\zeta(1-\zeta)}\frac{d\zeta}{dy}\theta_e^{5/2} + \frac{\alpha\zeta^2}{(1-\zeta)^{1/2}}\theta_e = f(y) \quad . \qquad (2\text{-}20)$$

$f(y)$ arises out of integrating with respect to τ and is determined by the initial conditions. If the initial condition is $\theta_e(y,0) = \theta_e^\circ(y)$, then (2-20) becomes

$$0 = \frac{2}{5}\frac{\partial}{\partial y}\left[\theta_e^{5/2} - \theta_e^{\circ 5/2}\right] - \frac{2}{5}\frac{1-\frac{1}{2}\zeta}{\zeta(1-\zeta)}\frac{d\zeta}{dy}\left[\theta_e^{5/2} - \theta_e^{\circ 5/2}\right] + \frac{\alpha\zeta^2}{(1-\zeta)^{1/2}}\left[\theta_e - \theta_e^\circ\right] \qquad (2\text{-}21)$$

This is the equation governing electron temperature for a stationary-frozen-nonconducting plasma.

It is noteworthy that although the dependent variable θ_e is a function of both y , and τ , (2-21) is essentially an ordinary differential equation in θ_e in that only the partial derivative with respect to y appears. The only precaution in considering (2-21) as an ordinary differential equation is that in the solution, arbitrary functions of τ arise instead of constants (as in the case of a real ordinary differential equation).

In order to formulate a well posed problem, appropriate boundary and initial conditions must accompany the governing equation (2-21). The initial condition is

$$\theta_e(y,0) = \theta_e^o(y) \qquad (2\text{-}22)$$

The density profile $\zeta(y)$ remains the same throughout the stationary process, and hence is the same as the initial density profile.

The basic boundary condition is that the intensity at the outer edge of the plasma equals the intensity delivered by the laser,

$$i(0,\tau) = d\phi/d\tau$$

But a boundary condition on temperature θ_e must be developed. (2-18) is rewritten as

$$\frac{\partial \theta_e^{5/2}}{\partial \tau} = \frac{5}{2} \frac{\alpha \zeta}{\sqrt{1-\zeta}} i$$

and the boundary condition is

$$\left.\frac{\partial \theta_e^{5/2}}{\partial \tau}\right|_{y=0} = \frac{5}{2} \frac{\alpha \zeta(0)}{\sqrt{1-\zeta(0)}} \frac{d\phi}{d\tau} \qquad (2\text{-}23)$$

If $\zeta(y)$ is such that $\zeta(0) = 0$, then the appropriate boundary condition is on the first derivative with respect to y

$$\left.\frac{\partial^2 \theta_e^{5/2}}{\partial y \partial \tau}\right|_{y=0} = \frac{5}{2} \alpha \left.\frac{d\zeta}{dy}\right|_{y=0} \frac{d\phi}{d\tau} \qquad (2\text{-}24)$$

for $\zeta(0) = 0$, and $d\zeta/dy\big|_{y=0} \neq 0$. It is necessary to resort to the derivative in this case because (2-23) will turn out to be satisfied automatically when $\zeta(0) = 0$. The same basic

boundary condition on the intensity governs both cases. Equation (2-24) could also be found by combining (2-18) and (2-19) at the edge of the plasma. (2-22) and (2-23) or (2-24) together with the governing differential equation (2-21) form a well posed problem.

2. Analytic Solution

A study of the governing equations shows that the nature of the heating depends on the size of the thickness parameter α. α large corresponds to ∇n_e sufficiently small such that the underdense portion of the plasma is optically thick. The result is a "bleaching wave" process whereby successive layers are heated until they become nearly transparent, allowing the beam to penetrate to a deeper layer. α small corresponds to ∇n_e sufficiently large such that the underdense portion of the plasma is optically thin. Then, the whole underdense region is heated simultaneously. If α is sufficiently small, the laser will have only a very small heating effect on the plasma and would be ineffective in the production of a thermonuclear plasma.

If the initial temperature of the plasma is much less than T_o, then another small parameter can be defined,

$$\theta_e^o(y) = \mu g(y) \tag{2-25}$$

where the maximum value of $g(y)$ is chosen to be one and μ is the small parameter. μ is called the initial temperature parameter since it is a measure of the initial temperature.

The governing equation is now

$$0 = \frac{2}{5}\frac{\partial}{\partial y}\left(\theta_e^{5/2} - \mu^{5/2} g^{5/2}\right) - \frac{2}{5}\frac{1 - \frac{1}{2}\zeta}{\zeta(1-\zeta)}\frac{d\zeta}{dy}\left(\theta_e^{5/2} - \mu^{5/2} g^{5/2}\right)$$

$$+ \frac{\alpha\zeta^2}{\sqrt{1-\zeta}}\left(\theta_e - \mu g\right) \qquad (2\text{-}26)$$

If the final electron temperature is in the neighborhood of T_o, then θ_e will be of order one. Hence, during the hotter stages of heating, the terms in μ will be relatively small. If only terms of order one are considered, (2-26) becomes

$$0 = \theta_e^{3/2}\frac{\partial\theta_e}{\partial y} - \frac{2}{5}\frac{1 - \frac{1}{2}\zeta}{\zeta(1-\zeta)}\frac{d\zeta}{dy}\theta_e^{5/2} + \frac{\alpha\zeta^2}{\sqrt{1-\zeta}}\theta_e + O(\mu) \qquad (2\text{-}27)$$

This is designated the "hot equation" since it corresponds to the hotter stages of the heating.

In the initial stages of the heating, θ_e will be near θ_e^o which is of order μ. For this case θ_e must be rescaled; $\theta_e = \mu\theta_\mu$ where θ_μ is of order one. Then, (2-26) becomes

$$0 = \frac{2}{5}\frac{\partial}{\partial y}\left(\theta_\mu^{5/2} - g^{5/2}\right) - \frac{2}{5}\frac{1 - \frac{1}{2}\zeta}{\zeta(1-\zeta)}\frac{d\zeta}{dy}\left(\theta_\mu^{5/2} - g^{5/2}\right)$$

$$+ \frac{\alpha}{\mu^{3/2}}\frac{\zeta^2}{\sqrt{1-\zeta}}\left(\theta_\mu - g\right) \qquad (2\text{-}28)$$

This is designated the "cold equation" since it corresponds to the colder stages of the heating.

Solving the problem for $\theta_e^{\circ} \ll 1$ involves solving (2-27) and (2-28) separately and then appropriately matching the two solutions to the boundary conditions, initial conditions, and to each other. Solving such a problem where different parts of the solution must be matched with each other requires the method of matched asymptotic expansions such as described in detail by Cole.[15]

a. Solution to the Cold Equation

A significant parameter $\alpha/\mu^{3/2}$ appears in the cold equation (2-28) which may be large or small. There are two important cases, $\alpha \gg \mu^{3/2}$ or $\alpha \ll \mu^{3/2}$, a thicker, or a thinner plasma, respectively.

For a thinner plasma $\alpha \ll \mu^{3/2}$, (2-28) becomes

$$0 = \frac{2}{5}\frac{\partial}{\partial y}\left(\theta_\mu^{5/2} - g^{5/2}\right) - \frac{2}{5}\frac{1 - \frac{1}{2}\zeta}{\zeta(1-\zeta)}\frac{d\zeta}{dy}\left(\theta_\mu^{5/2} - g^{5/2}\right) + O(\alpha/\mu^{3/2})$$

Rearranging this equation gives

$$\frac{\partial}{\partial y}\log\left(\theta_\mu^{5/2} - g^{5/2}\right) = \frac{\partial}{\partial y}\log\frac{\zeta}{\sqrt{1-\zeta}} + O(\alpha/\mu^{3/2})$$

which is integrated

$$\theta_\mu = \left[g^{5/2} + \frac{\ell(\tau)\,\zeta}{\sqrt{1-\zeta}} \right]^{2/5} + O(\alpha/\mu^{3/2}) \qquad (2\text{-}29)$$

$\ell(\tau)$ is an arbitrary function of τ that arises in the integration with respect to y. $\ell(\tau)$ is found by applying the boundary condition, which is (2-23) or (2-24). The result is

$$\frac{d\ell}{d\tau} = \frac{5}{2} \frac{\alpha}{\mu^{5/2}} \frac{d\phi}{d\tau}$$

which is integrable

$$\ell = \frac{\alpha}{\mu^{5/2}} \left(\frac{5}{2} \phi + a\right)$$

where a is the constant of integration. a can be evaluated by applying the initial condition (2-22). Since $\phi(0) = 0$, $a = 0$ also, and with (2-25), (2-29) becomes

$$\theta_\mu = \left(g^{5/2} + \frac{5}{2} \frac{\alpha}{\mu^{5/2}} \frac{\zeta\phi}{\sqrt{1 - \zeta}} \right)^{5/2} + O(\alpha/\mu^{3/2}) \quad , \qquad (2\text{-}30)$$

the solution to the cold equation when $\alpha \ll \mu^{3/2}$. Physically, this corresponds to the case where the entire underdense region of the plasma is simultaneously heated from the very beginning of the laser pulse.

For a thicker plasma $\alpha \gg \mu^{3/2}$, (2-28) becomes

$$0 = \frac{2}{5} \frac{\mu^{3/2}}{\alpha} \frac{\partial}{\partial y} \left(\theta_\mu^{5/2} - g^{5/2}\right) + \frac{\zeta^2}{\sqrt{1 - \zeta}} \left(\theta_\mu - g\right)$$

$$- \frac{2}{5} \frac{\mu^{3/2}}{\alpha} \frac{1 - \frac{1}{2}\zeta}{\zeta(1 - \zeta)} \frac{d\zeta}{dy} \left(\theta_\mu^{5/2} - g^{5/2}\right) \quad . \qquad (2\text{-}31)$$

Since the derivative term is multiplied by the small parameter $\mu^{3/2}/\alpha$, the method of singular perturbations must be used for the solution. Thus, the solution to (2-31) is composed of an outer solution, Θ_o, where terms of order $\mu^{3/2}/\alpha$ can be neglected, and an inner solution, Θ_i, where the temperature changes rapidly in a very short distance.

The outer solution is to order one,

$$\Theta_o = g + O(\mu^{3/2}/\alpha) \quad . \tag{2-32}$$

Physically this represents the unheated parts of the thick plasma.

Finding the inner solution requires expanding the scale of y ,

$$\bar{y} = \frac{y - y_o}{\mu^{3/2}/\alpha} \quad ,$$

where $y_o = y_o(\tau)$ gives the location of the "transition layer". The other functions in (2-31), $g(y)$ and $\zeta(y)$, will be constant to order one in the scale of $\bar{y}$. For example,

$$\zeta(y) = \zeta(y_o + \frac{\mu^{3/2}}{\alpha}\bar{y}) = \zeta(y_o) + \frac{\mu^{3/2}}{\alpha}\bar{y}\left.\frac{d\zeta}{dy}\right|_{y=y_o} + O(\mu^3/\alpha^2)$$

Then to order one, the inner equation is

$$0 = \Theta_i^{3/2}\frac{\partial\Theta_i}{\partial\bar{y}} + \frac{\zeta^2(y_o)}{\sqrt{1-\zeta(y_o)}}\left(\Theta_i - g(y_o)\right) + O(\mu^{3/2}/\alpha)$$

which can be integrated

$$\int^{\Theta_i} \frac{\Theta_i^{3/2}\, d\Theta_i}{\Theta_i - g(y_o)} = m(\tau) - \frac{\zeta^2(y_o)}{\sqrt{1-\zeta(y_o)}}\,\bar{y} + O(\mu^{3/2}/\alpha) \,. \tag{2-33}$$

$m(\tau)$ is the function of time that arises in the integration with respect to $\bar{y}$

The integral on the left side of (2-33) can be evaluated using ordinary methods of integration. Conducting the integration, (2-33) becomes

$$\frac{2}{3}\left(\frac{\Theta_i}{g}\right)^{3/2} + 2\left(\frac{\Theta_i}{g}\right)^{1/2} + \log \frac{\left(\frac{\Theta_i}{g}\right)^{1/2} - 1}{\left(\frac{\Theta_i}{g}\right)^{1/2} + 1}$$

$$= \frac{1}{[g(y_o)]^{3/2}}\left[m(\tau) - \frac{\zeta^2(y_o)}{\sqrt{1-\zeta(y_o)}}\,\bar{y}\right] + (\mu^{3/2}/\alpha). \quad (2\text{-}34)$$

The complicated expression on the left side (2-34) can be expanded for limiting values of Θ_i/g .

For Θ_i/g near one, (2-34) can be solved as an expansion for Θ_i/g ,

$$\Theta_i = g\{1 + 4\exp\frac{1}{[g(y_o)]^{3/2}}\left[-\frac{8}{3} + m(\tau) - \frac{\zeta^2(y_o)}{\sqrt{1-\zeta(y_o)}}\,\bar{y}\right] + \ldots]$$

$$+ O(\mu^{3/2}/\alpha)$$

which is valid for $\Theta_i/g - 1 \ll 1$.

As $\bar{y}$ goes to positive infinity, Θ_i is seen to reduce exponentially fast to g which is just the outer solution (2-32). Thus, the inner solution (2-34) correctly matches the outer solution on the positive $\bar{y}$ side of the transition layer.

For Θ_i/g much larger than one, (2-34) can again be solved as an expansion,

$$\Theta_i = \left[\frac{3}{2}\,m(\tau) - \frac{3}{2}\,\frac{\zeta^2(y_o)}{\sqrt{1-\zeta(y_o)}}\,\bar{y}\right]^{2/3} + O(\mu^{3/2}/\alpha) \quad , \quad (2\text{-}35)$$

which is valid for $\Theta_i/g \gg 1$. Θ_i is seen to grow very large if $\bar{y}$ becomes large negative. Hence, for large negative $\bar{y}$, (2-35) must be made to match the solution to the hot equation. This inner solution corresponds physically to the front of a bleaching wave where the temperature begins to rise significantly above its initial value.

b. Solution to the Hot Equation

When the energy in the laser pulse is large compared with the initial internal energy of the plasma, then generally $(\theta_e)_{final}/\theta_e^\circ \gg 1$. In this case $(\theta_e)_{final}$ is essentially independent of $\theta_e^\circ(y)$. The "hot equation" (2-27) governs this case. Dividing (2-27) by θ_e gives a linear first order equation in $\theta_e^{3/2}$,

$$\frac{\partial \theta_e^{3/2}}{\partial y} - \frac{3}{5}\frac{1-\frac{1}{2}\zeta}{\zeta(1-\zeta)}\frac{d\zeta}{dy}\theta_e^{3/2} = -\frac{3}{2}\frac{\alpha\zeta^2}{\sqrt{1-\zeta}} + O(\mu) \quad ,$$

which can easily be solved to give

$$\theta_e = \frac{\zeta^{2/5}}{(1-\zeta)^{1/5}}\left[c(\tau) - \frac{3}{2}\alpha\int_0^y \frac{\zeta^{7/5}\,dy}{(1-\zeta)^{1/5}}\right]^{2/3} + O(\mu)$$

The function $c(\tau)$ that arises in the integration with respect to y is determined by applying the boundary condition (2-23) or (2-24)

$$\frac{d}{d\tau}[c(\tau)]^{5/3} = \frac{5}{2}\alpha\frac{d\phi}{d\tau}$$

or

$$c(\tau) = \alpha^{3/5}\left(\frac{5}{2}\phi + b\right)^{3/5}$$

b is the constant of integration and will be determined by the matching with the cold solution. Hence,

$$\theta_e = \frac{\alpha^{2/5}\zeta^{2/5}}{(1-\zeta)^{1/5}}\left[\left(\frac{5}{2}\,\phi + b\right)^{3/5} - \frac{3}{2}\,\alpha^{2/5}\int_0^y \frac{\zeta^{7/5}dy}{(1-\zeta)^{1/5}}\right]^{2/3} + O(\mu) \tag{2-36}$$

The expression (2-36) is only physically realistic when the term in brackets is greater than or equal to zero. It is seen that given a τ, this term is positive for y less than a certain value.

The physical impossibility of its being negative is seen if the resulting expression for $i(y,\tau)$ is written using (2-18),

$$i = \left[\left(\frac{5}{2}\,\phi + b\right)^{3/5} - \frac{3}{2}\,\alpha^{2/5}\int_0^y \frac{\zeta^{7/5}dy}{(1-\zeta)^{1/5}}\right]^{5/3} \frac{\frac{d\phi}{d\tau}}{\left(\frac{5}{2}\,\phi\right)^{2/5}}$$

The term in brackets becoming negative corresponds to the intensity becoming negative which is impossible. The hot solution is only valid for positive values of the term in brackets. The cold solution must be used elsewhere. Physically, (2-36) describes the temperatures behind the bleaching wave.

If $\alpha^{2/5} \ll 1$, (36) can be expanded with $\alpha^{2/5}$ as the small parameter,

$$\theta_e = \frac{\alpha^{2/5}\zeta^{2/5}}{(1-\zeta)^{1/5}}\left(\frac{5}{2}\,\phi + b\right)^{2/5} + O(\alpha^{4/5}, \mu) \tag{2-37}$$

This limit corresponds to the physical case of thin plasmas when the entire underdense region is heated simultaneously.

c. Matching Hot and Cold Solutions

In the various expressions that compose the solution (2-30), (2-32), (2-34), and (2-36), various unknowns arose: b, $m(\tau)$, and $y_o(\tau)$. These unknowns will be determined by matching the different components with each other for the possible ranges of the parameter α.

$$\alpha \ll \mu^{5/2}$$

This limit corresponds to a very thin plasma. The cold solution is given by (2-30). The first term in the parentheses is of order one and the second term is of order $\alpha/\mu^{5/2}$ and is relatively small. Then, (2-30) can be expanded about $g(y)$ (where g is non-vanishing) giving

$$\theta_\mu = g + \frac{\alpha}{\mu^{5/2}} \frac{\zeta_\xi}{g^{3/2}\sqrt{1-\zeta}} + O(\alpha/\mu^{3/2}) \quad . \qquad (2\text{-}38)$$

It is immediately seen that at the end of the heating ($\xi=1$), the term in $\alpha/\mu^{5/2}$ is still small compared with g and thus there is no need to seek a hot regime. The temperature θ_e remains in the cold regime throughout the laser pulse and is governed by (2-38)

Physically, this means that very little of the laser energy is actually absorbed by the plasma. The whole underdense region is penetrated by the beam so that a reflected light wave will arise. Since the intensity of the reflected light will be imperceptibly diminished due to weak absorption, its effect will be to roughly double the heating due to the incident light, i.e., the term in $\alpha/\mu^{5/2}$ is doubled.

Neglecting the effect of the reflected wave, the temperature produced is

$$\theta_e = \theta_e^{\circ}(y) + \frac{\alpha}{[\theta_e^{\circ}(y)]^{3/2}} \frac{\zeta\Phi}{\sqrt{1-\zeta}} + O(\alpha/\mu^{1/2})$$

This is shown schematically in Figure 6 for a linear density gradient, a constant initial temperature, and for $\alpha/\mu^{5/2} = 1/10$.

$$\mu^{5/2} \ll \alpha \ll \mu^{3/2}$$

This limit corresponds to a plasma sufficiently thick that significant heating occurs, but thin enough that the heating is done simultaneously even at the beginning.

The cold solution is again given by (2-30), but now the term in $\alpha/\mu^{5/2}$ dominates the term of order one. Expanding about the term in α (where Φ, ζ are non-vanishing) gives

$$\theta_\mu = \frac{\alpha^{2/5}}{\mu} \frac{\zeta^{2/5}(\frac{5}{2}\Phi)^{2/5}}{(1-\zeta)^{1/5}} + O(1) \quad . \qquad (2\text{-}39)$$

This must match with the small α limit of the hot solution (2-37). The matching requires that the constant b in (2-37) be zero. Once again the entire underdense region is heated and a reflected light wave will arise whose intensity has very little attenuation since α is small. The effect of the reflected wave then is to double the temperature in (2-39).

Neglecting the effect of the reflected wave, a composite solution can be constructed which possesses the features of the hot solution (2-37) and cold solution (2-30),

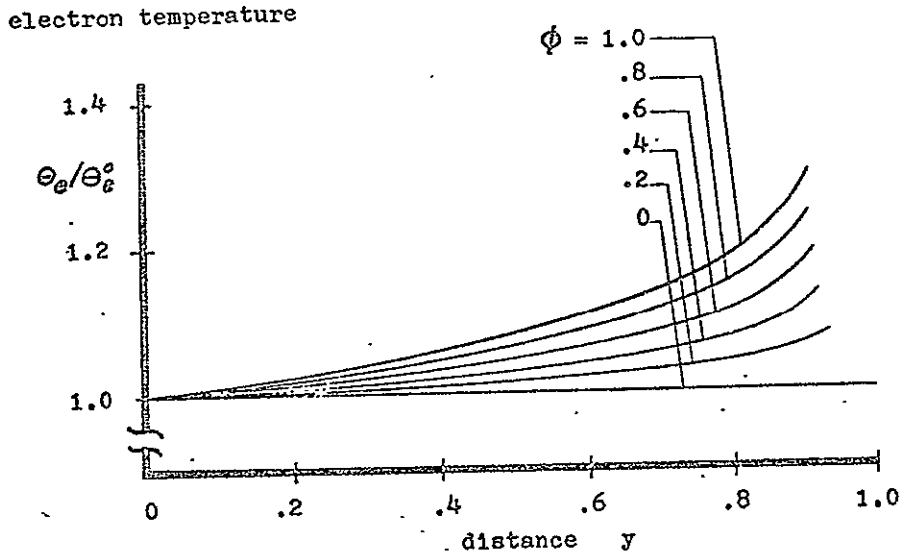

Figure 6. Temperature distribution for a very thin plasma: $\alpha/\mu^{5/2} = 0.10$

$$\theta_e = \left(\theta_e^{\circ 5/2} + \frac{5}{2}\frac{\alpha\zeta^{\circ}}{\sqrt{1-\zeta}}\right)^{2/5} + O(\alpha/\mu^{1/2})$$

$$\mu^{3/2} \ll \alpha$$

This limit corresponds to a plasma that is heated at the beginning by a bleaching wave. The cold solution is given by an outer solution (2-32) and a transition layer solution (2-34). As was seen before, the transition layer (located at $y_o(\tau)$) was matched with the outer solution for $y > y_o(\tau)$. Now (2-34) must be matched with the hot solution (2-36). The asymptotic limit for Θ_i large is given by (2-35). The limit of θ_e small in the hot solution must be calculated. This matching problem is demonstrated schematically in Figure 7. θ_e in (2-36) achieves small values near the point where the term in brackets vanishes. Given τ , the term in brackets vanishes at some $y_w = y_w(\tau)$. Expand the scale of y in the neighborhood of y_w ,

$$y_\nu = \frac{y-y_w}{\nu}$$

where ν is a small parameter to be determined in the matching. Then (2-36) becomes

$$\theta_e = \left[\frac{3}{2}\,\alpha\nu\,\frac{\zeta^2(y_w)}{\sqrt{1-\zeta(y_w)}}\,(-y_\nu)\right]^{2/3} + O(\mu)$$

This can be matched to (2-35) if $\nu = \mu^{3/2}/\alpha$, $m(\tau) = 0$, and $y_o(\tau) = y_w(\tau)$, in which case $y_\nu = \bar{y}$.

A composite solution valid over all y cannot be written in this case but the components can be summarized,

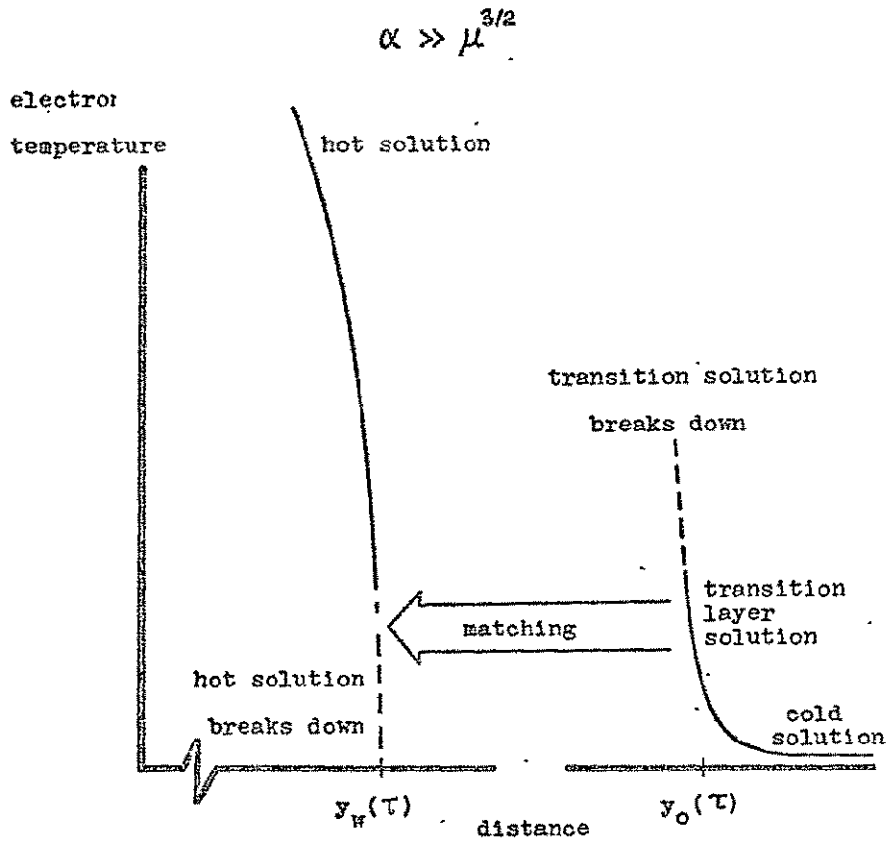

Figure 7. Matching of the hot solution, transition layer and the cold solution

$$\theta_e = \frac{\alpha^{2/5}\zeta^{2/5}}{(1-\zeta)^{1/5}}\left[\left(\frac{5}{2}\Phi\right)^{3/5} - \frac{3}{2}\alpha^{2/5}\int_0^y \frac{\zeta^{7/5}dy}{(1-\zeta)^{1/5}}\right]^{2/3} + O(\mu) \qquad (2\text{-}40)$$

for $y < y_w(\tau)$,

$$\theta_e = \theta_e^{\circ} + O(\mu^{5/2}/\alpha) \text{ for } y > y_w(\tau) , \qquad (2\text{-}41)$$

$$\left[\theta_e^{\circ}(y_w)\right]^{3/2}\left\{\frac{2}{3}\left[\frac{\theta_e}{\theta_e^{\circ}(y_w)}\right]^{3/2} + 2\left[\frac{\theta_e}{\theta_e^{\circ}(y_w)}\right]^{1/2} + \log\frac{\left[\frac{\theta_e}{\theta_e^{\circ}(y_w)}\right]^{1/2} - 1}{\left[\frac{\theta_e}{\theta_e^{\circ}(y_w)}\right]^{1/2} + 1}\right\} = \frac{-\alpha\zeta^2(y_w)}{\sqrt{1-\zeta(y_w)}}\left[y-y_w\right] + O(\mu^3/\alpha) \qquad (2\text{-}42)$$

for $y-y_w = O(\mu^{3/2}/\alpha)$.

A bleaching wave is seen to arise which separates hot parts of the plasma from cold parts. The location of the wave, $y_w(\tau)$ is given implicitly by

$$\left(\frac{5}{2}\Phi\right)^{3/5} = \frac{3}{2}\alpha^{2/5}\int_0^{y_w(\tau)} \frac{\zeta^{7/5}dy}{(1-\zeta)^{1/5}} \qquad (2\text{-}43)$$

As Φ increases from zero, y_w is seen to increase monotonically with Φ . The velocity of the bleaching wave can be found by taking the implicit derivative of (2-43),

$$V_w = \frac{d\Phi}{d\tau}\left(\frac{5}{2}\alpha\Phi\right)^{-2/5}\left[1-\zeta(y_w)\right]^{1/5} \Big/ \zeta(y_w)^{7/5}$$

For a laser pulse with $i \sim \tau$, $V_w \sim \tau^{1/5}$ for a constant density. A positive density gradient has the effect of limiting

the maximum velocity of the wave and eventually causing it to decrease.

If α is very small, the wave speed approaches the speed of light and reaches the critical density very early in the laser pulse. From that time on, the laser heats the entire underdense portion of the plasma simultaneously and the temperature profile produced is

$$\theta_e = \left(\frac{5}{2}\frac{\alpha\zeta\bar{\varepsilon}}{\sqrt{1-\zeta}}\right)^{2/5} + O(\alpha^{4/5},\mu) \qquad (2\text{-}44)$$

A "hot spot" is generated near $\zeta = 1$, the critical density. Of course, the original expression for absorption coefficient (2-11) breaks down very near $\zeta = 1$ and remains finite at the critical density. Nevertheless, a hot spot is produced in this region. This limit is called the "simultaneous heating case". In this case the actual temperature produced will be roughly twice that given in (2-36) since the light wave is reflected at the critical density and travels backwards through the region with very little intensity attenuation (see 2-10)). Hence, most of the laser radiation is lost to reflection.

If the thickness parameter α is larger than a certain value α_c the wave travels much more slowly and does not even reach the critical density by the end of the laser pulse. α_c is a critical value of α that depends on the density profile, but is always of order one. Hence, in this case there is no isolated hot spot as for α small. This limit can be termed the "bleaching wave case" since a bleaching wave continues to move into the plasma throughout the laser pulse. The heating

is by no means "simultaneous". In this case all of the laser energy is absorbed.

In summary, stationary-frozen-nonconducting heating of a cool plasma will occur in one of four regimes depending on the sizes of the thickness parameter α and the initial temperature parameter μ. If $\alpha \ll \mu^{5/2}$, then the plasma is only slightly heated and the heating is simultaneous. A weak hot spot occurs at the critical density and nearly all the laser energy is lost to reflection. If $\mu^{5/2} \ll \alpha \ll \mu^{3/2}$, the plasma is heated to temperatures much hotter than the initial temperature but still most of the laser energy is lost to reflection. The heating is simultaneous and a stronger hot spot appears. If $\mu^{3/2} \ll \alpha < \alpha_c$, a very rapid bleaching wave traverses the underdense region early in the pulse. After that the heating is simultaneous and a significant hot spot appears at the critical density. During the simultaneous heating stage, a significant part of the laser energy is lost to reflection but not as much as in the previous cases. If $\alpha > \alpha_c$, a much slower bleaching wave propagates into the plasma and the wave does not penetrate all the way to the critical density. No hot spot or reflected wave appears, and all of the laser energy is absorbed.

3. Application to a Linear Density Profile

The solutions given in the last section can easily be calculated for a linear density profile, $\zeta = y$. These results for three different values of the parameter α are shown in Figures 8, 9, 10. For a linear density profile, $\alpha_c = 5.2$.

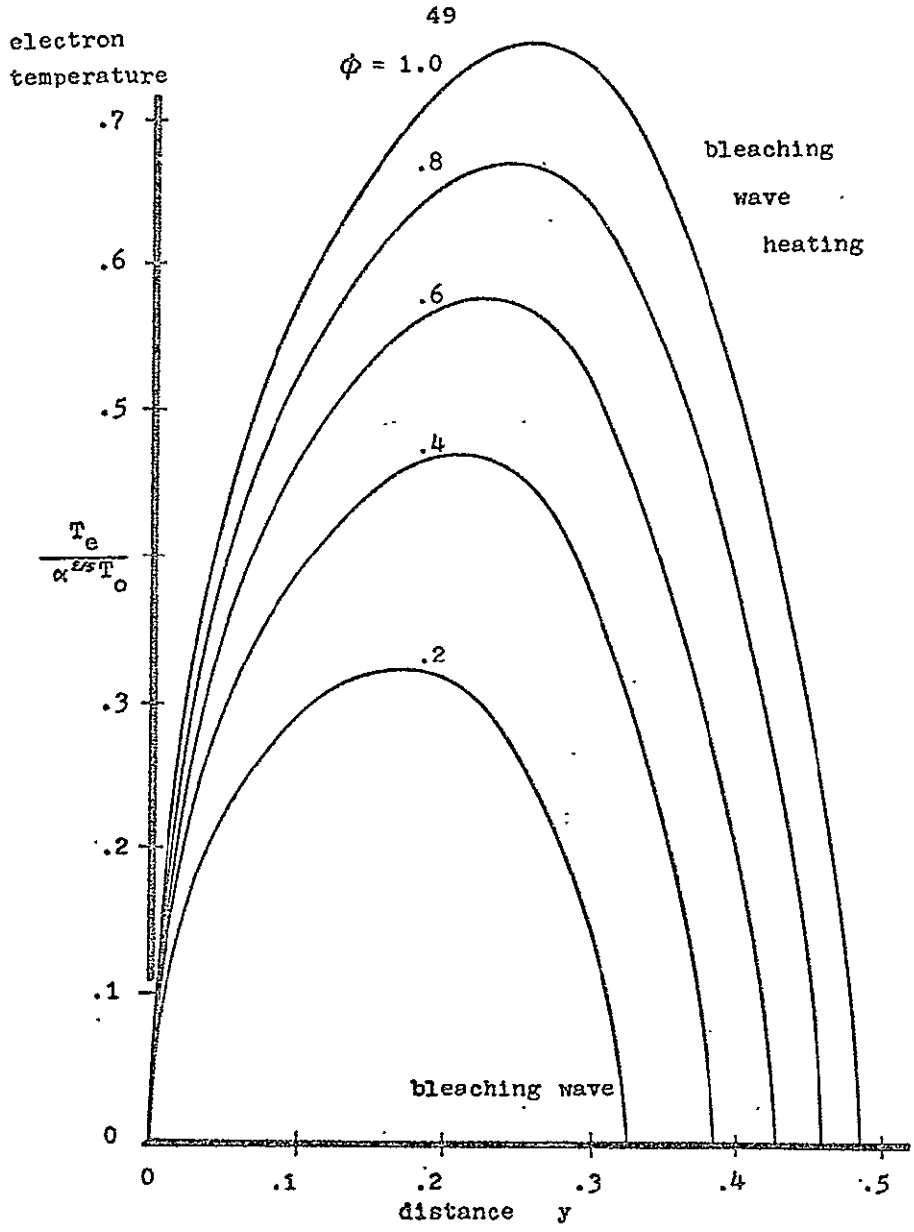

Figure 8. Temperature distribution for a linear density gradient with $\alpha = 1000$

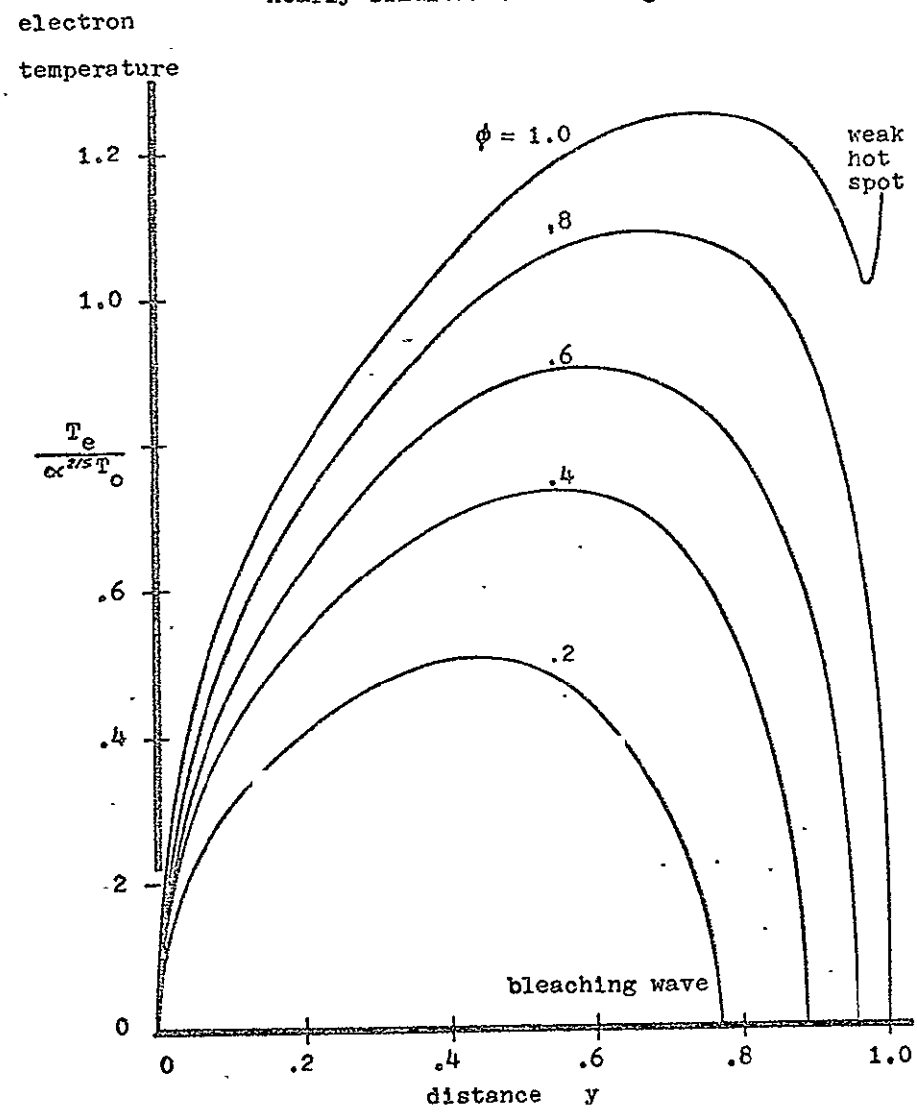

Figure 9. Temperature distribution for a linear density profile with $\alpha = 4$

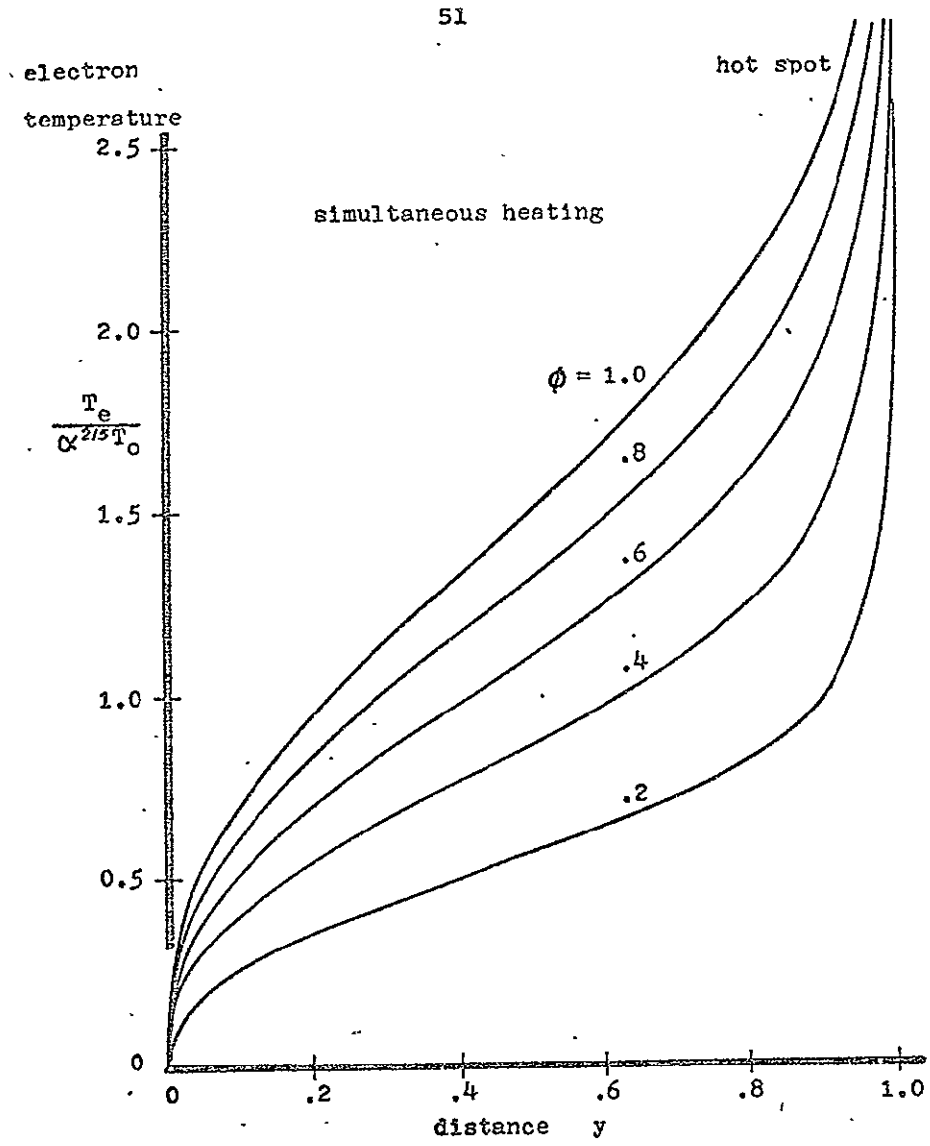

Figure 10. Temperature distribution for a linear density profile with $\mu^{5/2} \ll \alpha \ll 1$

Figure 8 clearly demonstrates the bleaching wave moving into the plasma. In this case ($\alpha = 1000$) corresponding to an optically thick plasma, the bleaching wave only propagates about halfway across the underdense portion of the plasma by the end of the laser pulse. In Figure 9 ($\alpha = 4$) corresponding to a medium thickness plasma, the bleaching wave reaches the critical density just before the end of the laser pulse, and a weak hot spot is generated at the critical density. In Figure 10 ($\alpha \ll 1$) corresponding to an optically thin plasma, the bleaching wave travels almost infinitely fast in traversing the underdense region and hence is not shown. A strong hot spot arises at the critical density.

While Figures 8, 9, and 10 give the analytical features of the solutions, they are given in terms of dimensionless quantities and do not show clearly the temperatures and other conditions that are attained. Figures 11 and 12 are summary plots for laser wave lengths $\lambda_o = 1.06\mu$ and 10.6μ, respectively. The "maximum temperatures" given are the maximum temperatures without the hot spot. Naturally, when a hot spot appears, there will be a much hotter temperature in a very localized region. In the simultaneous heating part, the temperature is of order $\alpha^{2/5}T_o$. In the bleaching wave part, it is of order $\alpha^{1/3}T_o$ since smaller densities are heated. The expressions for the maximum temperature are,

$$T_{e_{max}} \cong 1.08\,(J_o/A)^{2/5} \text{ eV for } \mu \ll \alpha < 5.2$$

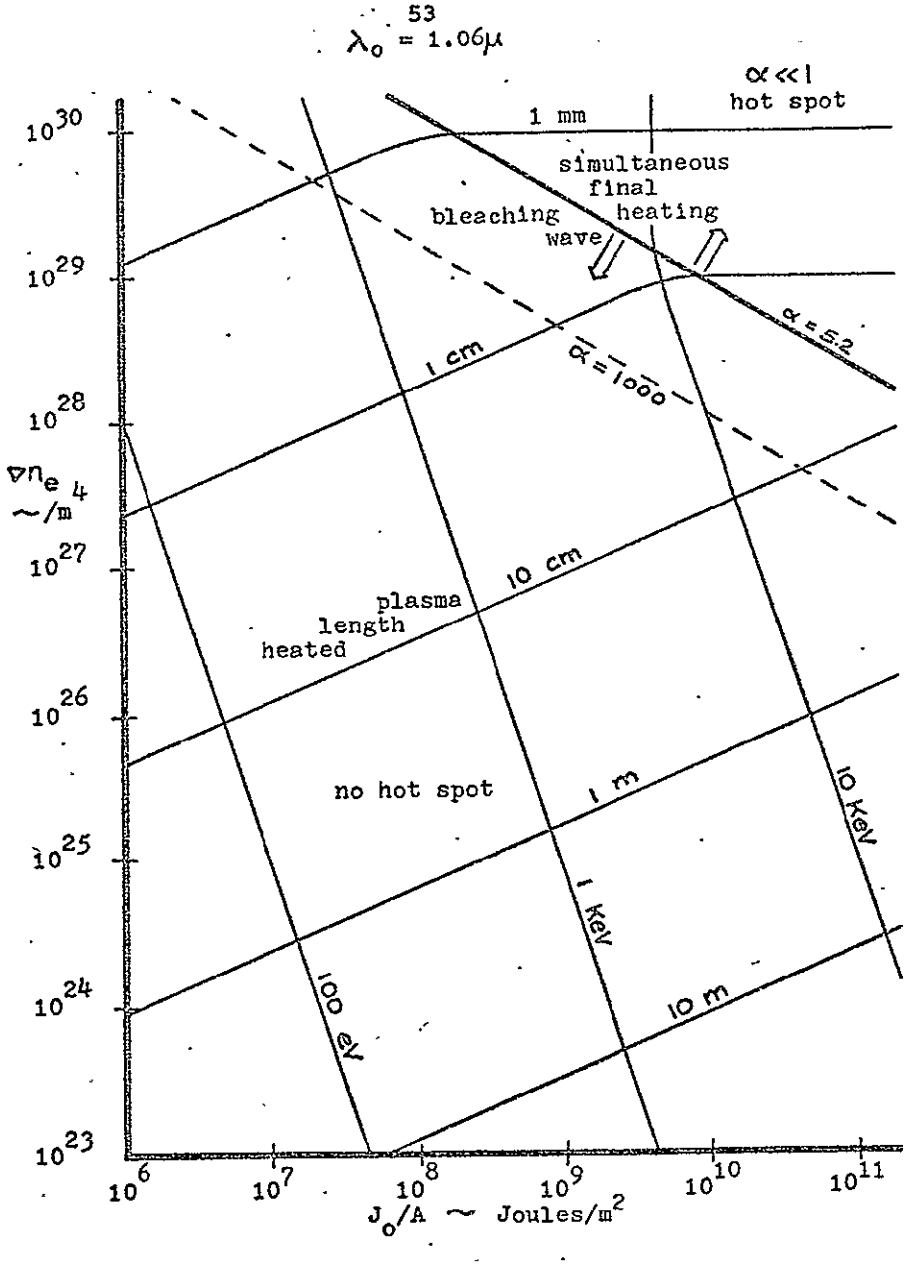

Figure 11. Summary of plasma conditions which can be achieved for a linear density profile with a Nd^+ glass laser

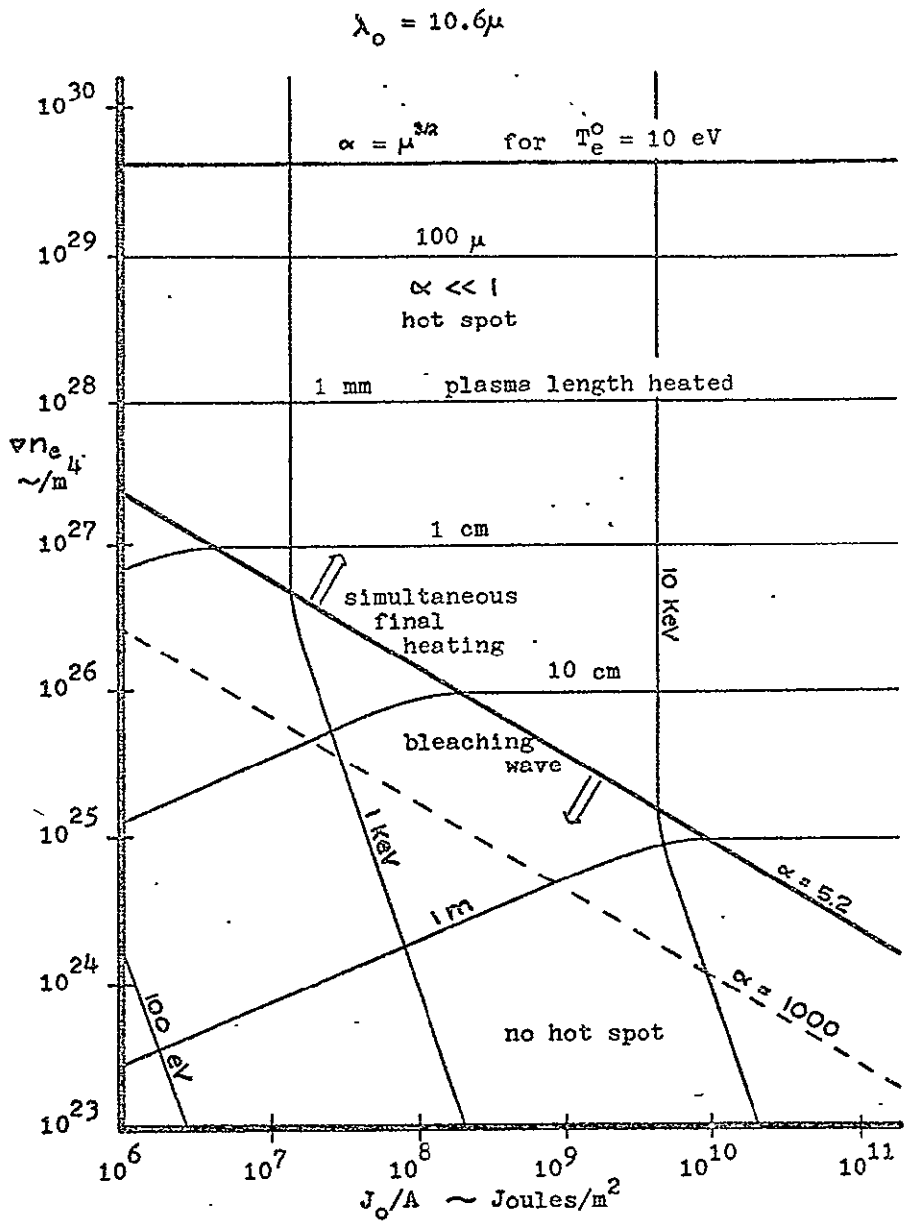

Figure 12. Summary of plasma conditions which can be achieved for a linear density profile with a CO_2 gas laser

$$T_{e_{max}} \simeq 1.64 \times 10^{-6} (J_o/A)^{1/2} (\nabla n_e)^{1/6} \lambda_o^{2/3} \text{ for } \alpha > 5.2 \ . \quad (2\text{-}45)$$

The "plasma length" is defined as the thickness of the plasma that is irradiated by the laser. This thickness will be R for the simultaneous heating case, but will be of order $\alpha^{-1/6} R$ for the bleaching wave case,

$$L = R = 1.12 \times 10^{27} (\nabla n_e)^{-1} \lambda_o^{-2} \text{ for } \mu << \alpha < 5.2$$

$$L \simeq \frac{1.53R}{\alpha^{1/6}} = 3.18 \times 10^{12} (J_o/A)^{1/4} (\nabla n_e)^{-7/12} \lambda_o^{-1/3} \text{ for } \alpha > 5.2 \quad (2\text{-}46)$$

where L is in meters.

The maximum density heated is equal to the dimensionless length heated for the case of a linear density gradient. Then the maximum density heated is one for the simultaneous part, and $1.53\alpha^{-1/6}$ for the bleaching wave part. These are not shown on the summary figures.

It is noted that the 10.6μ radiation heats in the simultaneous heating regime for much smaller electron density gradients than does the 1.06μ radiation, i.e., a relatively long plasma may be in the simultaneous heating regime under 10.6μ radiation but in the bleaching wave regime under 1.06μ radiation. By comparing Figures 11 and 12, it is also seen that the temperatures achieved are independent of the laser wave length in the simultaneous heating regime. However, the longer wave length heating produces higher temperatures in the bleaching wave regime.

It has been previously noted that not all the radiation is absorbed in the simultaneous heating case but that much is lost to reflection. It is important to know what fraction of energy is absorbed--both from the standpoint of efficiency and from the fact that reflected radiation may damage the laser. Integrating the temperature (2-44) for the thickness parameter $\alpha \ll 1$ over the width of the underdense region, the fraction of energy absorbed can be calculated. This fraction is doubled to take into account the absorption of reflected light, and the result is

$$\frac{J_{abs}}{J_o} = 2\left(\frac{5}{2}\alpha\right)^{2/5} \int_o^1 \frac{\zeta^{7/5} dy}{(1-\zeta)^{1/5}}$$

which for a linear density profile reduces to

$$\frac{J_{abs}}{J_o} = 1.72\ \alpha^{2/5}$$

These results are shown in Figure 13. For $\alpha > 5.2$ there is total absorption and for $\alpha \ll 1$ the absorption is given by the above equation. Intermediate values of α are represented by the dashed line which is an interpolation.

It has been shown recently that another effect may nearly eliminate the reflected light for sufficiently high intensities. This is the anomalous absorption effect that occurs near the critical density. This effect was studied theoretically by Kruer et.al.,[16] and is confirmed by an earlier experiment by Gekker and Sizukhin.[17]

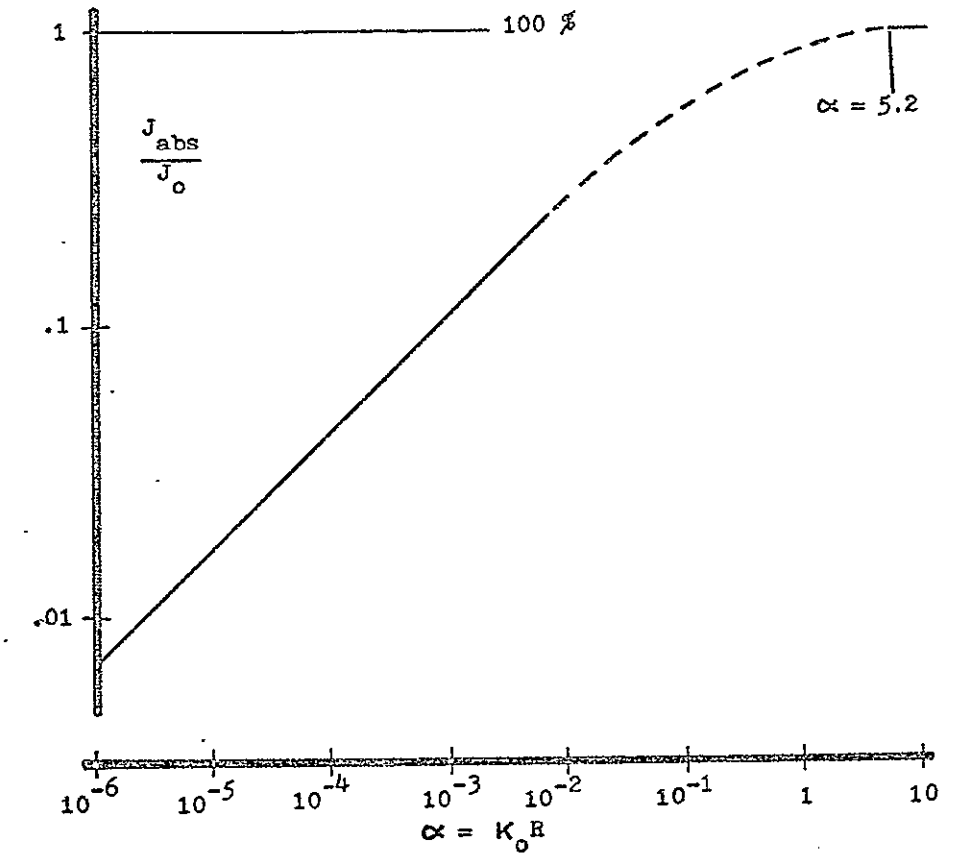

Figure 13. Fraction of laser energy absorbed for a linear density profile plasma

4. Summary

Analytic solutions have been developed for the laser heating of a one-dimensional plasma under the assumption that the plasma is stationary, non-thermally conducting, and that only the electrons are heated (the ions being frozen at their initial temperature). These assumptions were found to be reasonable for many cases of interest. In these cases, the laser pulse is sufficiently short so that the processes of plasma motion, thermal conduction, and electron-ion equilibration do not have time to make a significant effect. These assumptions reduce the problem (aside from equations of state) to a pair of equations; a radiative transfer equation and an equation for the temperature containing an energy source term. These equations were combined and solved for all ranges of the thickness parameter α by the method of matched asymptotic expansions.

The use of a one-dimensional plasma was motivated by the need to make the mathematics tractable. No real plasma is strictly one-dimensional but many plasma geometries of interest are nearly one-dimensional and the analytic results of this study can be applied to such plasmas with reasonable accuracy. An example of thermonuclear interest is the longitudinal heating of a column of plasma that has a uniform density across the column, such as might be found in a plasma focus or a theta pinch. Another example is the radial heating of such a column which is quasi-one-dimensional if the absorption length $1/\kappa_o$ is less than the radius of the column. Such a plasma with a number density of $10^{19}/cm^3$ heated by a longitudinally

aimed laser of wave length 10.6μ to a temperature of 10 KeV could be contained with a magnetic field of 3 MG (as might be developed in a plasma focus). For plasmas that are not nearly one-dimensional, the results of this study are still valuable in understanding qualitative results.

The analytic solution shows markedly different behavior for different ranges of the thickness parameter α. For thick plasmas (corresponding to α large) the response is characterized by a bleaching wave proceeding into the plasma. Behind the wave is a hot nearly transparent plasma being irradiated by the laser. Ahead of the wave is an unheated opaque plasma. Physically, the motion of the wave corresponds to the heating of successive layers of opaque plasma to temperatures at which they become transparent and allow the radiation to pass on to deeper layers. For α greater than a certain distinct value α_c which depends on the density profile, the bleaching wave fails to penetrate to the critical density by the end of the laser pulse. Then none of the radiation is reflected back at the critical density.

For α less than α_c, the bleaching wave reaches the critical density before the laser pulse ends. At that time, reflection occurs at the critical density and some of the light is reflected. Although the heating is simultaneous once the bleaching wave traverses the underdense region, it is by no means uniform--an extreme hot spot is created at the critical density point. For relatively thin plasmas (α somewhat less than one) the bleaching wave traverses the underdense region extremely fast and all but the earliest stages of the heating are "simultaneous".

For the thickness parameter α smaller than the small parameter $\mu^{3/2}$, the entire heating process is simultaneous with no bleaching wave at all. μ is the initial temperature parameter. The efficiency of the heating drops further as more of the laser energy is lost to reflection. For α even smaller (less than $\mu^{5/2}$), the heating is so ineffective that the temperature is scarcely changed at all.

It is clear that in the preparation of the plasma to be heated, the temperatures (or other conditions sought) can be optimized by proper choice of the thickness parameter α. For a given laser energy per unit area and wave length, α depends on the density gradient. Hence, proper tailoring of the density gradient beforehand will give the best results, whether that be maximum temperature or maximum yield from a thermonuclear reaction.

The solution found in this section is only for a stationary, nonconducting, frozen ion plasma. But the solutions for a stationary-frozen-conducting plasma, and a stationary-equilibrium-nonconducting plasma are closely related. In the stationary-frozen-conducting regime, the effect of conduction will simply be to smooth out the nonuniformities in temperature that are produced. This case is studied in more detail in the next section. In the stationary-equilibrium-nonconducting regime, the effect of the equilibration will be to divide the energy equally between the electrons and ions. In this case, the result is almost identical to the frozen ion solution presented in this section.

C. STATIONARY-FROZEN-CONDUCTING PLASMAS

For sufficiently thin plasmas, thermal conduction effects become important. When thermal conduction is strong enough to smooth out major temperature nonuniformities, then one has the stationary-frozen-conducting regime. This regime is similar to that studied in the last section except that thermal conduction effects are dominant. In this section, a simple solution is developed for the stationary-frozen-conducting regime. It is not intended that this solution be as rigorous as that of section B since it is desired only to demonstrate its major features.

1. Equations

The requirements for this regime are $\epsilon \ll 1$, $\lambda \ll 1$, $\lambda\theta_e/\theta_i \ll 1$ as before, but now a different condition $\eta_e \gg 1$. Ion conductivity η_i is always small compared to electron conductivity and is neglected. It is assumed that ϵ, λ, $\lambda\theta_e/\theta_i$ are actually zero, and $\eta_e \gg 1$. Then as before, the solutions to the continuity and momentum equations are $\zeta = \zeta(y)$ and $U = 0$, respectively. The electron entropy equation (2-8) becomes

$$\frac{\partial \sigma_e}{\partial \tau} = \frac{\alpha K}{\zeta}\frac{i}{\theta_e} + \eta_e \frac{2/7}{\zeta\theta_e}\frac{\partial^2 \theta_e^{7/2}}{\partial y^2}$$

This can be combined with an equation of state (2-13) to eliminate the electron entropy,

$$\zeta \frac{\partial \theta_e}{\partial \tau} = \alpha K i + \frac{2}{7} \eta_e \frac{\partial^2 \theta_e^{7/2}}{\partial y^2}$$

Using the absorption coefficient (2-11) this becomes,

$$\zeta \frac{\partial \theta_e}{\partial \tau} = \alpha \frac{\zeta^2}{\theta_e^{3/2}(1-\zeta)^{1/2}} i + \frac{2}{7} \eta_e \frac{\partial^2 \theta_e^{7/2}}{\partial y^2} \quad . \qquad (2\text{-}47)$$

In the stationary-frozen-conducting regime, the thickness parameter α is always small (see figures 2-5). The stationary-frozen-nonconducting solution has the temperature θ_e of order $\alpha^{2/5}$ as seen in the last section (in the simultaneous part of the regime). Since the primary effect of thermal conduction will be to smooth temperature nonuniformities, it is reasonable that the same temperature scale would appear in the adjacent conducting regime. Taking $\theta_e = \alpha^{2/5}\theta_\alpha$, (2-47) becomes

$$\zeta \frac{\partial \theta_\alpha}{\partial \tau} = \frac{\zeta^2}{\theta_\alpha^{3/2}(1-\zeta)^{1/2}} i + \frac{2}{7} \alpha\eta_e \frac{\partial^2 \theta_\alpha^{7/2}}{\partial y^2} \qquad (2\text{-}48)$$

If $\alpha\eta_e \ll 1$ the conduction term is negligible and the solution is stationary-frozen-nonconducting. If $\alpha\eta_e \gg 1$ then thermal conduction is dominant and the solution is stationary-frozen-conducting. Thus it is seen that $\alpha\eta_e$ (not η_e) is the important parameter that determines whether the plasma is thermally conducting or not. This will doubtless shift the boundary between these two regimes as will be discussed in section D.

Two unknowns remain in (2-48); θ_α and i. But in the stationary-frozen-conducting regime, $\alpha \ll 1$ so the laser intensity is only weakly diminished in passing through the plasma. The intensity is $i = \phi'(\tau)[1 + O(\alpha^{2/5})]$ as seen by comparing the radiative transfer equation (2-10) and the absorption coefficient (2-11). In view of this fact (2-48) becomes,

$$0 = \frac{2}{7}\frac{\partial^2 \theta_\alpha^{7/2}}{\partial y^2} + \frac{1}{\alpha\eta_e}\left[\zeta \frac{\partial \theta_\alpha}{\partial \tau} - \frac{\zeta^2 \phi'(\tau)}{\theta_\alpha^{3/2}(1-\zeta)^{1/2}}\right] + O\left(\frac{\alpha^{2/5}}{\alpha\eta_e}\right) . \qquad (2\text{-}49)$$

Still needed to form a well posed problem are the boundary and initial conditions. It is not the intent of this discussion to include the details of finite initial temperature as done in section B for the nonconducting solution, so the initial condition is taken to be $\theta_\alpha(y,0) = 0$. The boundary conditions are on the thermal conduction at both ends of the plasma. Since there is a vacuum at the front end, $y = 0$, there can be no thermal conduction, so $\partial\theta_\alpha/\partial y\big|_{y=0} = 0$. The same condition would apply at the rear edge of the plasma.

2. Analytic Solution

Consider the asymptotic expansion, $\theta_\alpha = \theta_o + \frac{1}{\alpha\eta_e}\theta_1 + \ldots$ Then (2-49) becomes

$$0 = \frac{2}{7}\frac{\partial^2 \theta_o^{7/2}}{\partial y^2} + \frac{1}{\alpha\eta_e}\left[\frac{\partial^2 \theta_o^{5/2}\theta_1}{\partial y^2} - \zeta\frac{\partial \theta_o}{\partial \tau} + \frac{\zeta^2 \phi'(\tau)}{\theta_o^{3/2}(1-\zeta)^{1/2}}\right] + O\left(\frac{\alpha^{2/5}}{\alpha\eta_e}, \frac{1}{(\alpha\eta_e)^2}\right)$$

The equation to order one is $\partial^2\theta_o^{7/2}/\partial y^2 = 0$ and has solutions $\theta_o = [a_1(\tau)y + a_2(\tau)]^{2/7}$ where a_1 and a_2 are the arbitrary functions of τ that arise in the integration with respect to y. The adiabatic boundary condition at $y = 0$ requires that $a_1(\tau) = 0$ so that θ_o becomes purely a function of τ. The equation to order $1/\alpha\eta_e$ then becomes,

$$0 = \theta_o^{5/2}\frac{\partial^2\theta_1}{\partial y^2} - \zeta\frac{\partial\theta_o}{\partial\tau} + \frac{\zeta^2\dot{\phi}'(\tau)}{\theta_o^{3/2}(1-\zeta)^{1/2}}$$

Integrating once and applying the boundary condition at $y = 0$ to order $1/\alpha\eta_e$ yields,

$$0 = \theta_o^{5/2}\frac{\partial\theta_1}{\partial y} - \frac{\partial\theta_o}{\partial\tau}\int_o^y\zeta dy + \frac{\dot{\phi}'(\tau)}{\theta_o^{3/2}}\int_o^y\frac{\zeta^2 dy}{(1-\zeta)^{1/2}}$$

Integrating again and solving for θ_1 yields,

$$\theta_1 = \frac{1}{\theta_o^{5/2}}\left[\frac{\partial\theta_o}{\partial\tau}\int_0^y\left\{\int_0^y\zeta dy\right\}dy - \frac{\dot{\phi}'(\tau)}{\theta_o^{3/2}}\int_0^y\left\{\int_0^y\frac{\zeta^2 dy}{0(1-\zeta)^{1/2}}\right\}dy\right] + a_3(\tau), \quad (2\text{-}50)$$

where $a_3(\tau)$ is the arbitrary function of time that arises in the integration with respect to y. Then,

$$\theta_\alpha = \theta_o(\tau) + \frac{1}{\alpha\eta_e\theta_o^{5/2}}\left[\frac{\partial\theta_o}{\partial\tau}\int_0^y\left\{\int_0^y\zeta dy\right\}dy - \frac{\dot{\phi}'(\tau)}{\theta_o^{3/2}}\int_0^y\left\{\int_0^y\frac{\zeta^2 dy}{0(1-\zeta)^{1/2}}\right\}dy + a_3(\tau)\right] + O\left(\frac{\alpha^{2/5}}{\alpha\eta_e}, \frac{1}{(\alpha\eta_e)^2}\right)$$

a. Underdense Plasmas

First suppose that there is no thermal conduction through the point $y = 1$. This is the case where the plasma doesn't achieve critical density anywhere and $y = 1$ is the rear edge. Then the rear boundary condition is $\partial\theta_\alpha/\partial y|_{y=1} = 0$. This is satisfied automatically to order one. The order $1/\alpha\eta_e$ equation gives,

$$\theta_o^{3/2} \frac{\partial\theta_o}{\partial\tau} = \Phi'(\tau) \int_0^1 \frac{\zeta^2 dy}{(1-\zeta)^{1/2}} \left\{\int_0^1 \zeta dy\right\}^{-1}$$

Integrating with respect to time, and applying the initial condition of zero temperature,

$$\theta_o = \left[\frac{5}{2} \Phi \int_0^1 \frac{\zeta^2 dy}{(1-\zeta)^{1/2}} \left\{\int_0^1 \zeta dy\right\}^{-1}\right]^{2/5} . \qquad (2\text{-}51)$$

Thus it is seen that applying the rear boundary condition to order $1/\alpha\eta_e$ determines the unknown function $\theta_o(\tau)$ in the term to order one. Applying the rear boundary condition to the next higher order would determine the unknown function $a_3(\tau)$ in the term to order $1/\alpha\eta_e$.

b. Overdense Plasmas

Suppose that the plasma does achieve critical density and that the portion beyond the critical density (the dark part) is heated by thermal conduction from the irradiated portion which is heated by absorption. This is shown schematically in figure 14. If the mass of the dark part is of the same order of magnitude as the mass of the light part, then the presence

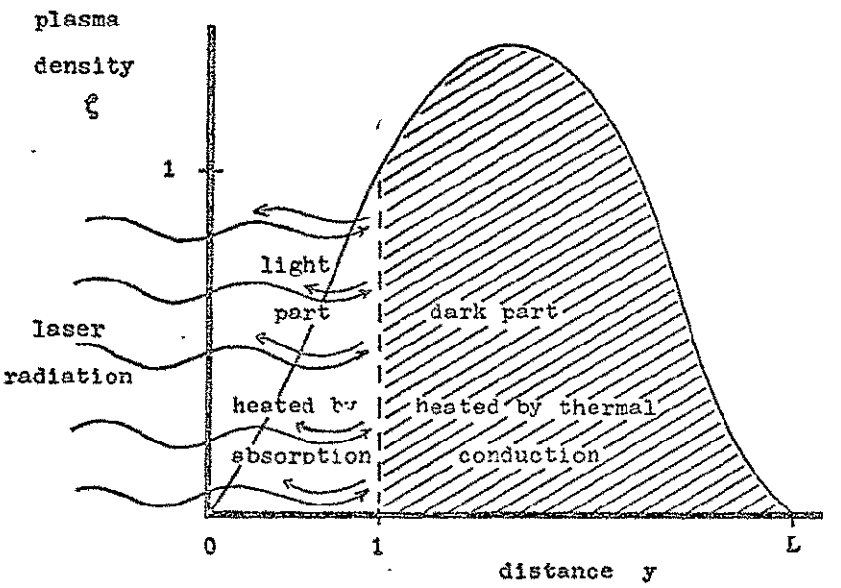

Figure 14. Laser heating of an overdense plasma in the stationary-frozen-conducting regime

of the dark part will not alter the basic character of the solution, i.e., that it is dominated by thermal conduction. However, the temperature produced will be less since a greater mass of plasma is being heated.

To construct the solution in this case, one must solve (2-46) for both the light part, $\theta_{\alpha\ell}$, and dark part $\theta_{\alpha d}$, separately. Then the two solutions are matched at the point $y = 1$ with the condition that thermal conduction at the junction is the same for both. Thus $(\theta_{\alpha\ell} - \theta_{\alpha d})\big|_{y=1} = 0$ and $(\partial\theta_{\alpha\ell}/\partial y - \partial\theta_{\alpha d}/\partial y)\big|_{y=1} = 0$. The dark form of (2-49) is the same as the light form except that the absorption term (that containing $\phi'(\tau)$) is missing in the dark equation.

The order one dark equation is the same as that for the light equation; $\partial^2\theta_{od}^{7/2}/\partial y^2 = 0$, and its solution is $\theta_{od} = [b_1(\tau)y + b_2(\tau)]^{7/2}$. Applying the adiabatic boundary condition at the rear edge ($y = L$) of the plasma, $\partial\theta_\alpha/\partial y\big|_{y=L} = 0$ requires that $b_1(\tau) = 0$ so that $\theta_{od} = \theta_{od}(\tau)$. Matching this to the light solution to order one requires that $\theta_{od}(\tau) = \theta_{o\ell}(\tau) = \theta_o(\tau)$. The order $1/\alpha\eta_e$ equation is,

$$\zeta \frac{\partial\theta_o}{\partial\tau} = \theta_o^{5/2} \frac{\partial^2\theta_{1d}}{\partial y^2}$$

Integrating with respect to y and applying the boundary condition at $y = L$ gives,

$$\frac{\partial\theta_{1d}}{\partial y} = -\frac{1}{\theta_o^{5/2}} \frac{\partial\theta_o}{\partial\tau} \int_y^L \zeta dy$$

Integrating again gives,

$$\theta_{1d} = \frac{1}{\theta_o^{5/2}} \frac{\partial \theta_o}{\partial \tau} \int_y^L \left\{ \int_y^L \zeta dy \right\} dy + b_3(\tau) ,$$

where $b_3(\tau)$ is the arbitrary function arising in the integration. Matching to the light solution (2-50), $\theta_{1d}(1,\tau) = \theta_{1\ell}(1,\tau)$ merely forms a relation between the two unknown functions of time $a_3(\tau)$ and $b_3(\tau)$. But the matching of the first derivatives $\partial\theta_{1d}/\partial y|_{y=1} = \partial\theta_{1\ell}/\partial y|_{y=1}$ gives,

$$\frac{1}{\theta_o^{5/2}} \left[\frac{\partial \theta_o}{\partial \tau} \int_0^1 \zeta dy - \frac{\Phi'(\tau)}{\theta_o^{3/2}} \int_0^1 \frac{\zeta^2 dy}{(1-\zeta)^{1/2}} \right] = \frac{1}{\theta_o^{5/2}} \left[- \frac{\partial \theta_o}{\partial \tau} \int_1^L \zeta dy \right]$$

Hence,

$$\theta_o^{3/2} \frac{\partial \theta_o}{\partial \tau} = \Phi'(\tau) \int_0^1 \frac{\zeta^2 dy}{(1-\zeta)^{1/2}} \left\{ \int_0^L \zeta dy \right\}^{-1}$$

Integrating with respect to τ and applying the zero initial temperature condition,

$$\theta_o = \left[\frac{5}{2} \Phi \int_0^1 \frac{\zeta^2 dy}{(1-\zeta)^{1/2}} \left\{ \int_0^L \zeta dy \right\}^{-1} \right]^{2/5}$$

which is the same as the solution to the previously solved case except for the different range of integration in the denominator (over the whole plasma).

Then the usual nondimensional electron temperature is,

$$\theta_e = \alpha^{2/5} \theta_\alpha = \left[\frac{5}{2} \alpha \Phi \int_0^1 \frac{\zeta^2 dy}{(1-\zeta)^{1/2}} \left\{ \int_0^L \zeta dy \right\}^{-1} \right]^{2/5} + O\left(\frac{\alpha^{2/5}}{\alpha \eta_e}\right) . \qquad (2\text{-}52)$$

Thus, for the stationary-frozen-conducting plasma, the temperature is seen to rise--uniformly--with the two-fifths power of the laser energy released (as measured by Φ). This agrees with the fact that thermal conduction dominates and also with the fact that as the plasma heats up, it becomes more and more transparent to the radiation, thus heating more and more slowly. The fall off in the rate of heating is clearly seen in figure 15 which is the time history of the electron temperature θ_e for a plasma with a parabolic density profile, $\zeta = \frac{3}{2} y - \frac{1}{2} y^2$, heated by a constant intensity laser pulse for which $\Phi = \tau$. This solution is based on the assumption that the masses of the light and dark parts of the plasma are of the same order.

Suppose that the dark part of the plasma is much larger than the light part. Then, even though the light part is dominated by thermal conduction and has a nearly uniform temperature, the dark part may be quite nonuniform. If the dark part is large enough, then it will have a nonuniform temperature profile diffusing with time into the dark part. Since the thermal conduction coefficient of a fully ionized plasma is proportional to the five-halves power of the temperature, the thermal diffusion is nonlinear. It will proceed into the cold dark part as a "thermal wave" resembling the "bleaching wave" found in the stationary-frozen-nonconducting regime. The close relation of these two phenomena is discussed in detail in chapter IV.

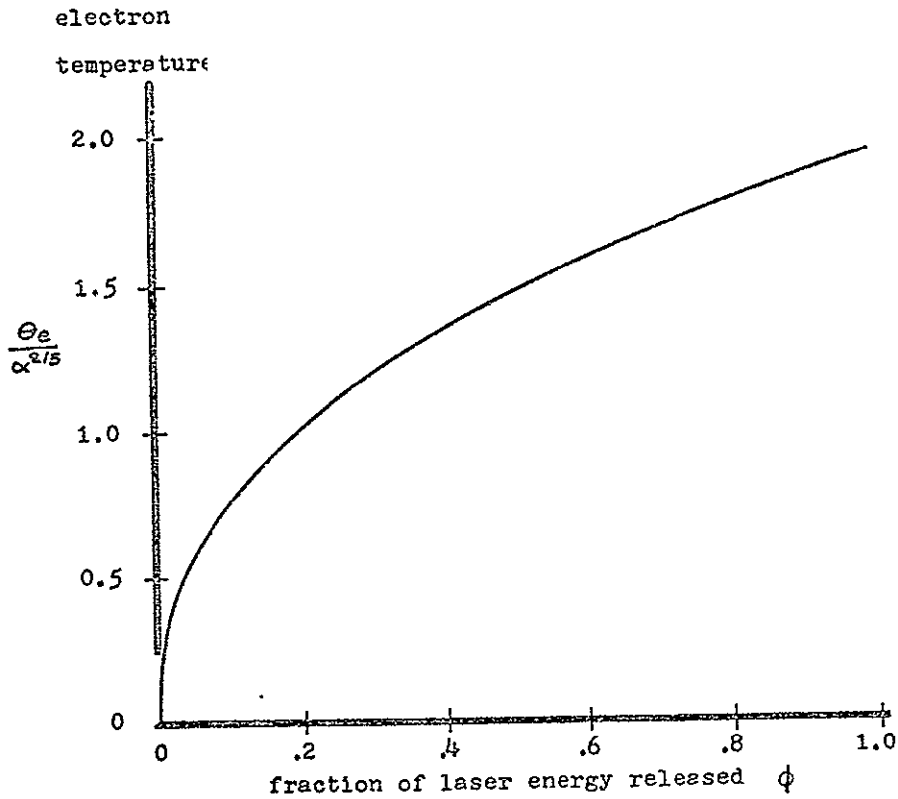

Figure 15. Time history of electron temperature of a plasma in the stationary-frozen-conducting regime

D. RE-EXAMINATION OF HEATING REGIMES

As was previously mentioned, it is necessary to take any solution found and reconsider the regimes in which it is valid. This is especially true in this study since the dimensionless electron temperature θ_e varies over many orders of magnitude. θ_e is of order $\alpha^{2/5}$ in the stationary-frozen-conducting regime and in the simultaneous heating part of the stationary-frozen-nonconducting regime. For the bleaching wave portion of the stationary-frozen-nonconducting regime $\theta \sim \alpha^{1/3}$. α is a parameter that may either be much larger or much smaller than one.

Any locally extreme values that may occur in θ_e or its derivatives may also invalidate the solutions. Indeed such a singularity does occur in the neighborhood of the critical density where a temperature singularity does occur (in the stationary-frozen-nonconducting regime). However, it is not the purpose of this discussion to probe the fine points of local phenomena--such as that very near the critical density. Rather it is intended to re-examine the overall behavior and to find the correct boundaries of the various regimes since θ_e is not of order one.

1. Onset of Motion

The original estimate of the plasma regimes (section A 3) indicated that the onset of motion occurs toward the upper right corner of the summary charts (figures 2-5), i.e., for higher values of ∇n_e and J_0/A. A study of the governing

equations with cognizance of the correct temperature scale reveals that the original estimate is too conservative, and that the onset of motion occurs for even higher ∇n_e .

The appropriate criterion to determine the onset of motion is the conditions for which the plasma motion begins to significantly affect the temperature that is produced. Consider the asymptotic expansions,

$$\begin{aligned} \zeta &= \nu_o(\alpha)\zeta_o + \nu_1(\alpha,\epsilon)\zeta_1 + \cdots \\ U &= \qquad\quad \xi_1(\alpha,\epsilon)U_1 + \cdots \\ \theta_e &= \lambda_o(\alpha)\theta_o + \lambda_1(\alpha,\epsilon)\theta_1 + \cdots \\ i &= i_o \qquad + \delta_1(\alpha,\epsilon)i_1 + \cdots \\ y &= \beta\tilde{y} \end{aligned} \tag{2-53}$$

where $\lambda_o(\alpha)$ and $\nu_o(\alpha)$ are the orders of magnitude of the temperature and density for the stationary solution. β is the appropriate length scale. They are to be determined by the nature of the stationary solution. The terms of order ν_1, ξ_1, λ_1, δ_1 contain the lowest order effect of motion. The terms of order one, ν_o and λ_o give the stationary solution. The object of this discussion is to find λ_1/λ_o which is the ratio of motion induced temperature change to the stationary temperature.

Applying the expansions (2-53) to the momentum equation (2-7) together with the equation of state (2-12) gives

$$\left[\ 0\ \right] + \left[\xi_1 \frac{\partial U_1}{\partial \tau} + \frac{\Lambda_o \epsilon}{\beta} \cdot \frac{3}{5} \cdot \frac{1}{\zeta_o} \cdot \frac{\partial}{\partial \tilde{y}} (\zeta_o \theta_o)\right] + \ldots \ = \ 0 \ . \quad (2\text{-}54)$$

In this and in subsequent equations, the first bracketed term represents the stationary terms and the second represents the lowest order effect of motion.

Applying the expansions (2-53) to the continuity equation (2-6) gives

$$\left[\nu_o \frac{\partial \zeta_o}{\partial \tau}\right] + \left[\nu_1 \frac{\partial \zeta_1}{\partial \tau} + \frac{\nu_o \xi_1 \epsilon}{\beta} \cdot \frac{\partial}{\partial \tilde{y}} (\zeta_o U_1)\right] + \ldots \ = \ 0 \ . \quad (2\text{-}55)$$

Applying the expansions (2-53) to the radiative transfer equation (2-10) with the absorption coefficient (2-11) gives

$$\left[\frac{1}{\beta} \frac{\partial i_o}{\partial \tilde{y}} + \frac{\nu_o^2 \alpha}{\Lambda_o^{3/2}} \cdot \frac{\zeta_o^2 i_o}{\theta_o^{3/2} \sqrt{1 - \nu_o \zeta_o + \ldots}}\right] + \left[\frac{\delta_1}{\beta} \cdot \frac{\partial i_1}{\partial \tilde{y}} + \frac{\delta_1 \nu_o^2 \alpha}{\Lambda_o^{3/2}} \cdot \frac{\zeta_o^2 i_1}{\theta_o^{3/2}} + \right.$$

$$\left. \frac{\nu_o \nu_1 \alpha}{\Lambda_o^{3/2}} \cdot \frac{2 \zeta_o \zeta_1 i_o}{\theta_o^{3/2}} - \frac{\nu_o^2 \Lambda_1 \alpha}{\Lambda_o^{5/2}} \cdot \frac{3 \zeta_o^2 i_o \theta_1}{2 \theta_o^{5/2}}\right] + \ldots \ = \ 0 \ . \quad (2\text{-}56)$$

Note that the radical $\sqrt{1 - \nu_o \zeta_o + \ldots}$ was not expanded. This factor becomes important only if the plasma becomes overdense at some point.

The electron energy equation is found by combining (2-8) with (2-11) and (2-13),

$$\zeta \frac{\partial \theta_e}{\partial \tau} - \frac{2\theta_e}{3} \cdot \frac{\partial \zeta}{\partial \tau} + \epsilon U \left(\zeta \frac{\partial \theta_e}{\partial y} - \frac{2\theta_e}{3} \cdot \frac{\partial \zeta}{\partial y}\right) = \alpha \frac{\zeta^2 i}{\theta_e^{3/2} \sqrt{1 - \zeta}} + \text{thermal conduction and equilibration terms}$$

The thermal conduction term is not written out since its only effect is to smooth out thermal nonuniformities. The equilibration term is not written since it can only affect the electron temperature by a factor of two. Applying the expansions (2-53) to the electron energy equation gives

$$\left[\nu_o\Lambda_o\left(\zeta_o\frac{\partial\theta_o}{\partial\tau} - \frac{2}{3}\theta_o\frac{\partial\zeta_o}{\partial\tau}\right) + \frac{\nu_o^2\alpha}{\Lambda_o^{3/2}}\cdot\frac{\zeta_o^2 i_o}{\theta_o^{3/2}\sqrt{1-\nu_o\zeta_o+\ldots}}\right] +$$

$$\left[\nu_o\Lambda_1\left(\zeta_o\frac{\partial\theta_1}{\partial\tau} + \frac{2}{3}\theta_o\frac{\partial\zeta_1}{\partial\tau}\right) + \nu_1\Lambda_o\left(\zeta_1\frac{\partial\theta_o}{\partial\tau} - \frac{2}{3}\theta_o\frac{\partial\zeta_1}{\partial\tau}\right) +\right.$$

$$\frac{\xi_1\nu_o\Lambda_o\epsilon}{\beta}\left(U_1\zeta_o\frac{\partial\theta_o}{\partial\tilde{Y}} - \frac{2}{3}U_1\theta_o\frac{\partial\zeta_o}{\partial\tilde{Y}}\right) + \frac{\nu_o\nu_1\alpha}{\Lambda_o^{3/2}}\cdot\frac{2\zeta_o\zeta_1 i_o}{\theta_o^{3/2}} +$$

$$\left.\frac{\nu_o^2\delta_1\alpha}{\Lambda_o^{3/2}}\cdot\frac{\zeta_o^2 i_1}{\theta_o^{3/2}} - \frac{\nu_o^2\Lambda_1\alpha}{\Lambda_o^{5/2}}\cdot\frac{3\zeta_o^2 i_o\theta_1}{2\theta_o^{5/2}}\right] + \ldots = 0 . \quad (2\text{-}57)$$

The most general equations are found when all terms within a pair of brackets are the same order of magnitude. Then from the stationary terms, one can conclude that

$$\frac{\Lambda_o^{3/2}}{\beta\nu_o^2} = \alpha ,$$

$$\frac{\Lambda_o^{5/2}}{\nu_o} = \alpha . \quad (2\text{-}58)$$

From the motion terms, one can conclude that

$$\xi_1 = \frac{\Lambda_o}{\beta}\epsilon ,$$

$$\nu_1 = \frac{\nu_0 \Lambda_0}{\beta^2}\epsilon^2$$

$$\delta_1 = \frac{\Lambda_0}{\beta^2}\epsilon^2 ,$$

$$\Lambda_1 = \frac{\Lambda_0^2}{\beta^2}\epsilon^2 . \qquad (2\text{-}59)$$

(2-58) and (2-59) are now examined for various cases to determine the appropriate variables for the onset of motion.

For a linear gradient plasma in the bleaching wave regime, $\nu_0 = \beta = \alpha^{-1/6}$ and $\Lambda_0 = \alpha^{1/3}$ (from section C) which is consistent with (2-58). Then (2-59) leads to $\xi_1 = \alpha^{1/2}\epsilon$, $\nu_1 = \alpha^{1/2}\epsilon^2$, $\delta_1 = \alpha^{2/3}\epsilon^2$, and $\Lambda_1 = \alpha\epsilon^2$. Thus $\Lambda_1/\Lambda_0 = \alpha^{2/3}\epsilon^2$ is the parameter determining the onset of motion in this regime.

For a linear gradient plasma in the simultaneous heating regime, $\nu_0 = \beta = 1$ and $\Lambda_0 = \alpha^{2/5}$. This is consistent with the second equation in (2-58) but not the first. The reason is that the characteristic length scale predicted by the radiative transfer equation is the absorption length, which is erroneous in this case since the characteristic length is the distance to the critical density where the heating ends. Then (2-59) leads to $\xi_1 = \alpha^{2/5}\epsilon$, $\nu_1 = \alpha^{2/5}\epsilon^2$, $\delta_1 = \alpha^{2/5}\epsilon^2$, $\Lambda_1 = \alpha^{4/5}\epsilon^2$. Then $\Lambda_1/\Lambda_0 = \alpha^{2/5}\epsilon^2$ is the parameter determining the onset of motion in this regime.

For a uniform plasma, ν_0 is the specified scale of the

density (which is constant). Then (2-58) leads to $\Lambda_o = (\alpha\nu_o)^{2/5}$; $\beta = \alpha^{-2/5}\nu_o^{-7/5}$. Thus (2-59) leads to $\xi_1 = \alpha^{4/5}\nu_o^{9/5}\epsilon$, $\nu_1 = \alpha^{6/5}\nu_o^{21/5}\epsilon^2$, $\delta_1 = \alpha^{6/5}\nu_o^{16/5}\epsilon^2$, and $\Lambda_1 = \alpha^{8/5}\nu_o^{18/5}\epsilon^2$. Then $\Lambda_1/\Lambda_o = \alpha^{6/5}\nu_o^{16/5}\epsilon^2$ is the parameter determining the onset of motion for a uniform plasma.

In a linear gradient plasma, the onset of motion will occur in the simultaneous heating regime for cases of interest. In this regime the important parameter is

$$\epsilon^* = \epsilon^2\alpha^{2/5} = 2.42 \times 10^{-47}(J_o/A)^{2/5}(\nabla n_e)^2\lambda_o^4 t_p^2 \quad (2\text{-}60)$$

If $\epsilon^2\alpha^{2/5} \ll 1$, then there is no motion during the laser pulse. If $\epsilon^2\alpha^{2/5} \gg 1$, significant motion occurs.

In a uniform plasma, the important parameter is

$$\epsilon^* = \alpha^{6/5}\nu_o^{16/5}\epsilon^2 = 1.20 \times 10^{24}(J_o/A)^{-4/5}\zeta^{16/5}\lambda_o^{-4}t_p^2 , \quad (2\text{-}61)$$

where ζ has replaced ν_o since they are identical for a uniform plasma. (2-61) fails very near $\zeta = 1$ since the radical $\sqrt{1 - \nu_o\zeta_o + \ldots}$ becomes very small in that case.

2. Onset of Thermal Conduction

In developing the stationary-frozen-conducting solution for $\alpha < 5.2$ (section C), it was found that αn_e is the parameter measuring the thermal conduction. However, thermal conduction will first become dominant in regions where $\alpha > 5.2$ and a different parameter is required to determine the onset of thermal conduction.

The energy equation including thermal conduction but not

the motion or equilibration terms, is

$$\zeta \frac{\partial \theta_e}{\partial \tau} = \alpha \frac{\zeta^2 i}{\theta_e^{3/2}\sqrt{1-\zeta}} + \frac{2}{7}\eta_e \frac{\partial^2 \theta_e^{7/2}}{\partial y^2} .$$

This was found by combining (2-8), (2-11), and (2-13). With the scaling $\zeta = \nu_o \zeta_o$, $\theta_e = \Lambda_o \theta_o$, $y = \beta \tilde{y}$, the energy equation becomes

$$\zeta_o \frac{\partial \theta_o}{\partial \tau} = \frac{\nu_o \alpha}{\Lambda_o^{5/2}} \frac{\zeta_o^2 i}{\theta_o^{3/2}\sqrt{1-\nu_o \zeta_o}} + \frac{\Lambda_o^{5/2}\eta_e}{\beta^2 \nu_o} \frac{2}{7} \frac{\partial^2 \theta_o^{7/2}}{\partial \tilde{y}^2} .$$

The scales are consistent if the parameter $\nu_o \alpha / \Lambda_o^{5/2} = 1$. Then onset of thermal conduction occurs when the parameter $\Lambda_o^{5/2}\eta_e/\beta^2\nu_o$ exceeds one. Eliminating ν_o , the key parameter is $\alpha\eta_e/\beta^2$.

For a linear gradient plasma in the bleaching wave regime $\beta = \alpha^{-1/6}$ and the onset of thermal conduction is determined by the parameter

$$\alpha^{4/3}\eta_e = 3.07 \times 10^{-30} (J_o/A)^{1/2} (\nabla n_e)^{7/6} \lambda_o^{8/3} t_p . \quad (2\text{-}62)$$

If $\alpha^{4/3}\eta_e \ll 1$, there is no thermal conduction, and if $\alpha^{4/3}\eta_e \gg 1$, thermal conduction is dominant.

For a uniform plasma, consideration of (2-40) indicates that the plasma length heated is $y_{max} = 1.13\, \alpha^{-2/5}\zeta^{-7/5}$, valid for ζ less than one. Then $\beta = \alpha^{-2/5}\zeta^{-7/5}$ is the appropriate choice and the thermal conduction parameter is

$$\eta^* = \alpha^{9/5}\eta_e\zeta^{14/5} = 5.51 \times 10^{11} (J_o/A)^{-1/5} \zeta^{14/5} \lambda_o^{-2} t_p . \quad (2\text{-}63)$$

3. Onset of Electron-Ion Equilibration

The electron and ion energy equations including equilibration but not thermal conduction and motion terms, are

$$\zeta\frac{\partial\theta_e}{\partial\tau} = \alpha\frac{\zeta^2 i}{\theta_e^{3/2}\sqrt{1-\zeta}} - \lambda\frac{\zeta^2}{\theta_e^{3/2}}(\theta_e - \theta_i) ,$$
$$\zeta\frac{\partial\theta_i}{\partial\tau} = + \lambda\frac{\zeta^2}{\theta_e^{3/2}}(\theta_e - \theta_i) . \qquad (2\text{-}64)$$

With the scaling $\zeta = \nu_o\zeta_o$, $\theta_e = \Lambda_o\theta_o$, $\theta_i = \Lambda_o\theta_{o_i}$, $y = \beta\tilde{y}$ the scale of the equilibration terms in (2-64) becomes $\nu_o\lambda/\Lambda_o^{3/2}$ which is the proper scaling when the ion temperature is of the same order as the electron temperature. If however, the ions are very cold (at the initial temperature) then μ is the proper scale for θ_i . In this case the coefficient of the equilibration term in the ion energy equation becomes $\nu_o\lambda/\Lambda_o^{1/2}\mu$ which determines the ion heating.

The parameter $\lambda^*_{eq} = \nu_o\lambda/\Lambda_o^{3/2}$ determines the bounds of the equilibrium regime. If $\lambda^*_{eq} \gg 1$ there is electron-ion equilibrium. If $\lambda^*_{eq} \ll 1$ the electron and ion temperatures are not in equilibrium. The parameter $\lambda^*_{fr} = \nu_o\lambda/\Lambda_o^{1/2}\mu$ determines the bounds of the frozen regime. If $\lambda^*_{fr} \gg 1$ some ion heating takes place, though equilibrium is not assured. If $\lambda^*_{fr} \ll 1$ the ions remain frozen at their initial temperature throughout the heating.

Before calculating these parameters it is necessary to know the expression for the small temperature parameter

$\mu = T_e^o/T_o$. Using (2-1),

$$\mu = 3.0 \times 10^{35}(J_o/A)^{-1}(\nabla n_e)^{-1}\lambda_o^{-4}T_e^o , \qquad (2\text{-}65)$$

where T_e^o is in eV and the other terms are in the usual units.

In a linear gradient plasma, in the bleaching wave regime $\Lambda_o = \alpha^{1/3}$ so that the equilibration parameter is

$$\lambda_{eq}^* = \lambda/\alpha^{2/3} = 7.05 \times 10^7 (J_o/A)^{-1/2}(\nabla n_e)^{1/6}\lambda_o^{-4/3}t_p \quad \text{for } \alpha > 5.2 , \qquad (2\text{-}66)$$

In the simultaneous heating regime where $\Lambda_o = \alpha^{2/5}$,

$$\lambda_{eq}^* = \lambda/\alpha^{3/5} = 5.48 \times 10^{13}(J_o/A)^{-3/5}\lambda_o^{-2}t_p \quad \text{for } \alpha < 5.2 \qquad (2\text{-}67)$$

The freezing parameter in the bleaching wave regime is

$$\lambda_{fr}^* = \lambda/\alpha^{1/3}\mu = 67.2\,(\nabla n_e)^{1/3}\lambda_o^{-2/3}T_e^{o\,-1}t_p \quad \text{for } \alpha > 5.2 \qquad (2\text{-}68)$$

In the simultaneous heating regime the freezing parameter is

$$\lambda_{fr}^* = \lambda/\alpha^{1/5}\mu = 4.08 \times 10^{13}(J_o/A)^{-1/5}\lambda_o^{-2}T_e^{o\,-1}t_p \quad \text{for } \alpha < 5.2 \qquad (2\text{-}69)$$

In a uniform plasma $\nu_o = \zeta$ and $\lambda = (\alpha\zeta)^{2/5}$ and the equilibration parameter is

$$\lambda_{eq}^* = 5.50 \times 10^{13}(J_o/A)^{-3/5}\zeta^{2/5}\lambda_o^{-2}t_p , \qquad (2\text{-}70)$$

and the freezing parameter is

$$\lambda_{fr}^* = 4.09 \times 10^{13}(J_o/A)^{-1/5}\zeta^{4/5}\lambda_o^{-2}T_e^{o\,-1}t_p . \qquad (2\text{-}71)$$

4. Summary

The results of calculating the various parameters are shown in figures 16, 17, 18, 19 for a linear gradient plasma, and figures 20, 21, 22, 23 for a uniform plasma. The lines bounding the regimes are extended on into the conducting regime as dashed lines even though these parameters were calculated from the nonconducting point of view.

The heating of a linear gradient plasma falls conveniently into several regimes. For short plasmas (high ∇n_e) the heating is nonstationary. For slightly lower values of ∇n_e the heating is stationary and conducting. For even lower ∇n_e (longer plasmas) the heating becomes stationary and nonconducting. Equilibration effects depend primarily on the energy deposition and the pulse time rather than on ∇n_e. The solution of section B applies in the stationary-frozen-conducting regime, and the solution of section C applies to the parts of the stationary-frozen regime above the line $\alpha = 5.2$.

These solutions can also be applied to the regions where some, or complete equilibration occurs. This fact is easily seen by observing the stationary energy equations for electrons and ions, (2-64). For the frozen case, the electron energy equation governs the heating as studied in sections B and C. For equilibrium regimes, $\theta_e = \theta_i$ and the two equations combine to give,

$$\zeta \frac{\partial \theta_e}{\partial \tau} = \frac{\alpha}{2} \cdot \frac{\zeta^2_i}{\theta_e^{3/2}\sqrt{1-\zeta}}$$

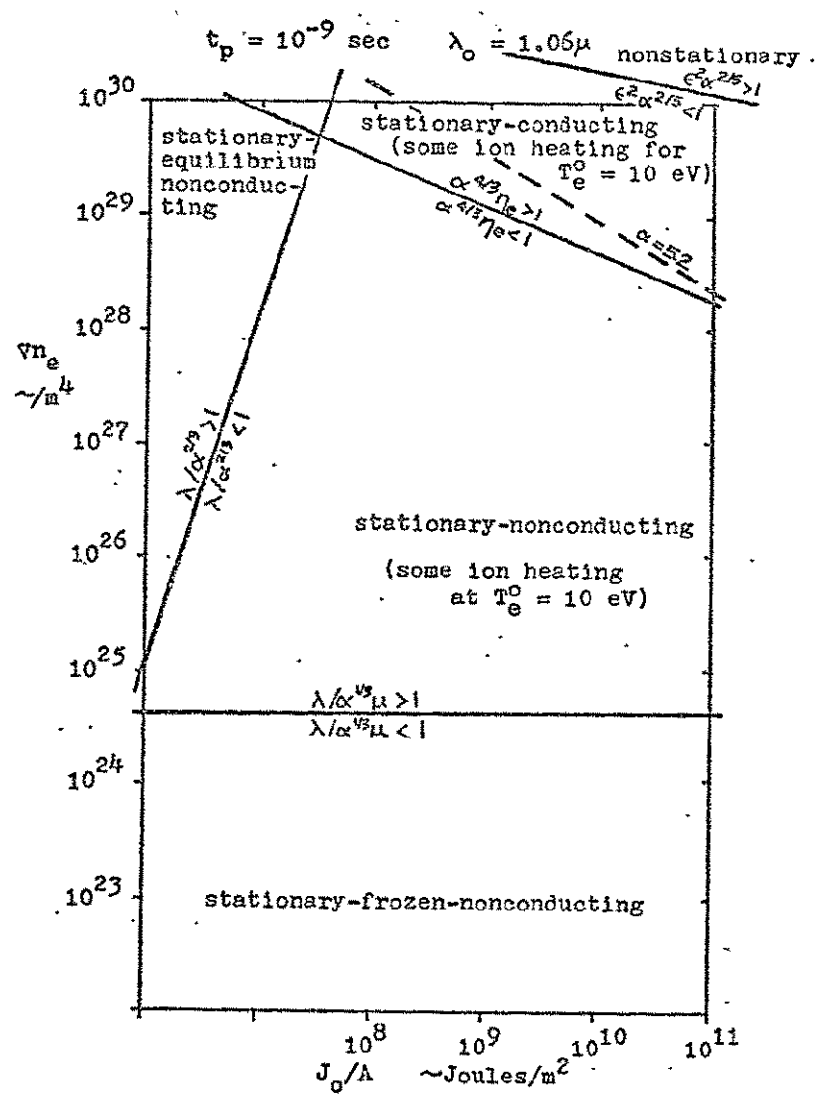

Figure 16.. Re-examined heating regimes for a nanosecond pulse from a Nd^+ glass laser

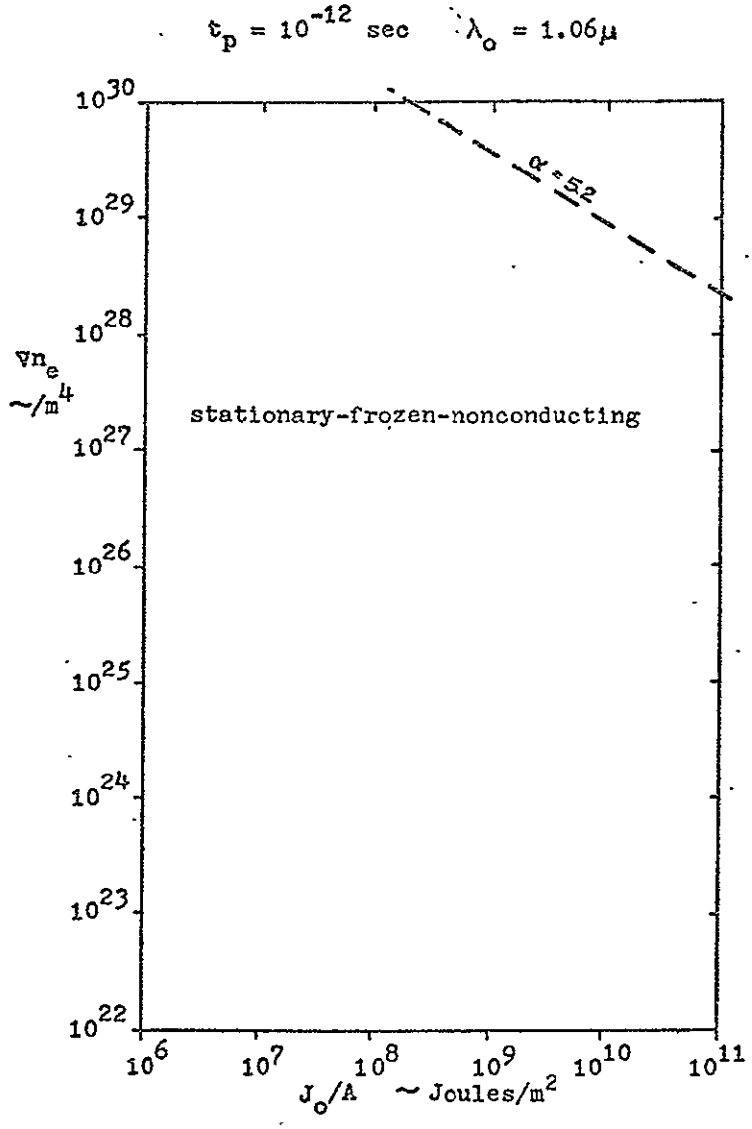

Figure 17. Re-examined heating regimes for a picosecond pulse from a Nd^+ glass laser

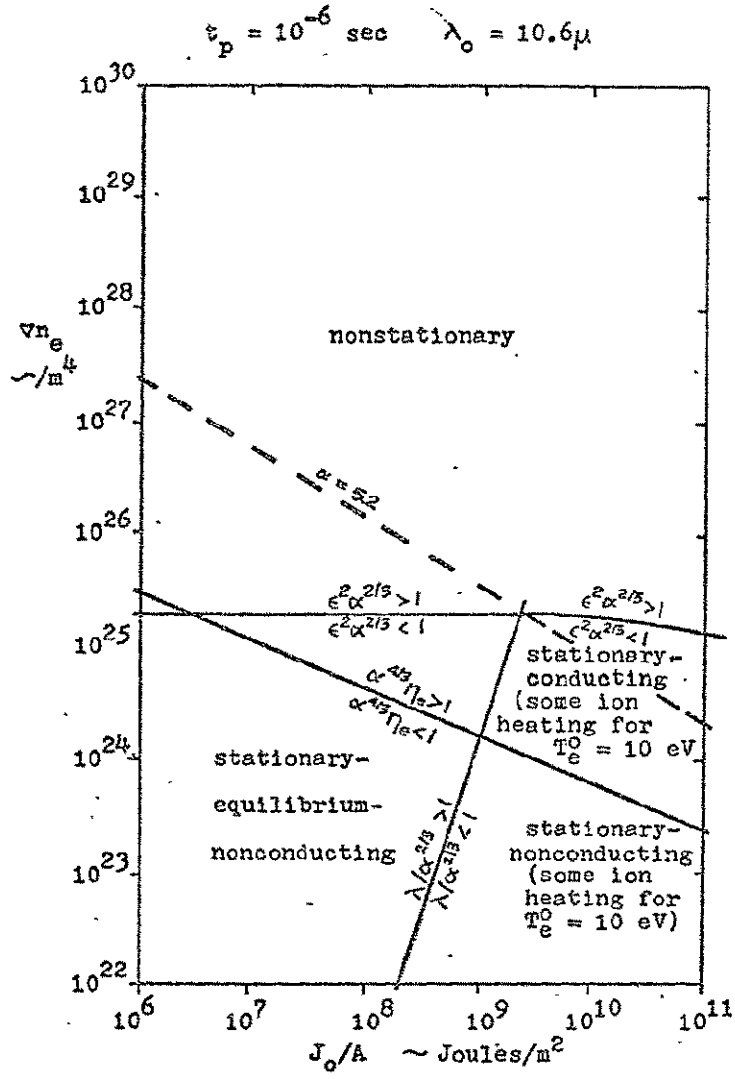

Figure 18. Re-examined heating regimes for a microsecond pulse from a CO_2 gas laser

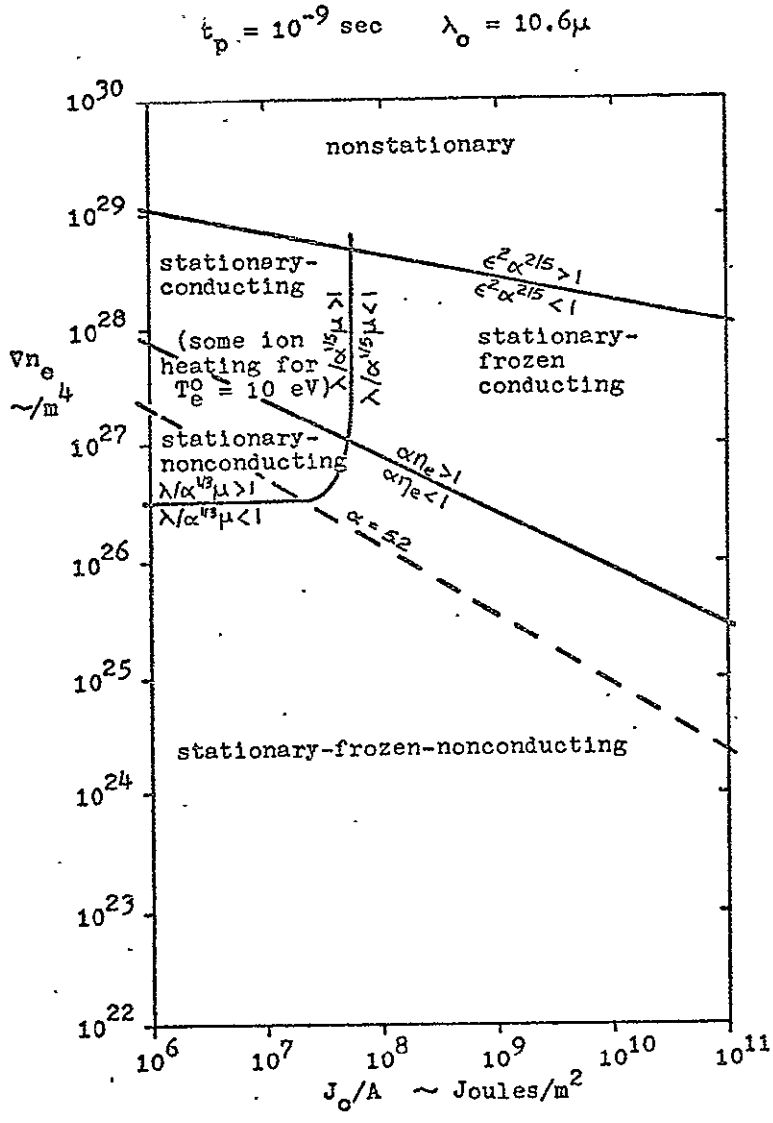

Figure 19. Re-examined heating regimes for a nanosecond pulse from a CO_2 gas laser

$t_p = 10^{-9}$ sec $\quad \lambda_o = 1.06\mu$

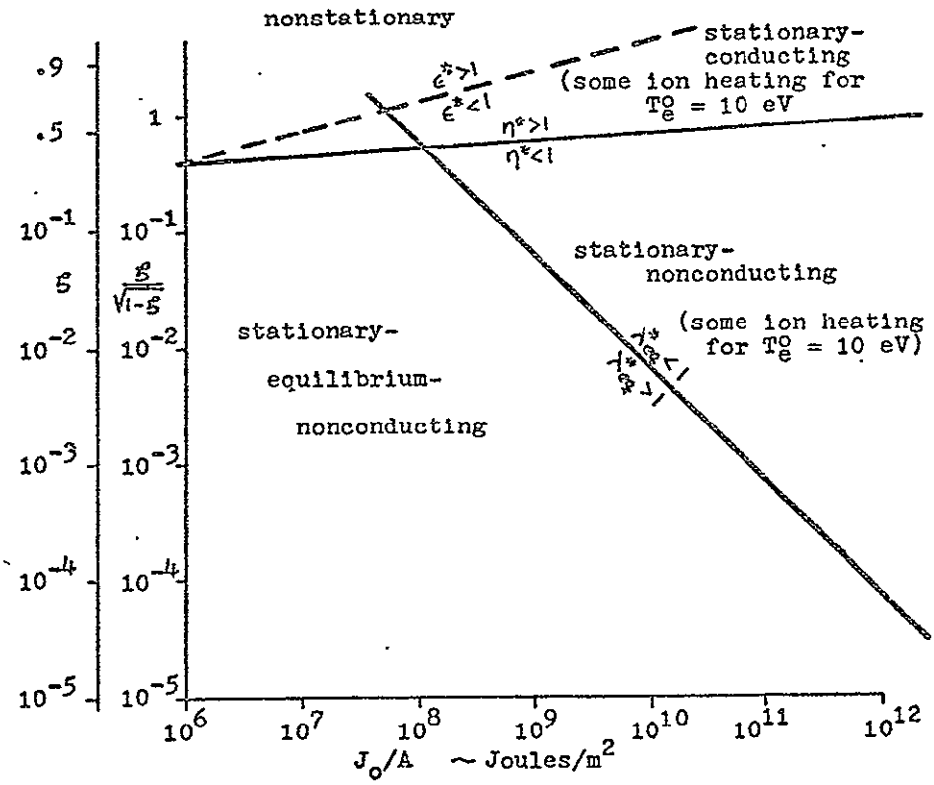

Figure 20. Heating regimes with a uniform plasma for a nanosecond pulse from a Nd^+ glass laser

$t_p = 10^{-12}$ sec $\lambda_o = 1.06\mu$

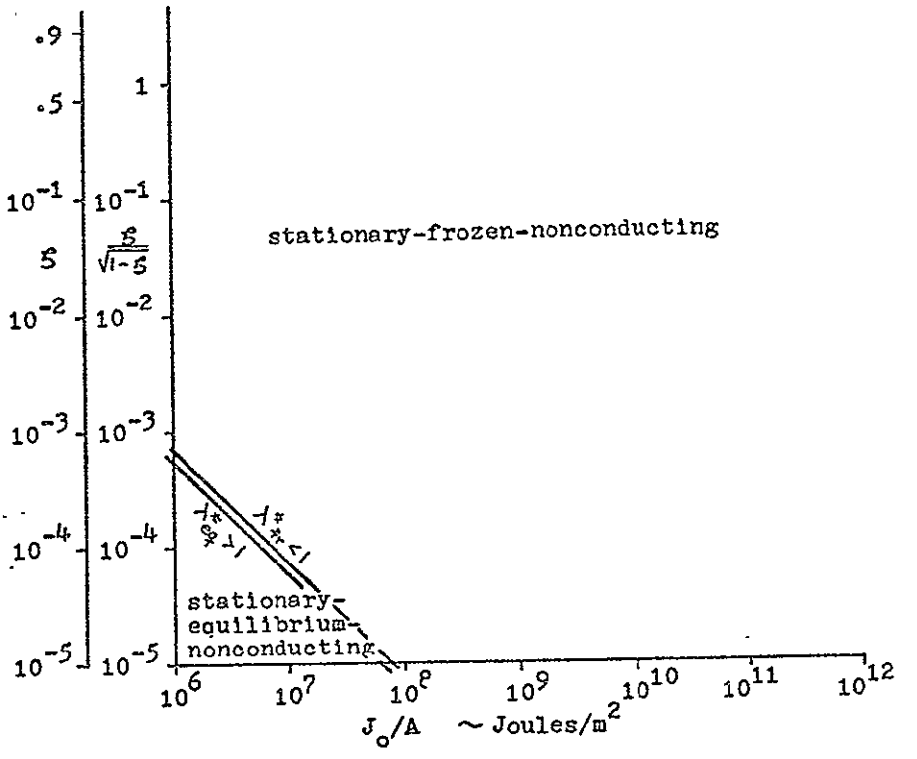

Figure 21. Heating regimes with a uniform plasma for a picosecond pulse from a Nd^+ glass laser

$t_p = 10^{-6}$ sec $\lambda_o = 10.6\mu$

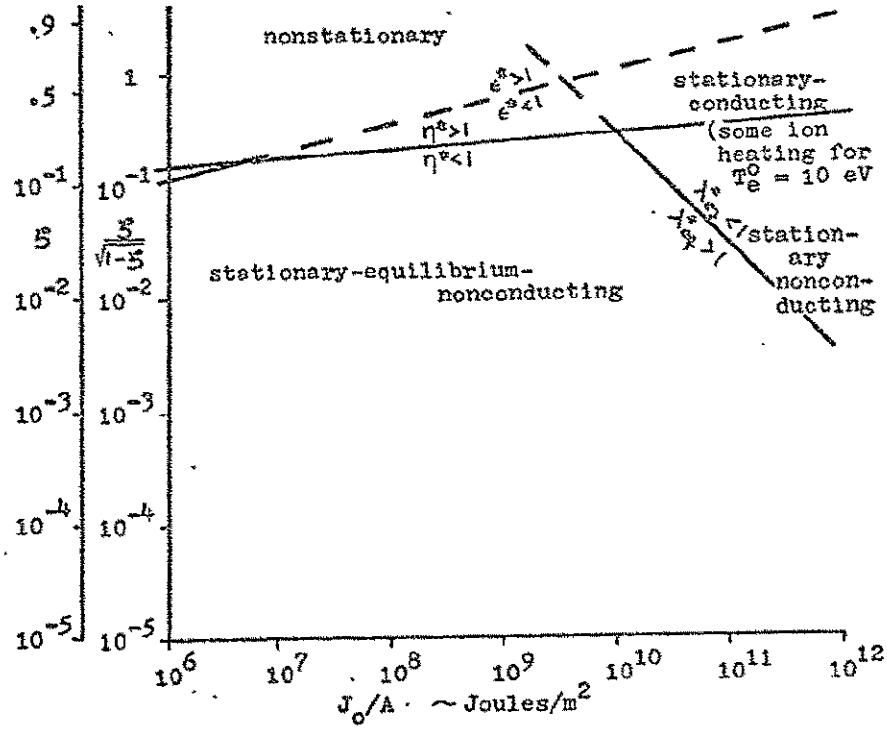

Figure 22. Heating regimes with a uniform plasma for a microsecond pulse from a CO_2 gas laser

$t_p = 10^{-9}$ sec $\quad \lambda_o = 10.6\mu$

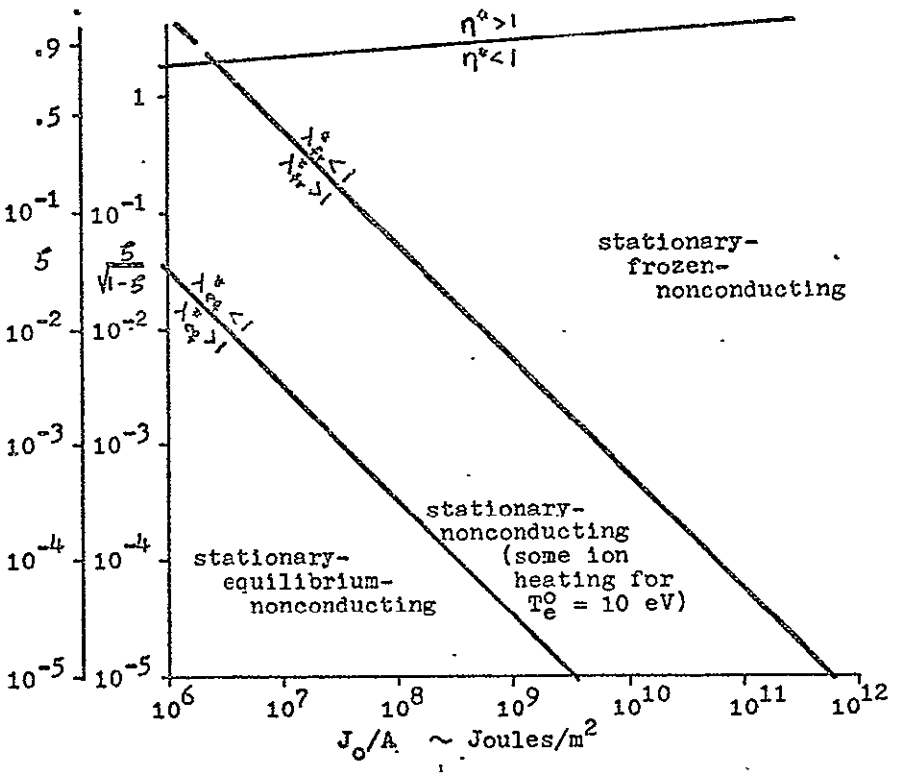

Figure 23. Heating regimes with a uniform plasma for a nanosecond pulse from a CO_2 gas laser

This is the same as the previous electron energy equation except that $\alpha/2$ has replaced α as the absorption parameter. Hence, the equilibrium solution is the same as the frozen solution except α is replaced by $\alpha/2$. If there is partial equilibration, the absorption parameter will be between $\alpha/2$ and α. A similar calculation including the thermal conduction term in the electron energy equation shows that in an equilibrium regime, the thermal conducting parameter is reduced by one half. Thus the solutions found in sections B and C apply to essentially all the nonstationary regimes.

The heating of a uniform plasma falls into the same basic regimes. For a uniform plasma, larger values of ζ correspond to shorter plasmas and vice versa. The length of the plasma is just the length that is heated. One noticeable difference of the uniform plasma from the linear gradient plasma is that even for large energy deposition, the heating may still be in an equilibrium regime for the longer pulse lengths.

As before, the solution found in section B applies in the stationary-nonconducting regimes whether equilibrium, frozen or somewhere in between. The solution of section C does not apply in the conducting regimes because there is no critical density point to cut off the radiation and limit its penetration.

No solution was developed for those conducting regimes where the critical density does not appear (such as in the uniform plasma) or where the critical density region may not

be irradiated (such as in the part of the stationary-conducting regimes below the $\alpha = 5.2$ line for the linear gradient plasma). It is expected that a wave like heating will occur in these regimes also, and the reasoning behind this is explained following. The thermal conduction will tend to move as a wave. Behind the wave is a hot transparent plasma, and ahead of the wave is a cold opaque plasma. Then the laser beam will tend to penetrate the transparent hot region and be absorbed near the front of the wave. Thus, even though thermal conduction is strong, it is expected that the speed of the "wave" will be governed primarily by the absorption of radiation in its front, i.e. as in the bleaching wave. Hence it is expected that the solution in this regime will be very similar to the stationary-frozen-nonconducting solution--both insofar as the temperatures achieved and the lengths heated. Of course, detailed phenomena of the two solutions may differ. Thus the extension of the lines for the onset of motion, freezing, and equilibration into the conducting regime in figures 17-23 is apparently justified.

E. POST-HEATING DYNAMICS

One objective of laser plasma heating is to achieve gain in a thermonuclear reaction. The general criterion for gain is governed by Lawson's criterion which is discussed in Appendix 2. Lawson's criterion requires that the product of the number density of the reactants (deuterium and tritium ions) and the time of confinement must exceed 10^{14} sec/cm^3, and the temperature must exceed 10 KeV. A certain minimum confinement time is required simply to get enough energy out of the reaction. For a CO_2 gas laser, the appropriate density would be on the order of the critical density, 10^{19}/cm^3. This calls for a confinement time of 10 μsec. For a Nd^+ glass laser, the appropriate density would be 10^{21}/cm^3. This calls for a confinement time of 100 nsec. Thus, the plasma must be contained for times significantly longer than the laser pulse that would heat it in a stationary regime. Hence, what happens to the plasma after the pulse is of critical importance.

1. Post-Heating Dynamics for a Linear Gradient

For a thermonuclear reaction to proceed at all, one condition must be met. The electrons must equilibrate with the ions before the plasma motion reduces the electron temperature and the densities. This is critically important because the thermonuclear reaction rate is strongly temperature dependent. Thus it it essential to find two time scales, the time scale for electron-ion equilibration, t_{eq}, and the time scale for significant plasma motion to arise, t_a. A third scale of

interest is the time scale for significant thermal conduction, t_{th}.

An examination of these time scales indicates that the post-heating dynamics falls into two regimes for conditions of interest. One regime is characterized by frozen-conducting dynamics, and the other by equilibrium-conducting dynamics.

a. Acoustic Time

The acoustic time is the time for an acoustic wave to traverse the heated region. The thickness of the heated region $y_{max}R$, and the maximum electron temperature, $T_{e_{max}}$ (which determines the acoustic speed using $a = 6.36 \times 10^3 \, T_e^{1/2}$ m/sec for T_e in eV), are given in section B. Then the acoustic time is

$$t_a = 2.54 \times 10^{11} (\nu n_e)^{-2/3} \lambda_o^{-2/3} \text{ sec} . \qquad (2\text{-}72)$$

This is for the bleaching wave part, $\alpha > 5.2$ since it is in this regime that the three effects, motion, equilibration and conduction, will compete.

b. Electron-Ion Equilibration Time

The correct electron-ion equilibration time corresponding to the maximum temperature and density in a linear gradient plasma is given by $t_{eq} = t_p/\lambda^*_{eq}$ (in the bleaching wave regime) where $\lambda^*_{eq} = \lambda/\alpha^{2/3}$ is the equilibration parameter calculated in section D. Then,

$$t_{eq} = 1.42 \times 10^{-8} (J_o/A)^{1/2} (\nu n_e)^{-1/6} \lambda_o^{4/3} \text{ sec} . \qquad (2\text{-}73)$$

c. Thermal Conduction Time

The thermal conduction time is the time for significant thermal conduction to diffuse accoss the thickness of the laser heated region and is given by

$$t_{th} = \frac{\rho_{max} C_v (y_{max} R)^2}{K_e} \qquad (2\text{-}74)$$

where K_e is the electron thermal conductivity given by Spitzer.[14] Applying the maximum temperature and density found in section B 3,

$$t_{th} = 3.26 \times 10^{29} (J_o/A)^{-1/2} (\nabla n_e)^{-7/6} \lambda_o^{-8/3} \text{ sec} \quad . \qquad (2\text{-}75)$$

The same result would be attained by taking $t_{th} = t_p/(\alpha^{4/3} \eta_e)$ where $\alpha^{4/3} \eta_e$ is the thermal conduction parameter found in section D.

d. Summary

The results of these calculations are presented in figures 24, and 25, for a Nd^+ glass laser and a CO_2 gas laser respectively. It is seen that post-heating behavior falls mainly into two regimes: the equilibrium-nonconducting regime where $t_{eq} \ll t_a \ll t_{th}$, and the frozen-conducting regime for which $t_{th} \ll t_a \ll t_{eq}$. In the former regime, nonconducting dynamics will occur and in the latter the dynamics will be isothermal, based on the isothermal speed of sound.

In the equilibrium-nonconducting regime, after the pulse, the temperatures equilibrate, and the subsequent motion is of an equilibrium nonconducting plasma. Thermal conduction never

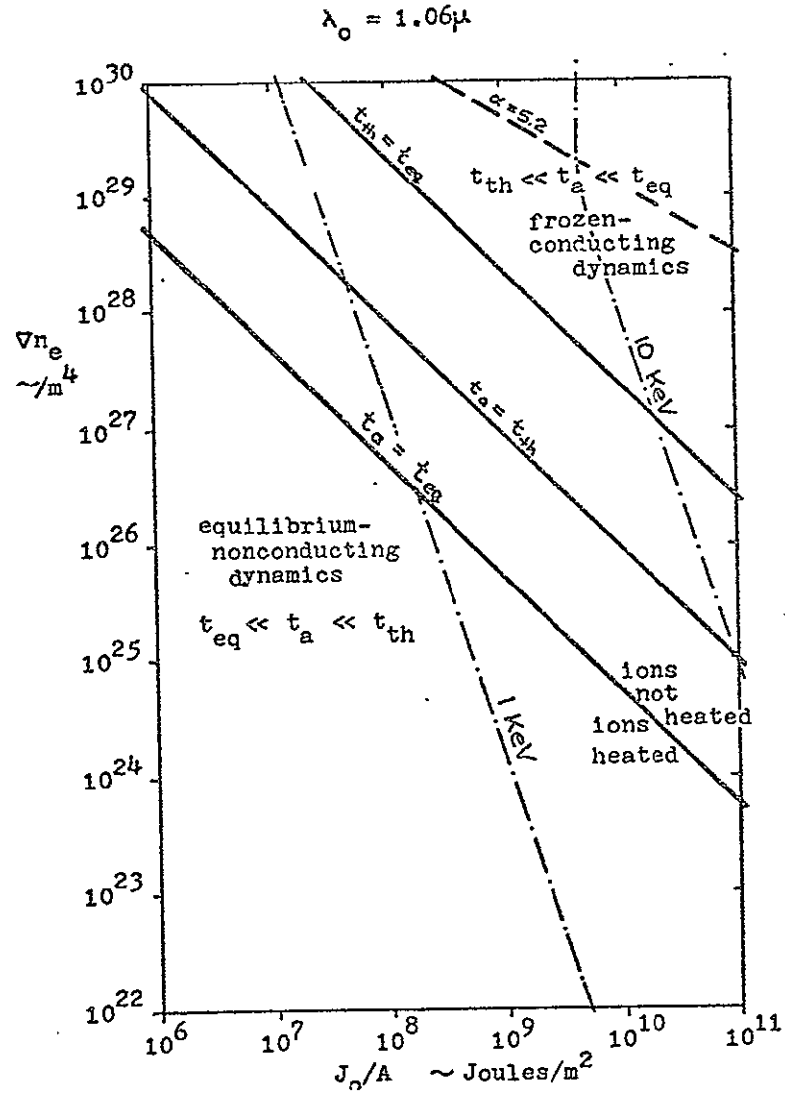

Figure 24. Post-heating dynamics for a linear density gradient plasma irradiated by a Nd^+ glass laser

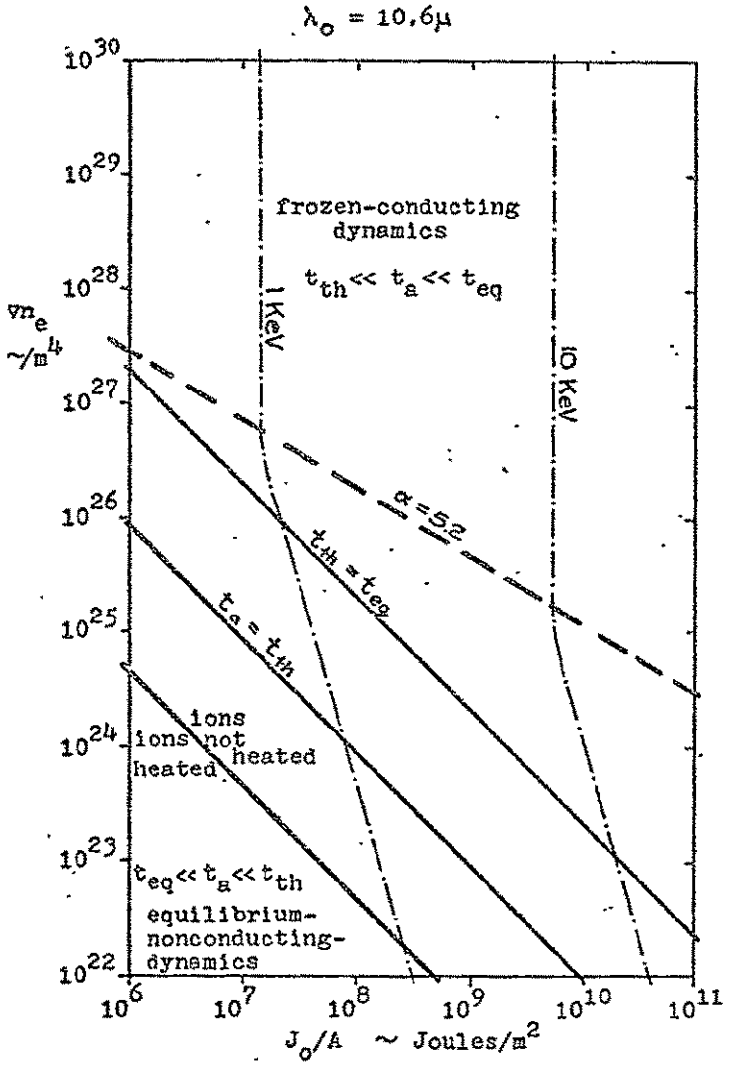

Figure 25. Post-heating dynamics for a linear density gradient plasma irradiated by a CO_2 gas laser

occurs.

In the frozen-conducting regime, after the end of the heating, strong thermal conduction smooths the nonuniformities in the temperature. Then the isothermal motion begins. Very little electron-ion equilibration occurs before the motion cools the plasma. At some point in the cooling, the equilibration time gets short enough that the ions equilibrate with the electrons--but at a much lower temperature than the original electron temperature.

Thus the issue is clear, for a thermonuclear reaction to occur during the confinement time of the plasma, the plasma must be in the equilibrium-nonconducting regime. Otherwise the ions never get heated to the temperatures required for a thermonuclear reaction. This criterion requires thicker plasmas (lower ∇n_e) , and the requirement is more stringent for greater laser energy (larger J_o/A).

2. Post-Heating Dynamics for a Uniform Plasma

In this geometry as well as the linear density gradient, the relative sizes of the equilibration and acoustic times are all important. These and the thermal conduction time from (2-74) can be easily calculated using the maximum temperature and density in a uniform laser heated plasma. The same results would be found by taking $t_{eq} = t_p/\lambda^*_{eq}$, and $t_{th} = t_p/\pi^*$. The time scales are,

$$t_a = 8.66 \times 10^{-13} (J_o/A)^{2/5} \zeta^{-8/5} \lambda_o^{\ 2} \text{ sec}$$

$$t_{eq} = 1.82 \times 10^{-14} (J_o/A)^{3/5} \zeta^{-2/5} \lambda_o^{\,2} \text{ sec} ,$$

$$t_{th} = 1.82 \times 10^{-12} (J_o/A)^{1/5} \zeta^{-14/5} \lambda_o^{\,2} \text{ sec} . \qquad (2\text{-}76)$$

The relative sizes of these time scales are presented in figure 26, along with the maximum temperature achieved (which is found by applying (2-40) to a uniform plasma). Also shown is the length of plasma heated, L corresponding to a 10.6μ CO_2 gas laser. The lengths for a 1.06μ Nd^+ glass laser are smaller by a factor of 100. The chart uses J_o/A and $\zeta/(1-\zeta)^{1/2}$ as the independent variables. A nonlinear scale for ζ is shown side by side with that for $\zeta/(1-\zeta)^{1/2}$. As with the linear density gradient, the post-heating behavior falls basically into two regimes: the same two in fact. Given a constant J_o/A, higher densities lead to frozen-conducting motion, and lower densities lead to equilibrium-nonconducting motion. This is the opposite of the natural tendency for t_{eq} to decrease with increasing density. The reason for this behavior is that for higher densities, the temperature is higher which tends to increase t_{eq} ($t_{eq} \sim T_e^{3/2}/n_e$). The temperature increase is greater than the density increase, hence the equilibriation time will be greater.

a. Wave Diagrams for a Uniform Plasma

It is appropriate to calculate a wave diagram for the motion that occurs in a uniform plasma. This calculation has been performed for a plasma in the equilibrium-nonconducting regime. This is the regime of interest for achieving a fusion

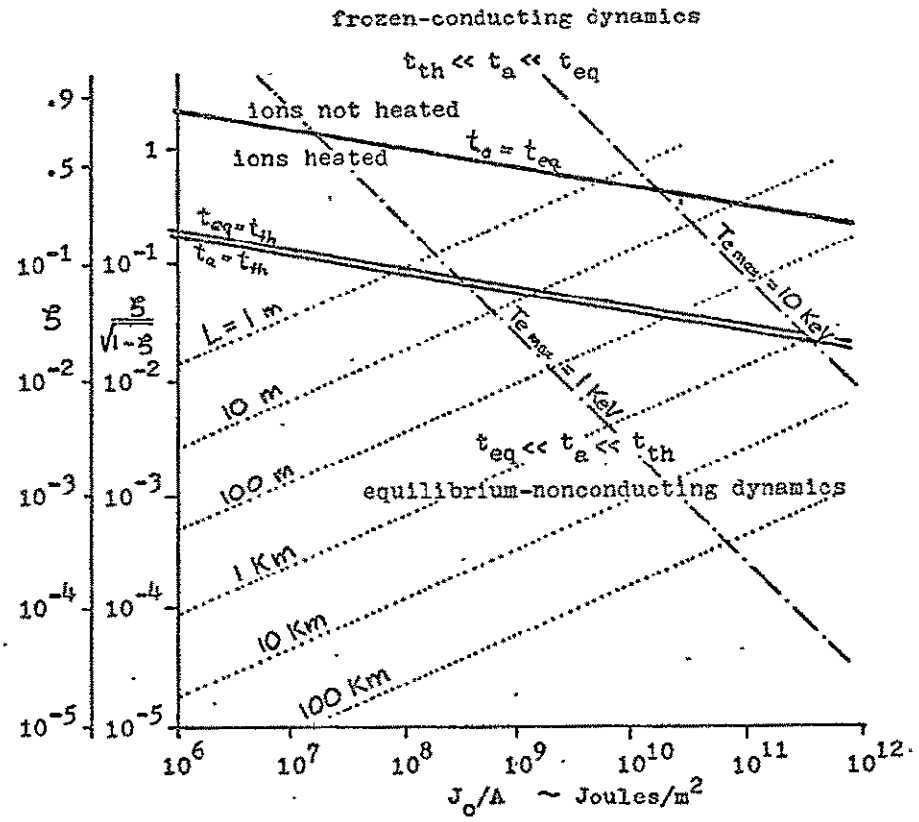

Plasma lengths are for a CO_2 gas laser.
Lengths for a Nd^+ glass laser are smaller by a factor of 100.

Figure 26. Post-heating dynamics for a uniform plasma

reaction, so this calculation will be applicable. To simplify the calculation, several assumptions were made: 1) neither thermonuclear energy release not bremsstrahlung alters the dynamics, 2) the temperature profile produced by laser heating was taken to be uniform at the average heated value, $\overline{T}$. The initial temperature was taken to be 1/100 of $\overline{T}$. The results of this calculation are presented in figure 27 which is the wave diagram, and figure 28 which shows the temperature profiles for successive times.

It is seen that the plasma expands freely into the vacuum at the plasma edge. A shock tube like phenomena occurs at the inner edge of the heated region. An expansion wave moves into the hot plasma and a shock wave moves into the unheated plasma. The shock wave heats the cold plasma to only 12% of the temperature of the laser heated region.

A similar calculation was performed for a uniform plasma with a solid wall at the inner edge of the heated region. Physically this corresponds to a plasma heated from both ends, designed so that the bleaching waves just meet in the center at the end of the laser pulse. The wave diagram for this case is shown in figure 29.

b. Release of Thermonuclear Energy

The usual estimate of thermonuclear energy release is to assume the plasma reacts at its initial temperature for exactly one acoustic time. Of course this is not the case because the temperature begins to reduce from the very beginning, and

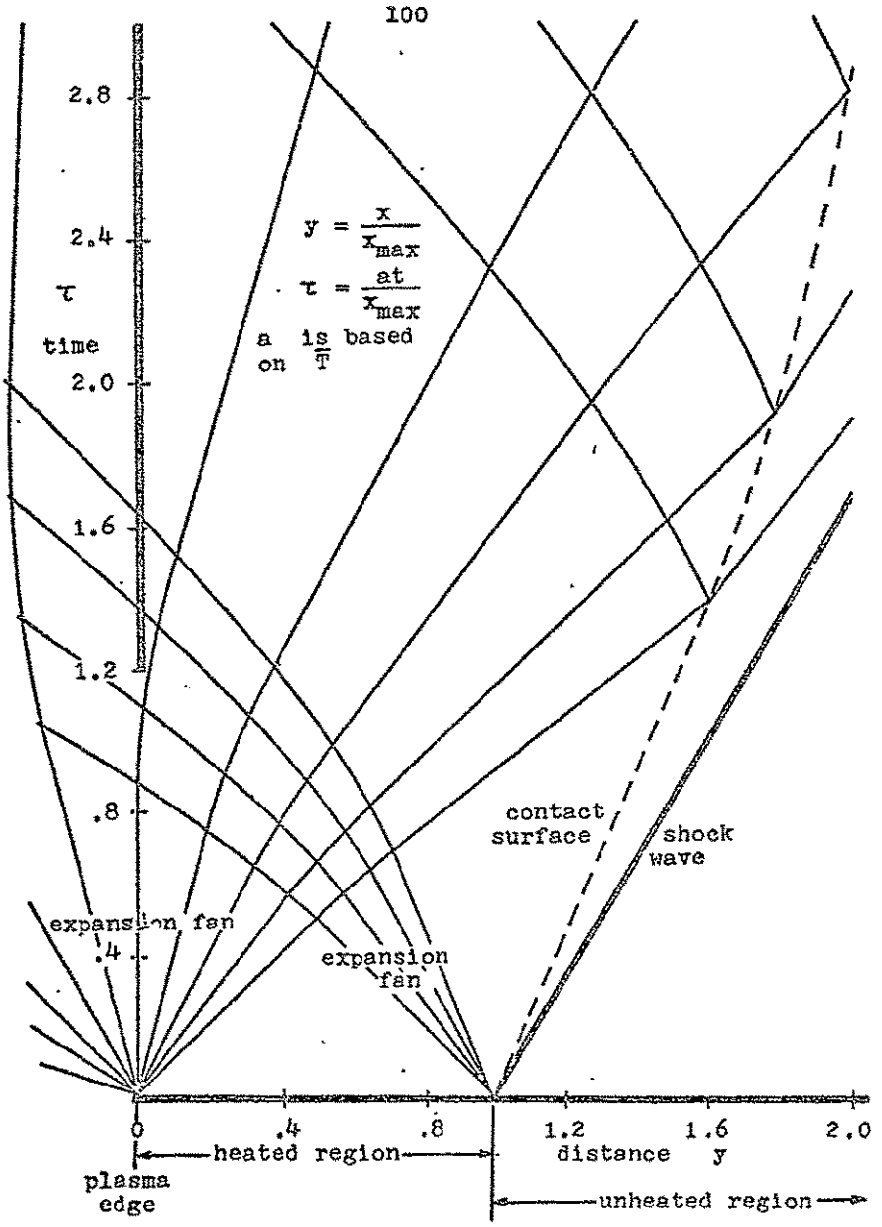

Figure 27. Wave diagram for a laser heated uniform plasma

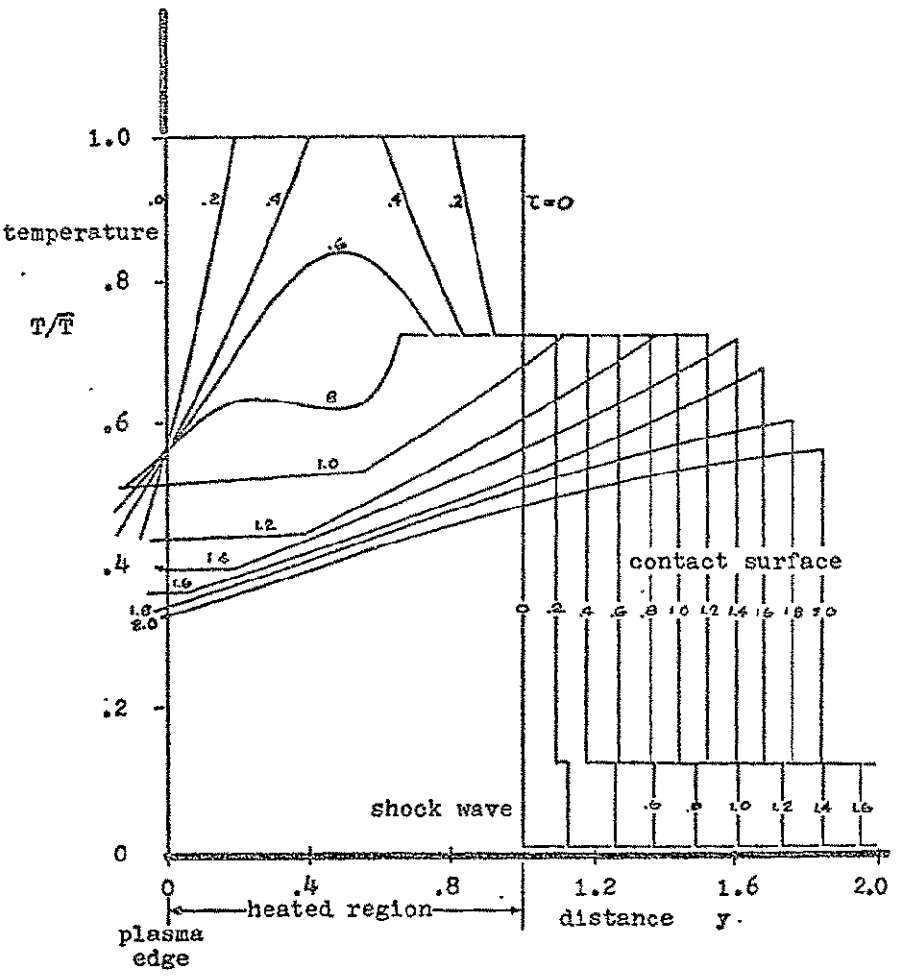

Figure 28. Temperature profiles

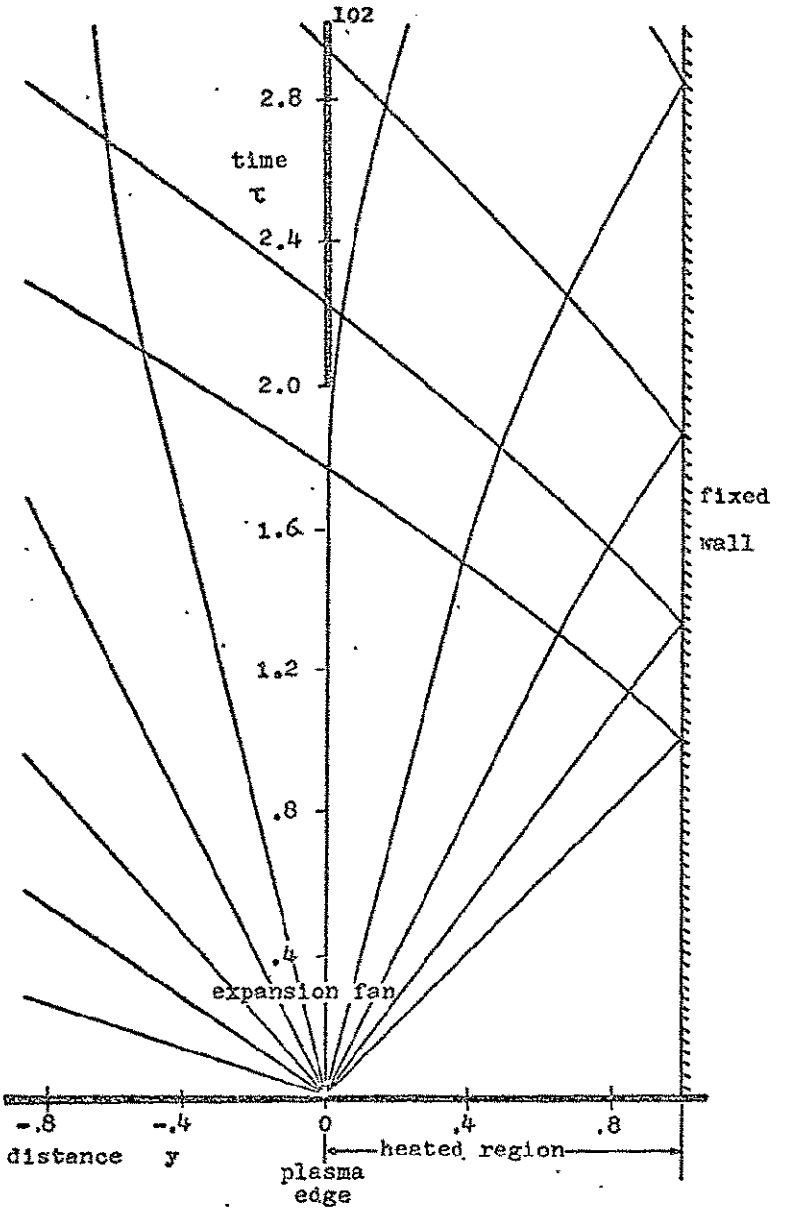

Figure 29. Wave diagram for a laser heated uniform plasma confined at the inner edge of the heated region

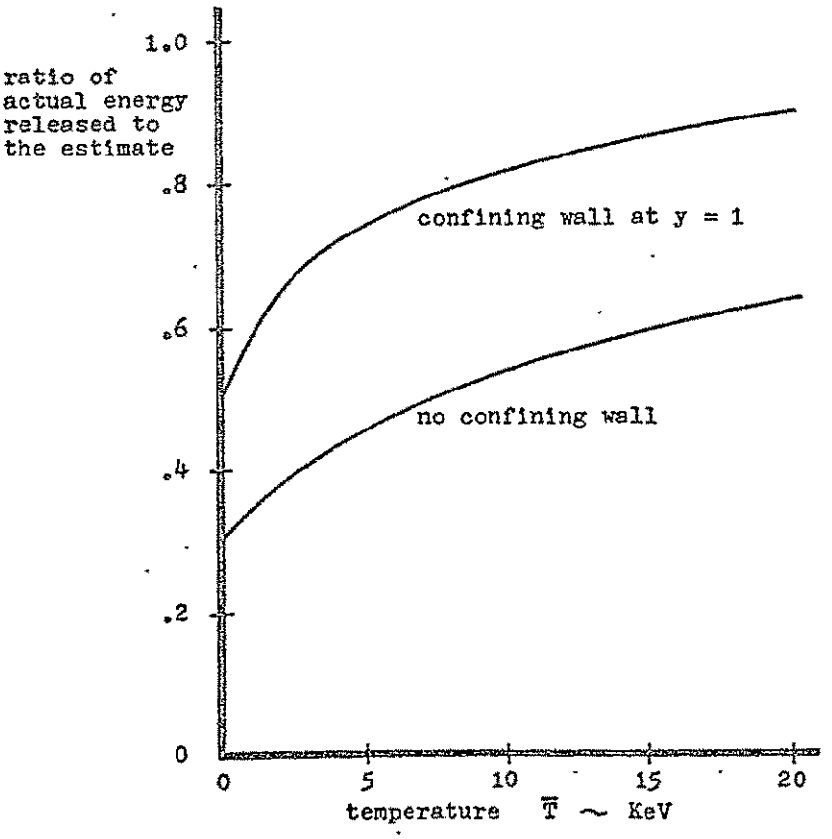

Figure 30. Comparison of thermonuclear energy release to the usual estimate

it does not cool abruptly at exactly one acoustic time. It is worthwhile then to use the solutions of motion in figures 27 and 29 to compare the actual release of thermonuclear energy to the estimate.

This calculation was performed assuming the results of the wave diagrams. The result is shown in figure 30. The ratio of the actual energy released by the D-T reaction per unit cross sectional area, E_{DT}, to the estimate of the same, $(E_{DT})_o$, is plotted versus the mean temperature to which the plasma is heated, $\overline{T}$. The actual energy release is lower than the estimate by only by 50% at 10 KeV (or 20% for the case of a confining wall at the inner edge of the heated region).

4. Summary

An examination has been conducted of the plasma dynamics following laser heating in a stationary regime. Post heating dynamics will appear in one of two regimes. Frozen-conducting dynamics will occur for denser plasmas (since higher densities lead to higher temperatures). In this regime, the electrons never equilibrate with the ions before motion dissipates and cools the plasma. No thermonuclear energy is released in this regime. For lower plasma densities, equilibrium-nonconducting dynamics occur. Here, the electrons equilibrate with the ions before the motion and thermonuclear energy is released if the initial temperature is high enough. The usual estimates of thermonuclear energy released are accurate to within a factor of two or better for 10 KeV temperatures.

F. APPENDICES

Appendix 1

Effect of Electromagnetic Forces

The primary thrust of this chapter is laser heating of a stationary plasma. Hence the effect of forces on the plasma does not appear in the solutions. Nevertheless, the size of the forces will affect the regime of validity of a stationary solution. The object of this section is to consider the size of the electromagnetic force that was included in neither the original equations, nor in any discussion of the regimes of validity.

Electromagnetic forces are proportional to the intensity of radiation. Thermal forces (pressure) are proportional to the time integral of the intensity since absorption builds the temperature and pressure with time. Thus it is possible with a sufficiently high intensity to have an electromagnetic force larger than the thermal force. But even a large force may have little effect if it operates for only a very short time. The largest electromagnetic forces will arise in picosecond laser pulses--which have the shortest duration as well. Thus the ratio of the two forces does not determine their relative importance. One must find the actual effect on the plasma motion. Previous investigations of electromagnetic forces have been made. Hora[18,19] discussed the electromagnetic forces associated with the radiation and drew some conclusions relating to its effect on plasma motion. Lindl and Kaw[20] studied

the effects of these forces when the radiation is not necessarily normal to the surface of the plasma. However, these two papers do not determine the relative effects of electromagnetic and thermal forces for typical laser produced plasmas. In this appendix, it is shown that electromagnetic forces have little effect on plasma motion in the stationary heating regimes with one exception, the case of a picosecond pulse with a CO_2 gas laser.

a. Calculation of Electromagnetic Forces

The dispersion relation for electromagnetic radiation subject to inverse-bremsstrahlung abosrption is,

$$\tilde{n} = n - ik = \left[1 - \frac{\omega_p^2}{\omega^2 + 1/\tau^2} - \frac{1}{\omega\tau}\frac{\omega_p^2}{\omega^2 + 1/\tau^2}\right]^{1/2} ,$$

where $\tilde{n}$ is the complex index of refraction, ω and ω_p are the laser and plasma frequencies respectively, and τ is the electron-ion collision time. For a sufficiently slow variation in the index of refraction, the approximation of geometrical optics can be used.[21]

The Lorentz force density can be written in terms of the Maxwell stress tensor and the Poynting vector. Following Hora, this force is,

$$\vec{f}_{em} = -\hat{i}_1 \frac{\partial}{\partial x}\frac{1}{2}(\epsilon E^2 + \mu H^2) - \frac{1}{c^2}\frac{\partial}{\partial t}\vec{E} \times \vec{H} ,$$

for a one-dimensional plasma with a density variation in the x direction with a plane electromagnetic wave traveling in the

+ x direction.

Only the time averaged value (over a few oscillations) of the force density is considered. Also, the time average of the Poynting term will be negligible for laser pulses much longer than the period of the wave. Then the time averaged force is,

$$\vec{f}_{em} = \hat{i}_1 \frac{\varepsilon E_o^2}{4} \frac{\partial}{\partial x} e^{-k}\left[(\mathrm{Re}\ \tilde{n}^{-1/2})^2 + (\mathrm{Re}\ \tilde{n}^{1/2})^2 + (\mathrm{Im}\ \tilde{n}^{-1/2})^2 + (\mathrm{Im}\ \tilde{n}^{1/2})^2 \right] ,$$

where k represents the damping of the wave,

$$k = 2\frac{\omega}{c}\int_0^x K\, dx$$

and E_o is the amplitude of the electric field of the radiation entering the plasma. $1/\omega\tau$ will be small for plasmas irradiated with a laser beam in the visible or longer wave lengths for a temperature greater than about 20 eV. The amplitude of the electric field is simply related to the intensity--and to the terminology introduced in section A,

$$\frac{\varepsilon E_o^2}{2} = \frac{I}{c} = \frac{J_o/A}{ct_p}\phi' ,$$

where $\phi' = d\phi/d\tau$. Moreover, the solution to the radiative transfer equation (10) is,

$$i = \phi' e^{-k}$$

Hence, the magnitude of the time averaged electromagnetic force is,

$$\bar{f}_{em} = \frac{J_o/A}{2Rct_p} \frac{\partial}{\partial y}\left[i\,(1/n + n) + \ldots\right]$$

where

$$n = (1-\zeta)^{1/2} + O[1/(\omega\tau)^2] \qquad (2\text{-}77)$$

In the stationary-frozen-conducting regime, in which $i = \phi'[1+O(\alpha^{2/5})]$,

$$f_{em} = \frac{J_o/A}{4Rct_p}\,\phi' \frac{\zeta}{(1-\zeta)^{3/2}} \frac{d\zeta}{dy} \qquad (2\text{-}78)$$

The apparent singularity at the critical density is not a real one since the expression used for the index of refraction (2-77) fails near that point. The stationary-frozen-conducting regime is presented since it is in that regime, if at all, that electromagnetic forces may be important.

b. Calculation of Thermal Forces

The thermal force density is simply the pressure gradient ∇p . Assuming the contribution of the cold ions to the pressure is negligible, the thermal force is,

$$|\nabla p| = \frac{\partial}{\partial x}\,(n_e k T_e) = \frac{2}{3}\,\frac{J_o/A}{R^2}\,\frac{\partial}{\partial y}\,(\zeta\theta_e)$$

In the stationary-frozen-conducting solution from (2-52),

$$|\nabla p| \cong \frac{2}{3}\,\frac{J_o/A}{R^2}\,(\tfrac{5}{2}\,\alpha\phi)^{2/5}\,\frac{d\zeta}{dy}$$

where the ratio of the two integrals in (2-52) was left out for brevity. This ratio is of order one if the dark part of the plasma is roughly the same size as the light part.

c. Comparison of Thermal and Electromagnetic Forces

The ratio of the forces is,

$$f_{em}/|\nabla p| = \left[R/ct_p(\tfrac{5}{2}\,\alpha)^{2/5}\right]\left[\frac{\dot{\varphi}'}{\dot{\varphi}^{2/5}}\right]\left[\frac{8-\frac{3}{2}\zeta}{\zeta^{2/5}(1-\zeta)^{3/10}(7-2\zeta)}\right]. \quad (2\text{-}79)$$

The first part of the expression, $R/ct_p(5/2\ \alpha)^{2/5}$, gives the order of magnitude of the ratio. The second part, $\dot{\varphi}'/\dot{\varphi}^{2/5}$ gives the time variation and is generally of order one or less. The third part, a complex function of ζ, gives the spatial variation, and it is of order one except near the critical density, $\zeta = 1$, where there is an apparent singularity. This is not a real singularity of course since the expressions used to derive (2-79) breakdown near the critical density. It is clearly seen that--holding other things constant--it is possible to make $\bar{f}_{em}/|\nabla p|$ as large as one wants if the pulse time t_p is made small enough.

The first factor is in the usual terminology,

$$R/ct_p(\tfrac{5}{2}\,\alpha)^{2/5} = 1.15 \times 10^{-17}(J_o/A)^{3/5}\lambda_o^{2}t_p^{-1}.$$

Given λ_o, t_p, then when J_o/A is larger than a certain value, the factor will exceed one. This gives the approximate size of J_o/A for which electromagnetic forces exceed thermal forces. The table below shows these values of J_o/A for typical pulses and wave lengths.

t_p / λ_0	1 nsec	1 psec
1.06 μ	1.6×10^{13}	1.6×10^{8}
10.6 μ	7.4×10^{9}	7.4×10^{4} joules/m^2

Clearly then, the electromagnetic forces will exceed the thermal forces for values of J_0/A well within the range of interest to laser plasma heating.

It is established then that electromagnetic forces may well exceed thermal forces. But this does not mean that they will have a major effect on the plasma motion, especially since the largest electromagnetic forces occur in the pulses of shortest duration. The real measure of their effect must be based on the total motion they generate.

d. The Overall Effect of Electromagnetic Forces

When a force acts on an object for a certain length of time, the object attains a certain velocity. Then the effect of electromagnetic forces is to impart a certain velocity to individual particles of the plasma. If that velocity is small compared to the local acoustic speed, a , then the effect of electromagnetic forces on the subsequent motion is small. If that velocity is of the same order or larger than a , then the electromagnetic forces strongly affect the motion.

A calculation is made of the velocity, V_{em}, generated in a nonuniform plasma by electromagnetic forces. For simplicity, it is assumed that only electromagnetic forces operate, and that each individual particle is accelerated by the force for the time t_p. The effect of any motion during the laser pulse on f_{em} is neglected. The calculation uses as the equation of motion,

$$\rho \frac{dV_{em}}{dt} = f_{em} \tag{2-80}$$

Integrating (2-80) from $t = 0$ to $t = t_p$ using f_{em} from (2-78) and an acoustic speed based on the stationary-frozen-conducting solution, the ratio of the electromagnetic to the acoustic velocity is found,

$$\frac{V_{em}}{a} = \left[\frac{J_o/A}{4m_i c n_{ec} R a_o (\frac{5}{2}\alpha)^{2/5}} \right] \left(\frac{d\zeta}{dy} \frac{1}{(1-\zeta)^{7/5} \zeta^{1/5}} \right), \tag{2-81}$$

where a_o is the acoustic speed based on the temperature T_o. The size of V_{em}/a is roughly the size of the term in brackets and is given in figures 31 and 32 for a Nd^+ glass laser and a CO_2 gas laser respectively.

It is recognized that the spatial variation given by the term in parenthesis may be much larger than one in two places, near the plasma edge, $\zeta = 0$, and near the critical density $\zeta = 1$. The motion near $\zeta = 0$ will be dominated by the dynamics of the adjacent denser parts of the plasma. The electromagnetic force does seem to have a significant effect near

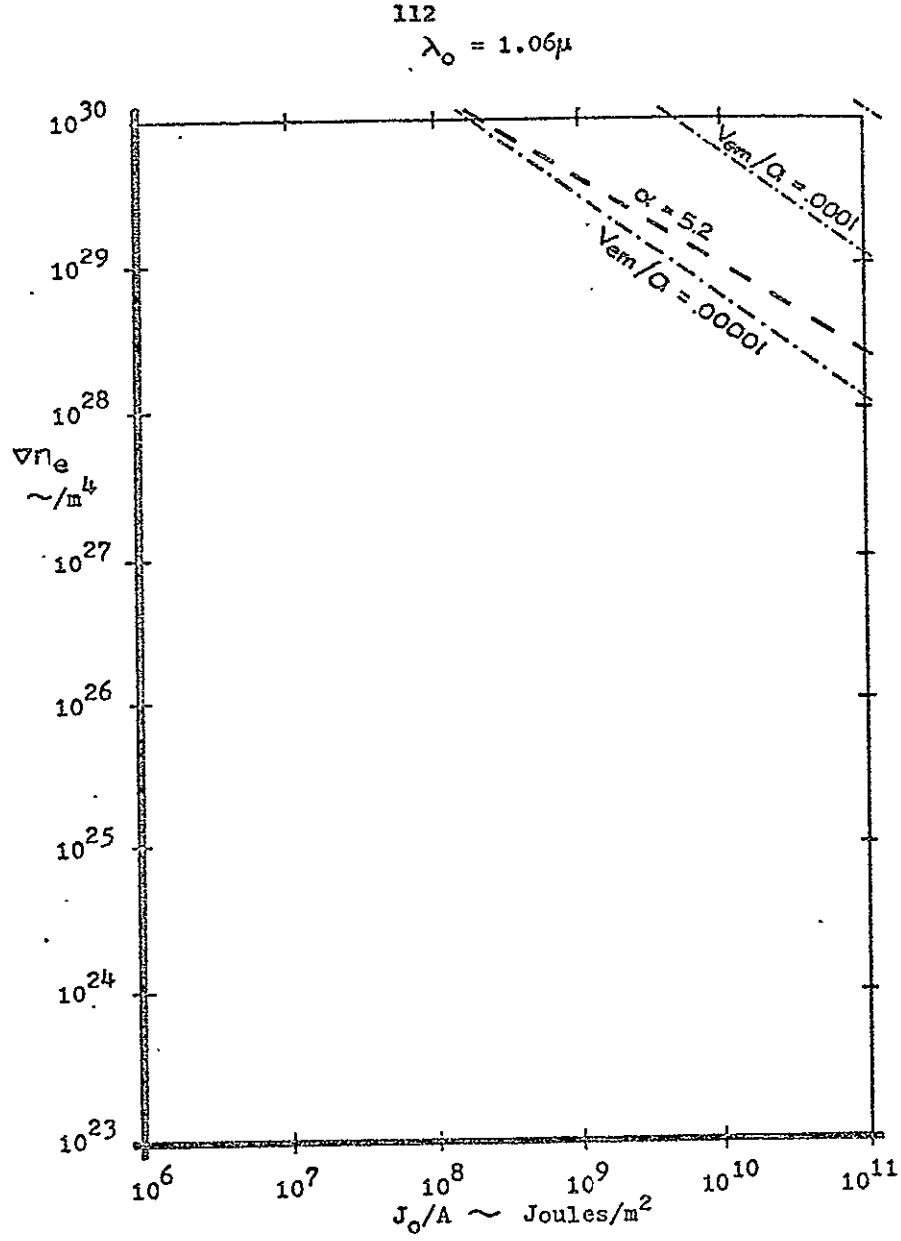

Figure 31. Electromagnetically generated velocities for a Nd^+ glass laser

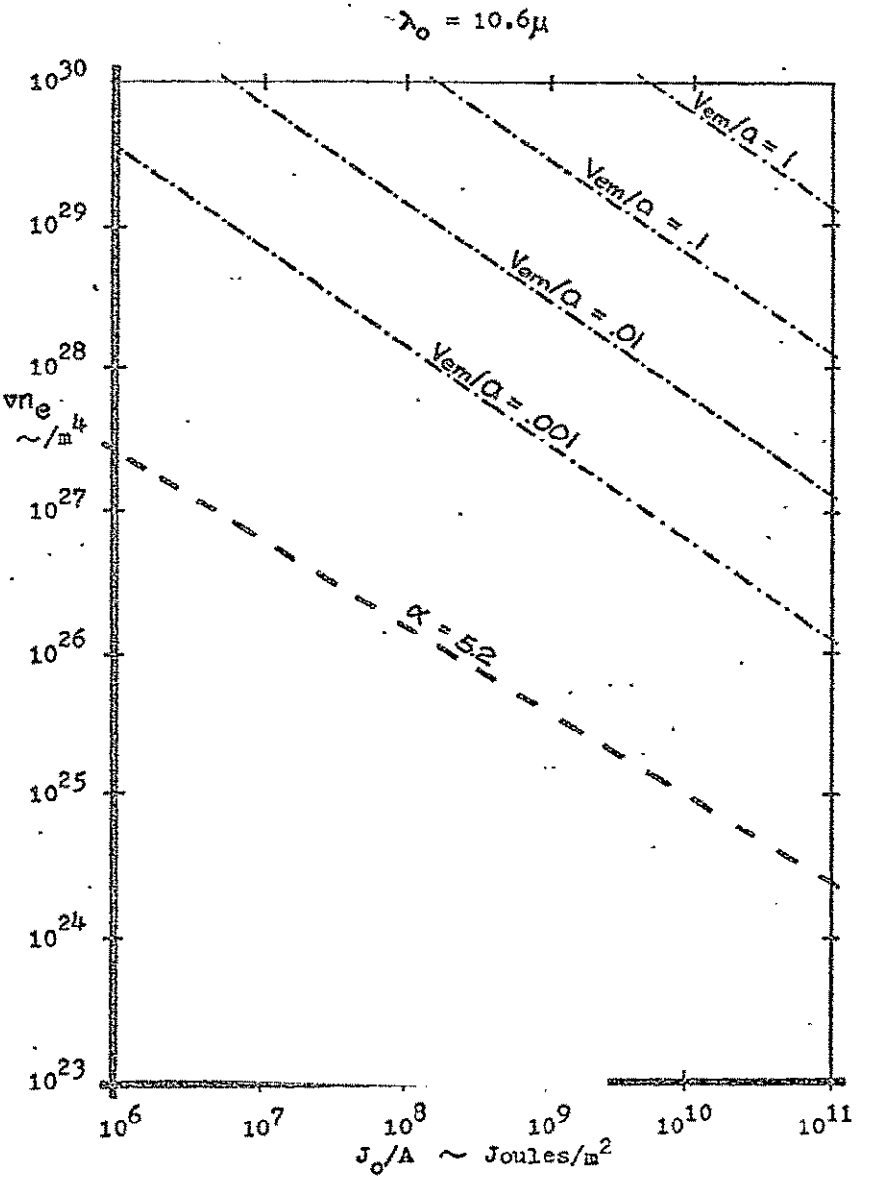

Figure 32. Electromagnetically generated velocities for a CO_2 gas laser

$\zeta = 1$ though, but the presence of anomalous absorption effects in this neighborhood will likewise generate high thermal forces which may well be more important. The anomalous absorption effect has been studied theoretically by Krüer et al.[16] and was seen to appear in an earlier experiment by Gekker and Sizukhin.[17]

The comparison of figures 31 and 32 with figures 16, 17, 18, and 19, the re-examined regime charts shows the regimes in which electromagnetic forces become important. It is seen that v_{em}/a becomes of order one only in a heating regime that is already nonstationary and hence not of interest to the problem of stationary laser plasma heating. The one exception is a picosecond pulse with a CO_2 laser where electromagnetic forces become important at the edge of the stationary-frozen-conducting regime. But even then the nonstationary regime is only extended slightly.

Appendix 2

The Lawson Criterion for Heating a Uniform Plasma

The focus of laser plasma heating as described in this work is to achieve a thermonuclear reaction that releases more energy than required to generate it, i.e., the achievement of gain. Thus it is appropriate to conclude this chapter with pertinent statements regarding the achievement of gain.

The standard requirement for gain in a pulsed reactor is known as the Lawson criterion.[3] The Lawson criterion is that the product of the number density of the reactants (equal parts Deuterium and Tritium) and the confinement time must

exceed 10^{14} sec/cm^3, and that the temperature of the reactants exceed 10 KeV,

$$nt > 10^{14} \text{ sec/cm}^3 \tag{2-82}$$

$$T_i > 10 \text{ KeV} \tag{2-83}$$

Physically this means that a sufficiently dense D-T plasma must react for a long enough time at a high enough temperature in order to release more energy than went into heating the plasma. The beauty of the Lawson criterion is seen by its very simplicity--and by its applicability to most any scheme or geometry. Of course, when the design stage is approached, a more exacting criterion will be needed to take into account the details of the thermonuclear reactor. For the analysis of a laser heated plasma the confinement time t is taken to be the ordinary acoustic time, t_a, from (2-76). The number density of the reactants is $n_i = n_e = 1.116 \times 10^{21} \varsigma/\lambda_o^2$ /cm^3. Thus the first part, (2-82) of Lawson's criterion becomes,

$$J_o/A > 3.60 \times 10^{12} \left(\frac{\varsigma}{\sqrt{1-\varsigma}} \right)^{3/2}$$

The second part, (2-83), of Lawson's criterion is that the ion temperature exceed 10 KeV. This is true if the electron temperature exceeds 10 KeV, and if there is electron-ion equilibrium, $t > t_{eq}$, (2-70). These are presented in figure 33 where the various requirements are plotted against laser energy per unit area, J_o/A, and the density, ς.

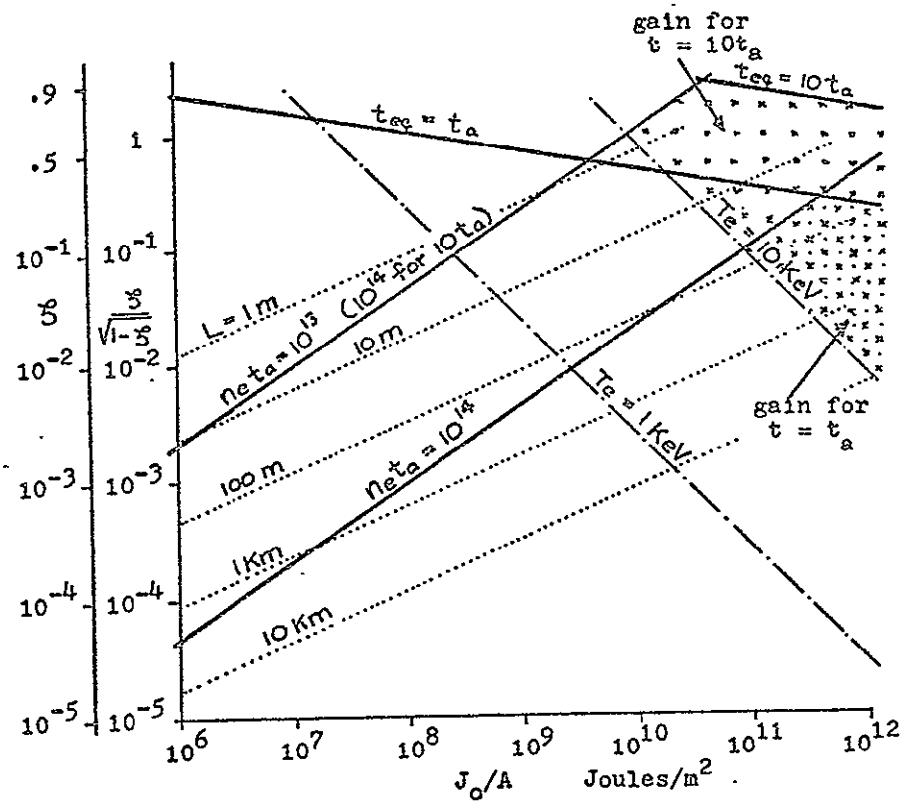

Figure 33. Lawson's criterion for a uniform laser heated plasma

The first part of Lawson's criterion requires ζ to be below the line $nt = 10^{14}$. The second part requires ζ to be below the line $t_a = t_{eq}$ and above the line $T_e > 10$ KeV. Lines are also shown supposing that the confinement time is ten acoustic times.

The minimum energy for achieving gain is 10^{11} Joules/m^2, large but probably feasible for future lasers. The corresponding density is $0.1n_{ec}$ and the plasma length is 60 m. For a CO_2 gas laser this corresponds to $n_e = 10^{18}$ cm^{-3}. A magnetic field of about a megagauss would be required to contain such a plasma. This is a large magnetic field, but not beyond possibility for the future. A 60 m length for such a magnetic field is a major engineering project to be sure.

If it were possible by some technique to confine the plasma for ten acoustic times (by a magnetic mirror effect possibly), then the minimum energy needed reduces to about 10^{10} Joules/m^2, corresponding to a density of 5×10^{18} for a CO_2 gas laser. The confining magnetic field needed is only increased by a factor of two, and the plasma length is a very reasonable 60 cm. This is an attractive possibility if the 2 MG magnetic field together with the enhanced confinement can be attained.

Appendix 3

Effect of Z-Doping on Lawson's Criterion

One of the characteristics of laser heating with a long wave length laser (such as the 10.6μ CO_2 gas laser) is a fairly long absorption length. A long absorption length

requires that the plasma volume be large and thus the laser energy required will also be large.

A possible solution to the problem of unwieldy absorption lengths has been suggested by Dawson,[22] and that is to dope the D-T plasma with an impurity having a high atomic number. The presence of the "high Z" impurity will increase the electrons significantly and thus increase the electron-ion collision time τ. Increasing τ shortens the absorption length. Specifically, the absorption length is proportional to $1/Z^{2/5}$ where Z is the effective atomic number of the ions. $Z = 1$ for a pure D-T plasma. It is appropriate then to examine the Z-doping approach in the light of achieving gain in a thermonuclear reaction.

First of all, the temperature will go up--simply because a shorter length of plasma is being heated. Raising the temperature will also raise the pressure. Now if the plasma is inertially confined, then an increase of pressure may be of no consequence. But in a magnetically confined plasma, only so much pressure can be contained. Thus the plasma must be initially at a lower density so that the higher pressure can be contained by the magnetic field. But reducing the density to keep the pressure fixed increases the absorption length and the net effect is that the absorption length is not reduced at all! Thus, Z-doping is of no value in a magnetically confined plasma.

Subsequent discussion assumes that the electron number density is held constant since it determines the refractive properties of the plasma (when reflection occurs, etc.). Then

the length of the plasma is reduced. This will immediately reduce the confinement time, which is detrimental with respect to achieving gain. Moreover, doping with an impurity (holding n_e constant) reduces the number density of the reactants--and hence the thermonuclear energy release. Also, bremsstrahlung losses will increase due to the increased ratio of electrons to ions.

A measure of the effect of Z-doping on gain has been made. There is a certain fixed amount of energy that must be added to a pure D-T plasma of a given electron density to raise its temperature to 10 KeV. A minimum nt is then needed to achieve gain from the reaction that follows. Suppose that exactly the same amount of energy is added to a doped D-T plasma which has the same electron density. Then a new minimum nt for the doped plasma can be calculated using the D-T reaction and the bremsstrahlung power densities,

$$P_{DT} = 2.59 \times 10^{-24} \frac{n^2}{T^{2/3}} \left[\exp - \frac{19.94}{T^{1/3}} \right] a_1 \text{ watt/cm}^3$$

$$P_{br} = 5.35 \times 10^{-31} n^2 T^{1/2} \cdot a_2 \text{ watt/cm}^3$$

where n is the number density in /cm^3 of all particles, and T is the temperature in KeV. An equilibrium plasma is assumed. a_1 and a_2 are factors depending on the doping,

$$a_1 = \frac{[1 + f(A-1)][1 + f(A^2-1)]}{[1 + \tfrac{1}{2}f(A-1)]^2}$$

$$a_2 = \frac{[1 - f]^2}{[1 + \tfrac{1}{2}f(A-1)]^2}$$

f is the impurity fraction of the ions and A is the atomic number of the impurity (assumed fully ionized). Then Lawson's criterion is

$$\frac{1}{nt} < \frac{\eta}{1-\eta} \frac{P_{DT}}{3n^2kT} - \frac{P_{br}}{3n^2kT} \qquad (2\text{-}84)$$

η is the efficiency of conversion of released energy into heating the next slug of plasma to thermonuclear temperatures. This calculation takes $\eta = 1/3$ after Lawson. Using the above equations, the required $n_e t$ for gain (i.e., satisfying the inequality (2-84) was calculated and is plotted in figure 34. Used in the calculation was $n = a_3 n_e$ where

$$a_3 = \frac{1 - f}{1 + f(A-1)}$$

Also used was $T = a_4 T_o$ where T is the temperature that is achieved in the doped plasma with the same amount of energy that produces the temperature T_o in the pure plasma. a_4 is given by

$$a_4 = \frac{[1 + f(A-1)]^{7/5}}{[1 + \tfrac{1}{2}f(A-1)]}$$

It is clearly seen that Z-doping always makes the Lawson criterion more difficult to attain, i.e., the minimum $n_e t$

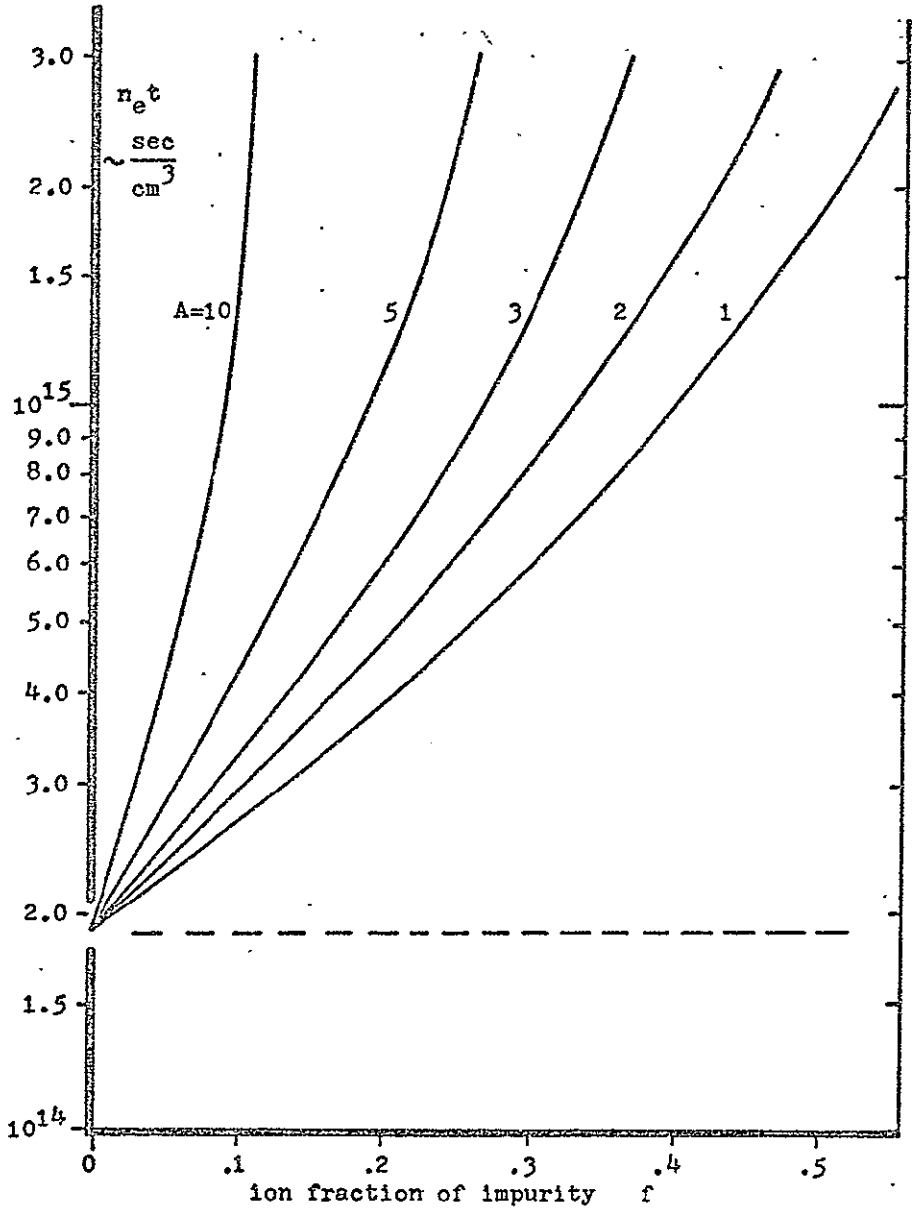

Figure 34. Lawson criterion for a high-Z doped DT plasma

is always raised. Moreover, Z-doping does not improve the electron-ion equilibration time. In fact it raises t_{eq} (2-76), since T_e is increased, and n_e is held constant. Thus the conclusion is obvious; Z-doping is to be discarded insofar as the goal of a thermonuclear reactor is concerned.

Chapter Three

LASER REFRACTION IN CYLINDRICAL PLASMAS

A. REFRACTION IN A STATIONARY PLASMA COLUMN

1. Introduction

One of the promising geometries for the production of a thermonuclear reaction is a long cylindrical plasma column. Such a column might be contained on the sides by a magnetic field which could be generated in several ways. But magnetic fields can only hold so much pressure, thus the plasma density must be made low enough so that the pressure at 10 KeV can be contained. Previously this was an impossible drawback to the laser heating of magnetically confined plasmas since the currently available magnetic fields (ca. 300 KG) could only contain a plasma density of ca. $10^{17}/cm^3$. The absorption length for a Nd+ glass laser in a $10^{17}/cm^3$, 10 KeV plasma is an incredible 450 miles!

However, the advent of powerful long wave length lasers has made a dramatic change in this situation. Dawson, Kidder, and Hertzberg[23] have proposed the use of a long wave length gas laser to heat such a magnetically confined plasma. Recent developments of high power pulsed CO_2 lasers[24,25,26] with $\lambda_0 = 10.6\mu$ show that gas laser development is becoming competitive with the solid state lasers in the production of high energy pulses. The significant advantage in using the long wave length, as first noted by Dawson, is that the laser energy can be better absorbed by plasmas at densities which can be confined in the magnetic fields that are currently feasible.

The mechanisms of absorption (with the exception of the recently discovered anomalous absorption[16]) are fairly well understood. The primary mechanism is inverse bremsstrahlung[14,27,28]. In addition, nonlinear[18] and resonance phenomena[11,29] have been examined. The actual character of the heating has also been studied (see references cited in Chapter II). But with one exception, nothing has been said about refractive effects in a columnar plasma: Vlases and Ahlstrom[30] studied the thermodynamic, absorption, and refraction problems associated with heating a magnetically confined plasma column with a long wave length laser.

This lack of previous work is not to indicate that refraction is not a problem. On the contrary, an attempt has been made to propagate a laser down a typical magnetically confined plasma (θ-pinch). The result was that the beam was refracted out of the column to the extent that no signal penetrated to the far end of the plasma[8]. Thus the refraction may play a very significant role in plasmas of this geometry. If it is not possible to keep the laser beam in the plasma column, then all the advantages of long wave length heating are lost, and it is critically important to study the refraction problem.

a. General Refraction Problem

When the geometry of a particular scheme is investigated it becomes obvious that refraction effects can play a dominant role. The density gradients in the plasma may refract the radiation out of the plasma before it has traveled far enough to be absorbed. The equation for the index of refraction in a gas composed of atoms, ions, and electrons is

$$\tilde{n} = 1 + (K_o + K_o' \lambda_o^{-2}) n_o + (K_i + K_i' \lambda_o^{-2}) n_i - 4.5 \times 10^{-22} n_e \lambda_o^2 ,$$

where $n_{o,e,i} \sim cm^{-3}$ and $\lambda_o \sim$ microns. This equation applies when the frequency ω is much greater than the plasma frequency ω_p and the cyclotron frequency. For $\lambda_o > 0.5\mu$ and a typical gas the contributions due to the atoms and the ions can be combined so that

$$\tilde{n} \approx 1 + 10^{-23}(n_o + n_i) - 4.5 \times 10^{-22} n_e \lambda_o^2 .$$

Thus it is clear that for $\lambda_o > 0.5\mu$ and ionization greater than 10% that $\tilde{n} - 1 < 0$ whereas for an un-ionized gas $\tilde{n} - 1 > 0$. Therefore in an un-ionized gas the refraction deflects the beam towards the higher density but in a fully ionized plasma the index of refraction decreases with increasing density so the refraction deflects the beam towards the lower density. Since all plasmas have $n_e \to 0$ at their boundaries, refraction could play a dominant role in the application of laser radiation to the production of CTR.

The simple equation relating the radius of curvature of a ray, R, to the index of refraction gradient is

$$\frac{1}{R} = \frac{\sin \psi}{\tilde{n}} \left| \text{ grad } \tilde{n} \right| ,$$

where ψ is the angle between the ray and the direction of grad $\tilde{n}$. It is particularly interesting to note that $R \to 0$ at the plasma critical density, i.e., where the laser frequency equals the plasma frequency. For laser heated plasmas,

the maximum density ρ_{max}, may be greater or equal to the critical density, ρ_c.

In this study only the problem of a cylindrical plasma with azimuthal symmetry irradiated in the axial direction is discussed. The results developed here indicate effects that would be important in other geometries as well, and the general trends can be carried over.

b. Unfavorable Density Profile

The most obvious geometry, where $\rho(r)$ is parabolic with ρ_{max} at $r = 0$, is considered first. The refraction effects are detrimental because of the unfavorable density gradient. It is shown that heating this type of plasma is very difficult due to the refraction losses.

If the incident laser beam is focused then it is shown that there exists a solution where the laser beam can be made to propagate indefinitely even in an unfavorable density gradient. Realistically some deviation from the ideal case would occur in practice. When a realistic deviation is allowed then it is shown that the propagation distance is improved by a factor of approximately three over the unfocused case.

c. Favorable Density Profile

The other possibility which exists is that the laser beam is propagated in a region where the density gradient is favorable, i.e., leads to self focusing. It is shown that for a favorable density variation a parallel incident beam is trapped as in a light pipe. Solutions for the wave fronts in a parabolic density profile are presented. These solutions based on geometrical optics show that the wave fronts are a family of

cusped curves that extend down the column, alternately collapsing and expanding. During this process envelopes of the wave fronts, caustics, are formed at the locus of points of the end of the cusps.

It is also shown that in a light pipe configuration of the plasma, the effective absorption length of the plasma can be reduced by as much as an order of magnitude.

2. Defocusing in a Parabolic Density Profile

a. Unfocused Laser Beam

The geometry considered is a long cylindrical plasma column with azimuthal symmetry and a density maximum on the axis with a monotonic decrease of the density in the radial direction. A laser beam is incident on the plasma column in the axial direction where it is assumed that the diffraction effects can be neglected and the laser beam is in the TEM_{00} mode with the intensity distribution approximated by a parabola. The general configuration is shown in figure 35. It is accurate to use geometrical optics as long as the plasma density is less than the critical density and caustics are not generated. The equations for the intensity and the abosrption must be modified near the critical density and caustics if the details are desired in these localized regions.

The Eikonal equation for a cylindrically symmetric geometry is

$$\frac{1}{c^2(r)} = \left(\frac{\partial u}{\partial x}\right)^2 + \left(\frac{\partial u}{\partial r}\right)^2 ,$$

where u corresponds to time and c is the phase velocity. This equation can be reduced to a differential equation for the

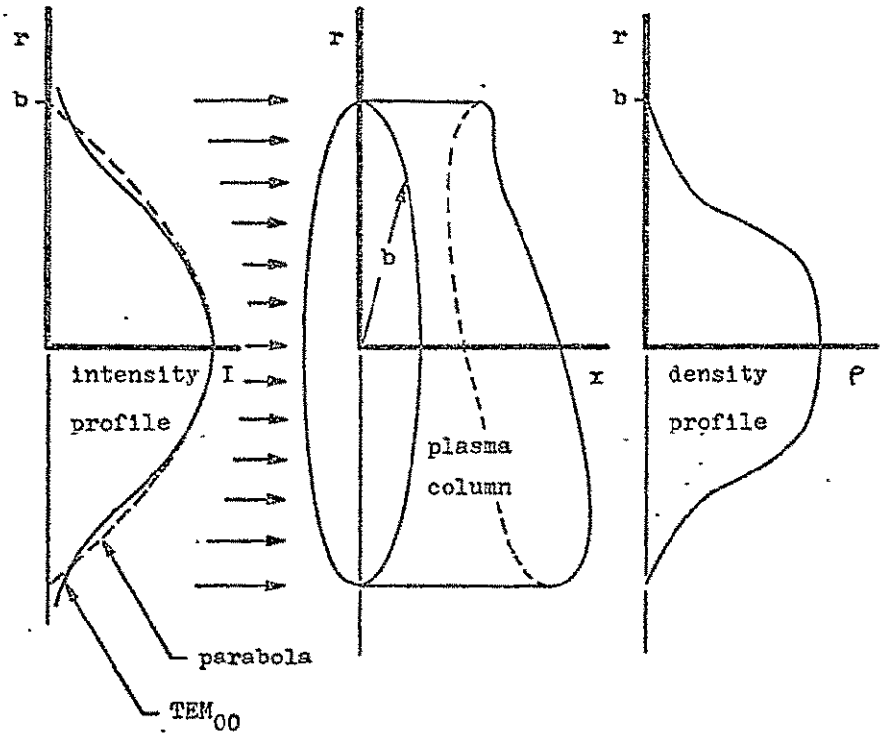

Figure 35. Laser pulse and plasma configuration

rays

$$c\frac{d^2r}{dx^2} + \left[1 + \left(\frac{dr}{dx}\right)^2\right]\frac{dc}{dr} = 0 , \qquad (3\text{-}1)$$

where the two boundary conditions are that

$$r(0) = r_o ,$$
$$\frac{dr}{dx}(0) = 0 . \qquad (3\text{-}2)$$

The integration of (3-1) leads to the ray equation

$$x = \int_{r_o}^{r} \frac{c\,dr}{\left[c^2(r_o) - c^2\right]^{1/2}} \qquad (3\text{-}3)$$

The phase velocity is given by

$$c = c_o(1-\zeta)^{-1/2} ,$$

where c_o is the speed of light in a vacuum and $\zeta = \frac{\omega_p^2}{\omega^2} = \frac{\rho}{\rho_c}$, the ratio of the density of the plasma to the critical density for the particular laser wave length. Thus (3-3) becomes

$$x = \sqrt{1-\zeta_o} \int_{r_o}^{r} \frac{dr}{\sqrt{\zeta_o - \zeta}} , \qquad (3\text{-}4)$$

where $\zeta_o = \zeta(r_o)$ and $\zeta = \zeta(r)$.

Now in order to evaluate the integral in (3-4), a parabolic density variation is assumed,

$$\zeta = \zeta_m\left[1 - \Gamma\left(\frac{r}{b}\right)^2\right] . \qquad (3\text{-}5)$$

$\Gamma = 1$ corresponds to $\zeta = 0$ at the edge of the plasma $r = b$;

and $\Gamma < 1$ corresponds to $\zeta = (1-\Gamma)\zeta_m$ at $r = b$. Thus for $\Gamma < 1$ the density profile is flatter as shown in figure 36.

The ray equation, (3-4), using (3-5) reduces to

$$\frac{r}{r_o} = \cosh\left\{\frac{x}{b}\left[\frac{\Gamma\zeta_m}{1 - \zeta_m(1 - \Gamma r_o^2/b^2)}\right]^{\frac{1}{2}}\right\} \qquad (3\text{-}6)$$

(3-6) can then be used to determine the distance that the laser beam propagates along the column. A measure of this distance is the value of x for which one half the laser beam energy has left the plasma column, $x_{\frac{1}{2}}$. Figure 37 shows the variation of $x_{\frac{1}{2}}/b$ with Γ for three values of ζ_m. For each of the values of ζ_m a value of the absorption length for $\lambda_o = 10.6\mu$ and $T_e = 10$ KeV is also given. It is clear that the radius of the plasma would have to be very large for any significant portion of the energy to be absorbed at 10 KeV and that Γ should be very small.

It should also be pointed out that the case $\Gamma < 1$ could be considered as a full parabolic plasma profile, $\Gamma = 1$, with a smaller radius laser beam r_b. For example if b is the plasma radius then $r_b/b = \frac{1}{3}$ corresponds to $\Gamma \doteq \frac{1}{10}$ and $r_b/b = \frac{1}{10}$ corresponds to $\Gamma \doteq \frac{1}{100}$. As long as the characteristic thermal conduction time in the lateral direction is much less than the longitudinal acoustic time, the whole plasma column would be heated.

Finally for this case it is straightforward to make a perturbation calculation of the percentage of the energy absorbed at any given temperature. Figure 38 shows that for a CO_2 laser and temperatures greater than 100 eV a significant fraction of

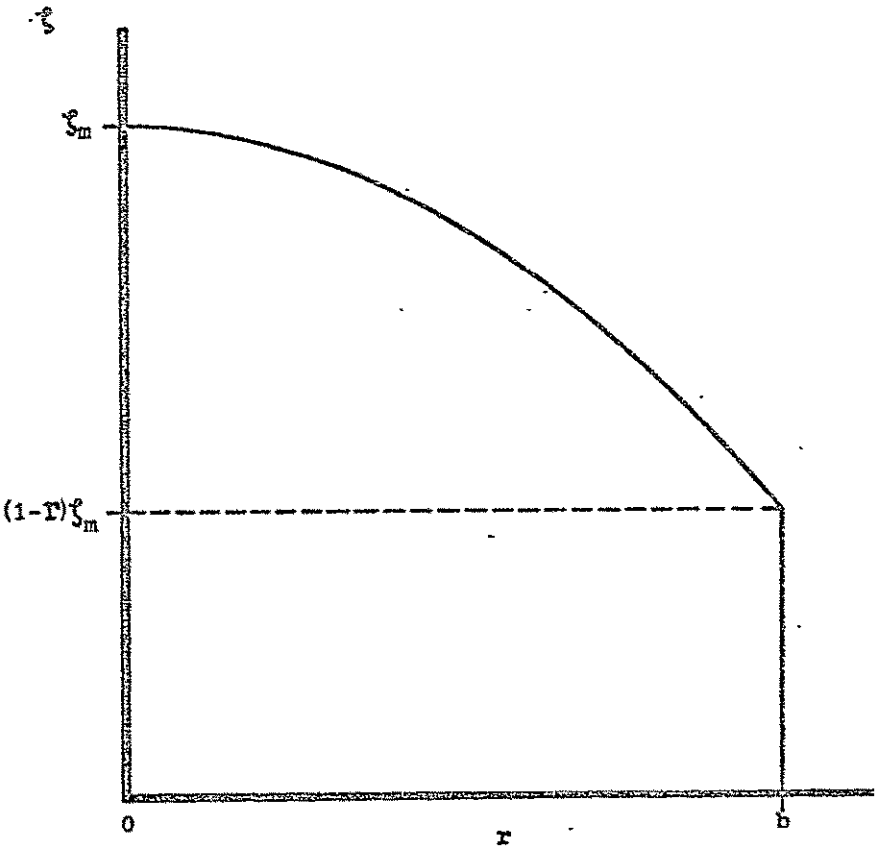

Figure 36. Typical density variation

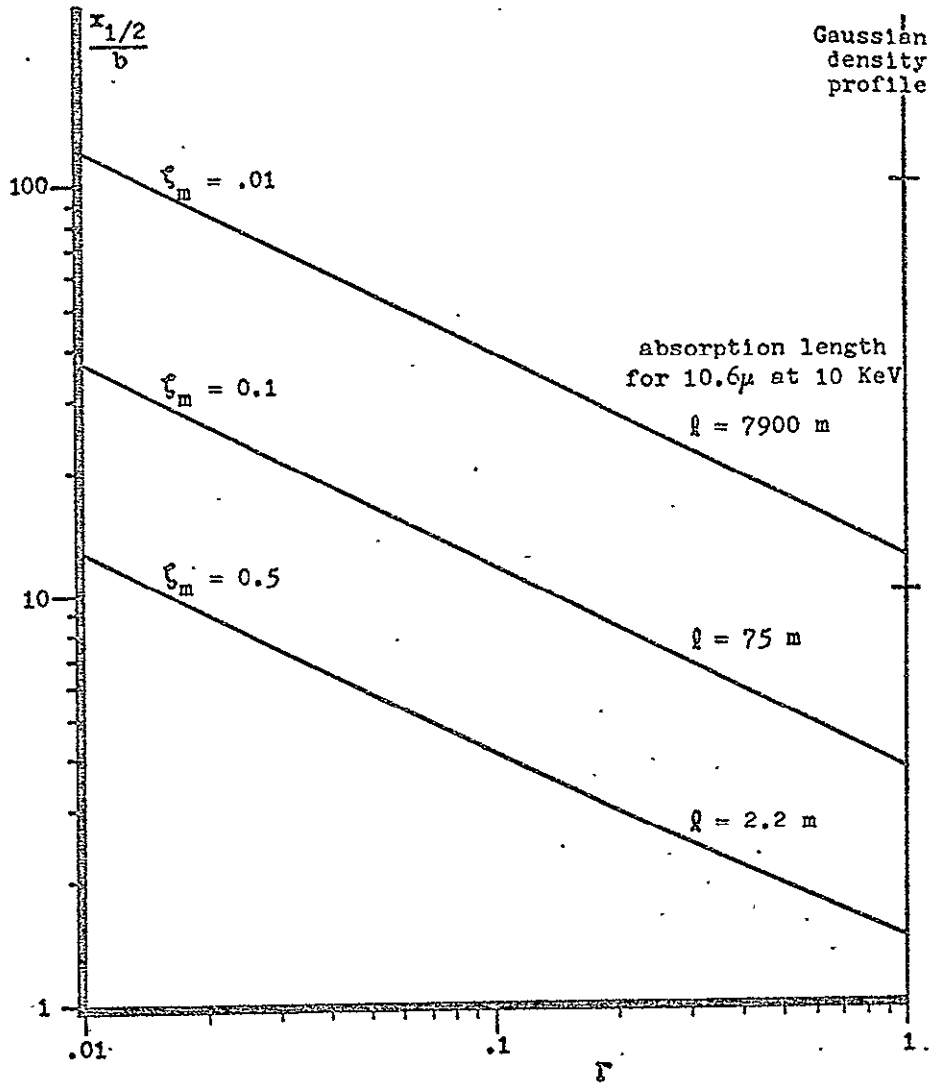

Figure 37. Distance in which half of the laser energy leaves the plasma, for a parabolic density, and intensity profile

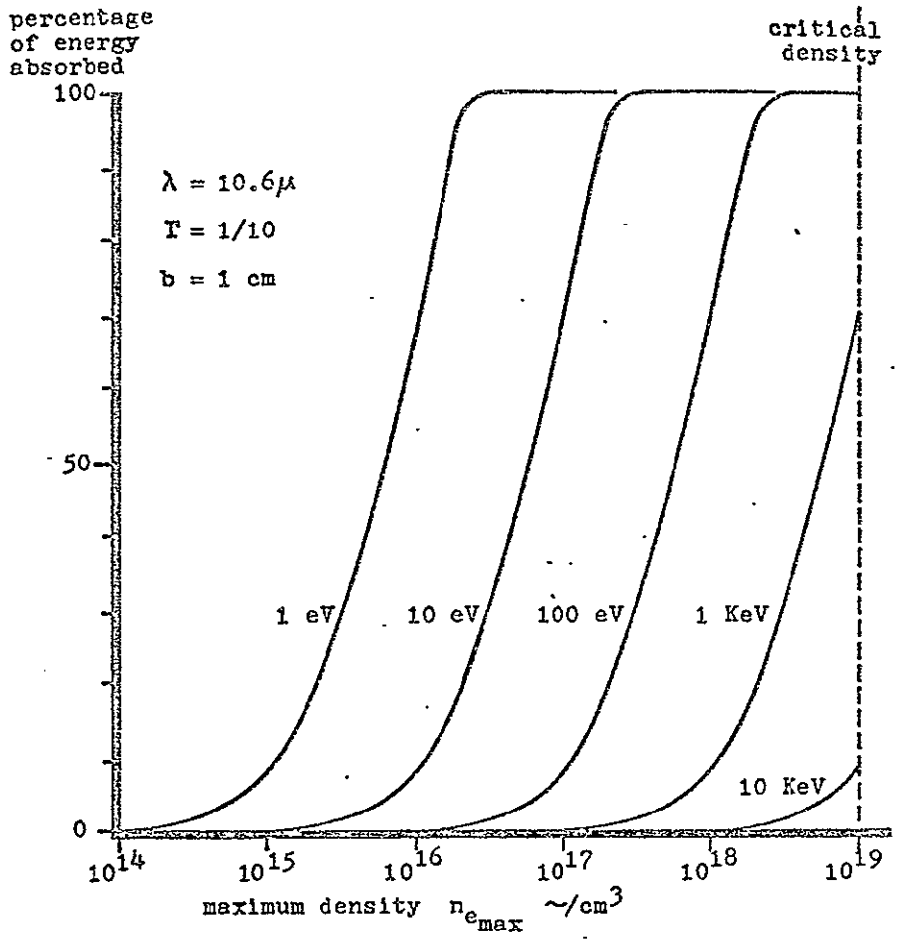

Figure 38. Energy absorbed in a perabolic density profile at a given temperature

the energy is not absorbed and at 10 KeV the percentage absorbed is negligible. These calculations were done for $b = 1.0$ cm and $\Gamma = 0.10$. For larger plasma diameters and smaller values of Γ the picture would of course be more favorable.

b. Focused Laser Beam

Now suppose for the parabolic density profile, the incident laser beam is focused by a lens such that in the absence of the plasma the focal point would be at $x = h$ as shown in figure 39. Before solving this case two limits are obvious. If $\frac{h}{b} \to \infty$ then this is the unfocused case discussed in the previous section. If $\frac{h}{b} \to 0$ then the radiation will traverse the plasma column and go out the other side. Solutions for finite values of h/b should give increased propagation distances; in fact it would seem reasonable to search for a solution such that the radiation is trapped.

The boundary conditions are now

$$r(0) = r_o \ , \qquad \frac{dr}{dx}(0) = -\frac{r_o}{h} \ . \tag{3-7}$$

The solution for this case has three forms:

$$\frac{x}{b} = \gamma\left\{\sinh^{-1}\frac{r}{b|\beta|} - \sinh^{-1}\frac{r_o}{b|\beta|}\right\} \quad \text{for} \quad \beta^2 > 0 \ , \tag{3-8}$$

$$\frac{x}{b} = \gamma\left\{\ln\frac{r}{b} - \ln\frac{r_o}{b}\right\} \quad \text{for} \quad \beta^2 = 0 \ , \tag{3-9}$$

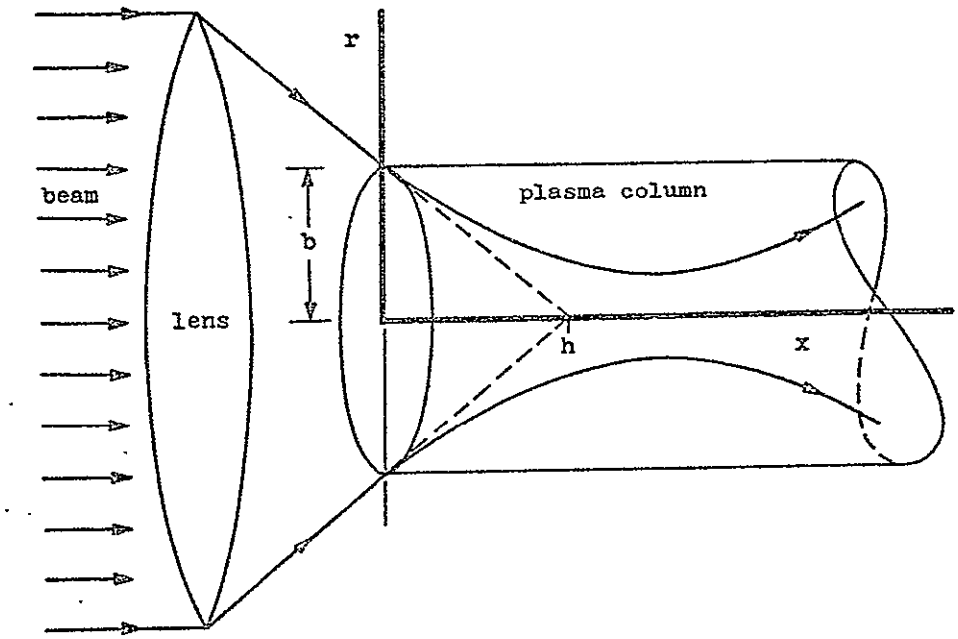

Figure 39. Focused beam configuration

$$\frac{x}{b} = \gamma\left\{\cosh^{-1}\frac{r}{b|\beta|} - \cosh^{-1}\frac{r_o}{b|\beta|}\right\} \quad \text{for} \quad \beta^2 < 0 \ , \qquad (3\text{-}10)$$

where

$$\beta^2 = \frac{1}{1 + \frac{h^2}{r_o^2}}\left\{\frac{1}{\Gamma}\left(\frac{1}{\zeta_m} - 1\right) - \frac{h^2}{b^2}\right\} \ ,$$

and

$$\gamma^2 = \frac{1}{1 + \frac{r_o^2}{h^2}}\left\{\frac{1}{\Gamma}\left(\frac{1}{\zeta_m} - 1\right) + \frac{r_o^2}{b^2}\right\} \ .$$

For $\beta^2 > 0$ the ray paths are overfocused so that they cross over the axis and exit from the plasma on the other side. For $\beta^2 < 0$ the ray paths are underfocused (as shown in figure 35). For $\beta^2 = 0$ all the ray paths approach the axis asymptotically. This condition requires

$$\frac{h^2}{b^2} = \frac{1}{\Gamma}\left(\frac{1}{\zeta_m} - 1\right) \ . \qquad (3\text{-}11)$$

It should be noted that in heating a plasma, this type of solution would only be useful if the characteristic thermal conduction time in the lateral direction is much less than the longitudinal acoustic time so that the whole plasma is heated.

As a practical matter it would be impossible to satisfy (3-11) exactly. Thus it is of interest to examine the effect of an error in e.g., Γ . (3-8) and (3-10) give

$$\frac{x_{\frac{1}{2}}}{b} \sim \ln\frac{\text{const.}}{|\Gamma - \Gamma|} \ ,$$

where Γ_c is the correct value for (3-11) to be satisfied. It is easily seen that only a small error in specifying Γ leads to values $\frac{x_{1/2}}{b}$ close to those obtained in the unfocused case. Figure 40 shows the variation of $\frac{x_{1/2}}{b}$ vs Γ for $\Gamma - \Gamma_c = 0.10\Gamma_c$ and $0.01\Gamma_c$. It is seen that $x_{1/2}/b$ is improved over the unfocused case by roughly factors of three and nine for $\Gamma - \Gamma_c = 0.10\Gamma_c$ and $0.01\Gamma_c$ respectively.

3. Refraction in a Favorable Density Profile

It is clear that if the density profile has a minimum the rays will be refracted into this region. It may even be possible to trap the rays in a minimum density region. The configuration considered is the same as that of Section A 2 except now it is assumed that a density minimum exists. In this case it is both convenient and interesting to use the equations in their characteristic form so that

$$\frac{dr}{ds} = \pm \frac{2}{c_o} \left[\zeta(r_o) - \zeta(r) \right]^{1/2} , \qquad (3\text{-}12)$$

and

$$\frac{dx}{ds} = \frac{2}{c_o} \left(1 - \zeta(r_o) \right)^{1/2} . \qquad (3\text{-}13)$$

Consider the density variation shown in figure 41. From (3-12) it is clear that any ray entering the column with $r_1 \le r_o \le r_2$ and $\frac{dr}{dx}(0) = 0$ will be trapped in this minimum region. Such a configuration could then be called a "light pipe" since the light is trapped in the plasma column.

In order to study the behavior of the radiation in a minimum region in more detail, it is instructive to assume a

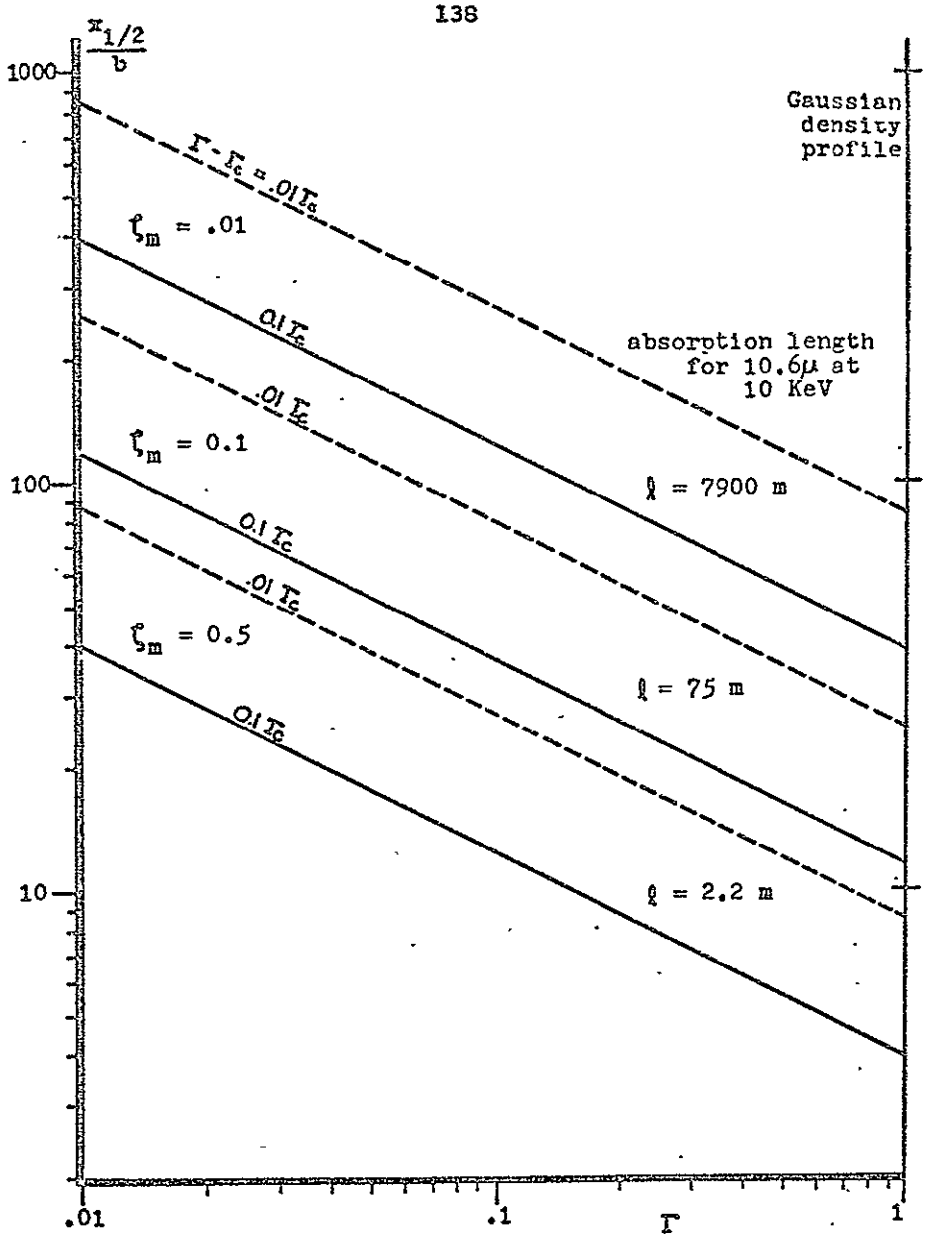

Figure 40. Distance in which half the energy of a focused laser beam leaves the plasma, for a parabolic density, and intensity profile

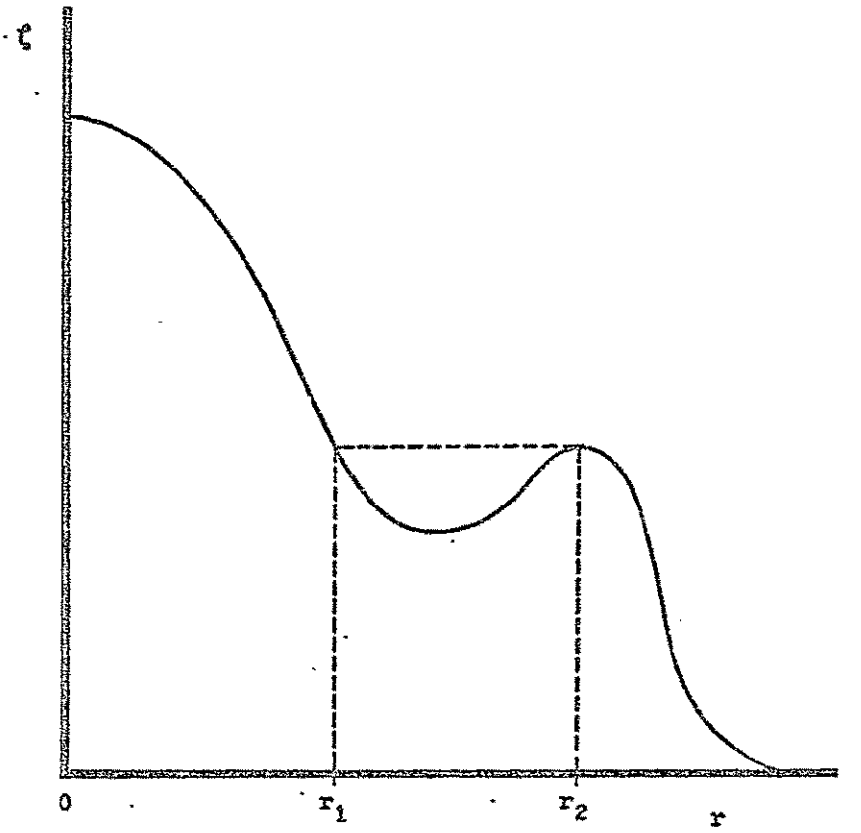

Figure 41. Density Variation with a general minimum

specific density profile and solve (3-12) and (3-13) for the ray paths and the wave fronts. The density variation chosen is

$$\zeta(r) = \zeta_m + (1-\zeta_m)\left(\frac{r}{b}\right)^2 . \qquad (3\text{-}14)$$

This is a parabolic curve with minimum density ζ_m at $r = 0$ and $\zeta = 1.0$ or $\rho = \rho_c$ at $r = b$. The radius of the laser beam is again assumed to be equal to b.

The equation for the rays is then

$$r = r_o \cos\left[\frac{x/b}{(1 - r_o^2/b^2)^{\frac{1}{2}}}\right] . \qquad (3\text{-}15)$$

The wave fronts are given parametrically by the equations

$$\frac{x}{b} = 2\sqrt{1-\zeta_m}\,\frac{s}{c_o b}\sqrt{1-\left(\frac{t}{b}\right)^2} ,$$

$$\frac{r}{b} = \frac{t}{b}\cos\left(2\sqrt{1-\zeta_m}\,\frac{s}{c_o b}\right) , \qquad (3\text{-}16)$$

$$\frac{uc_o}{b\sqrt{1-\zeta_m}} = 2\sqrt{1-\zeta_m}\,\frac{s}{c_o b} - \frac{1}{2}\left(\frac{t}{b}\right)^2\left[2\sqrt{1-\zeta_m}\,\frac{s}{c_o b} + \frac{1}{2}\sin\left(4\sqrt{1-\zeta_m}\,\frac{s}{c_o b}\right)\right] .$$

s and t are two parametric variables. The wave fronts arise for constant values of the time variable, u.

The general proof has already shown that all the rays would be trapped and is confirmed by (3-15). For this parabolic density profile all the rays are cosine functions where the wave length of the oscillating rays goes to zero as $r_o \to b$. Physically, this means that those rays entering the column near the critical density point are bent the most sharply and

oscillate back and forth across the column with a very short wave length. Those rays that enter the column near the center are only weakly deflected and oscillate back and forth very slowly. The ray that enters the column right on the axis will proceed along the axis without oscillation.

A series of wave fronts are shown in figure 42. They are a series of cusped curves that alternately collapse to the axis and then expand. This behavior leads to a series of envelopes or caustics at the points of reflection, i.e., where the wave front turns around and heads back toward the axis. Several caustics are shown in figure 43.

These solutions have infinities on the caustics which are due to the geometrical optics approximation. The behavior near a caustic is discussed in the first appendix. The axial symmetry also leads to a singularity at the axis. The behavior near the axis is also discussed in appendix one.

4. Absorption Length with a Favorable Density Profile

It is of interest to compare the absorption length in a uniform plasma to the absorption length in the plasma with a favorable density profile. Naturally, the absorption length in the "light pipe" is not a clearly defined quantity. The rays of the laser beam that enter the central region where the density is lowest will experience weaker absorption than those rays which enter near the periphery--at a higher density. Furthermore, all rays which do not enter at the density minimum will oscillate back and forth across the plasma as they move down its length. Thus, at any point in the column one finds a strange conglomeration of rays, whose intensity has been damped

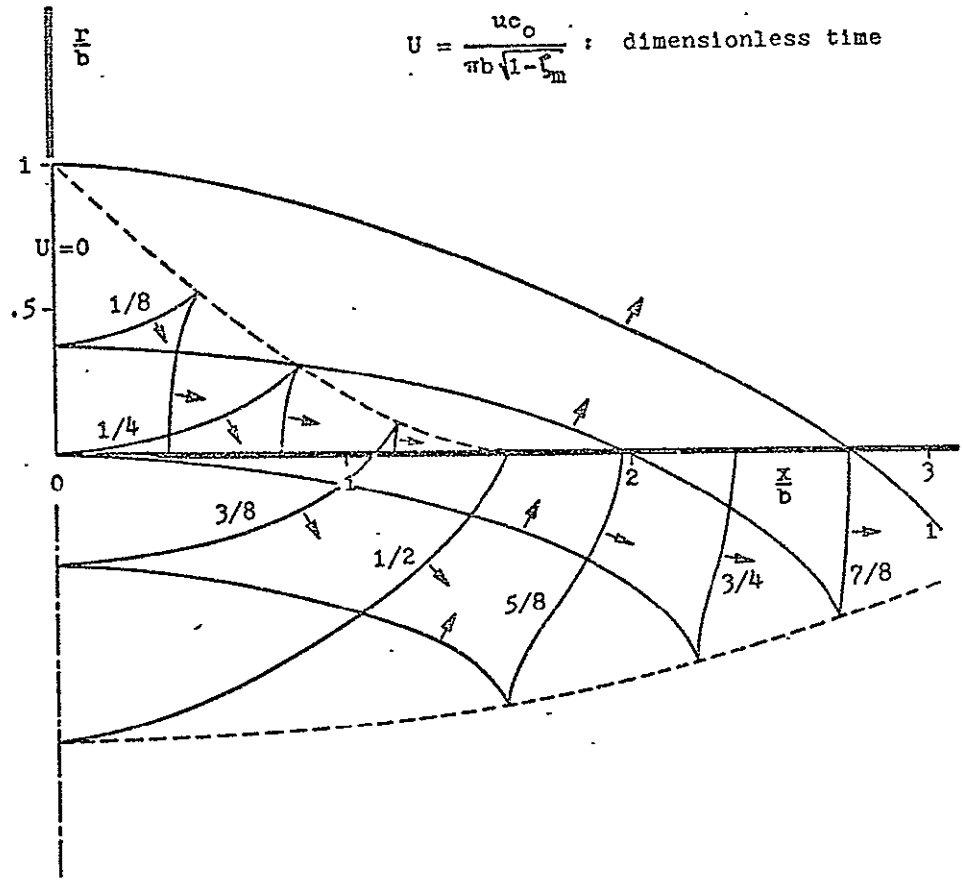

Figure 42. Wave fronts in a plasma column with a favorable parabolic density profile

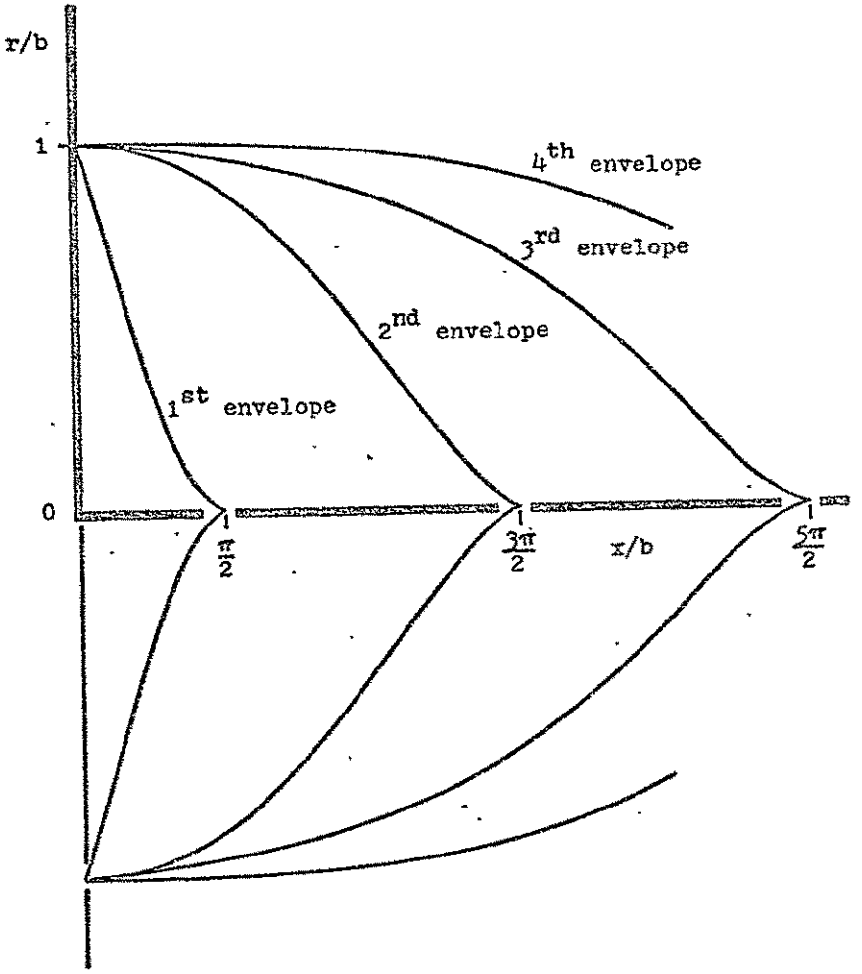

Figure 43. Envelopes of wave fronts for a favorable parabolic density variation

by widely varying amounts, and whose position seems to have no relationship to the origin of the rays.

The appropriate way to measure an "effective" absorption length for such a plasma is to calculate how the overall laser power diminishes in moving down the plasma column. The approach is to find first how each bundle of rays has diminished in intensity. Consider an annular bundle of rays of equal intensity,

$$dW(x,r_o) = I(r_o) \cdot 2\pi r_o dr_o \exp\left\{-\int_o^x K[r(x,r_o)]ds\right\} .$$

Where $dW(x,r_o)$ is the power at x of the radiation that entered the plasma between the circles $r = r_o$ and $r = r_o + dr_o$. $I(r_o)$ is the intensity profile of the laser; $K(r)$ is the absorption coefficient, and ds is an incremental distance along the ray which began at r_o . The total power in the cross section at x is found by integrating dW over all r_o ,

$$W(x) = 2\pi \int_o^b I(r_o) \cdot \exp\left[-\int_o^x Kds\right] r_o dr_o . \qquad (3\text{-}17)$$

The effective absorption length can be calculated by performing the integral (3-17) for a particular density profile. Weak oscillatory terms will arise in the calculation of $W(x)$ but these should be neglected giving $\overline{W}(x)$. The effective absorption length is then given by

$$\ell_{eff} = \left(-\overline{W}(x) \Big/ \frac{d\overline{W}(x)}{dx}\right)_{x=0} . \qquad (3\text{-}18)$$

Calculation of $\ell_{eff}/c_o\tau_{ei}$ was performed for the favorable parabolic density profile (3-14) using two different intensity profiles; $I(r) \sim 1 - (r/b)^2$ which approximates the TEM_{00} mode, and $I(r) \sim (r/b)^2[1-(r/b)^2]$ which approximates the TEM_{00+01} mode. c_o is the speed of light in a vacuum and τ_{ei} is the electron-ion collision time. The results are presented in figure 44 where they are compared to the absorption length in a uniform plasma at a density equal to the minimum density of the favorable profile. It is seen that there is significant enhancement of the absorption length. In fact there is an actual maximum absorption length which occurs approximately when the minimum density is half the critical density. There is at least an order of magnitude decrease in the absorption length for all densities less than about 0.4 of the critical density.

Thus, it is seen that the light pipe not only traps the laser radiation, but reduces the absorption lengths considerably from the often inconveniently long lengths which arise in a uniform density plasma.

5. Summary

The problem of propagating a laser beam along a long cylindrically symmetrical column of fully ionized plasmas has been considered using geometrical optics. For the case where the density has a maximum on the axis and decreases monotonically in the radial direction the ray paths are refracted out of the plasma column. The solutions show that it is very difficult to heat a long plasma column with this unfavorable density profile. By focusing the incident laser beam it is theoretically

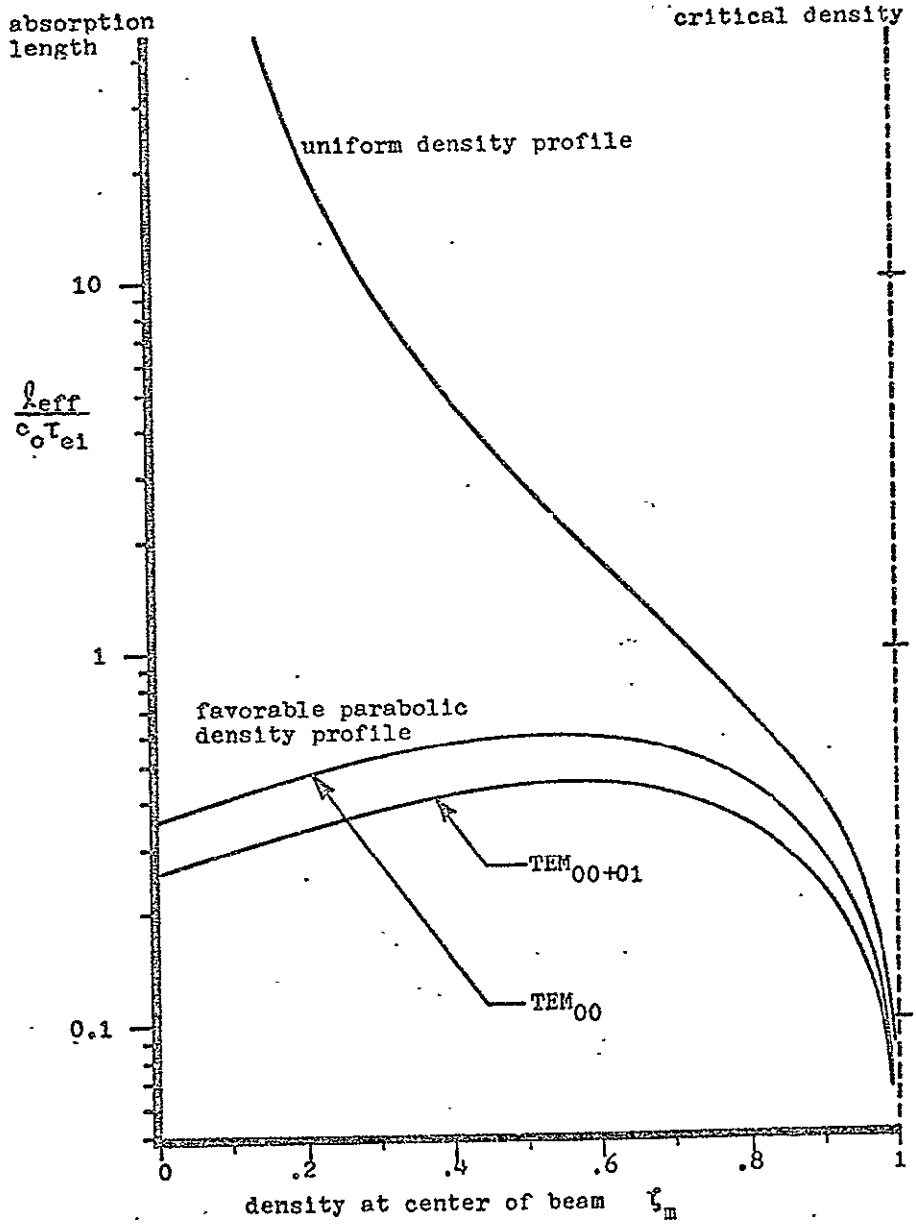

Figure 44. Effective absorption length in a plasma column with a favorable density profile

possible to keep the light from being refracted out of the plasma column. However, this solution can be compared to finding a neutral stability point in the middle of an unstable region. So that any deviation leads to a very rapid refraction of the laser beam out of the plasma.

A "light pipe" effect is found if there is a density minimum. For the general case of a density minimum it is shown that a parallel incident beam is trapped by the plasma column. A special case where the density variation is parabolic is considered, and the solution shows that the wave fronts are a family of cusped curves which alternately collapse to the axis and then expand until reflected back along a caustic. The intensity along the caustics is very large as is the intensity along the axis. Geometrical optics fails in these localized regions (see appendix one).

Finally it is shown that for the "light pipe" solutions there is a significant decrease in the effective absorption length due to the rays oscillating back and forth across the plasma. It is clear from these solutions that there are very significant advantages to the light pipe configuration for the production of a thermonuclear plasma.

B. DYNAMIC GENERATION OF FAVORABLE DENSITY PROFILES

1. Introduction

Since the plasma density profiles generally encountered are unfavorable with respect to refraction (such as in the quasi-steady stage of a θ-pinch), it is important to look for ways of creating a favorable profile. There are basically two approaches to this problem. The first approach is to catch the plasma during its formative stage when the density may not have settled down to its steady "unfavorable" state. The second approach is to take the quasi-steady unfavorable profile and change it to a favorable one, i.e., density profile tailoring.

The first approach can be applied to a pinch device. During the formation of the pinch, an axially symmetric shock wave collapses to the axis. Across the shock the density rises. So at any instant of time during the collapse, a favorable density profile is seen to appear: a lower density on the axis than farther out. The density profile during the "collapse phase" would resemble the solid line in figure 45.

After the collapse phase comes the "bounce phase" when the shock wave reflects from the axis. Due to the nature of the gas dynamics, a favorable density profile is left behind the reflected shock. The density profile corresponding to the bounce phase is the dashed line in figure 45.

If laser heating during the collapse phase is used, the laser pulse must be shorter than the time for the imploding shock to collapse through a distance equal to the radius of the beam. Likewise, for the bounce phase, the pulse must be

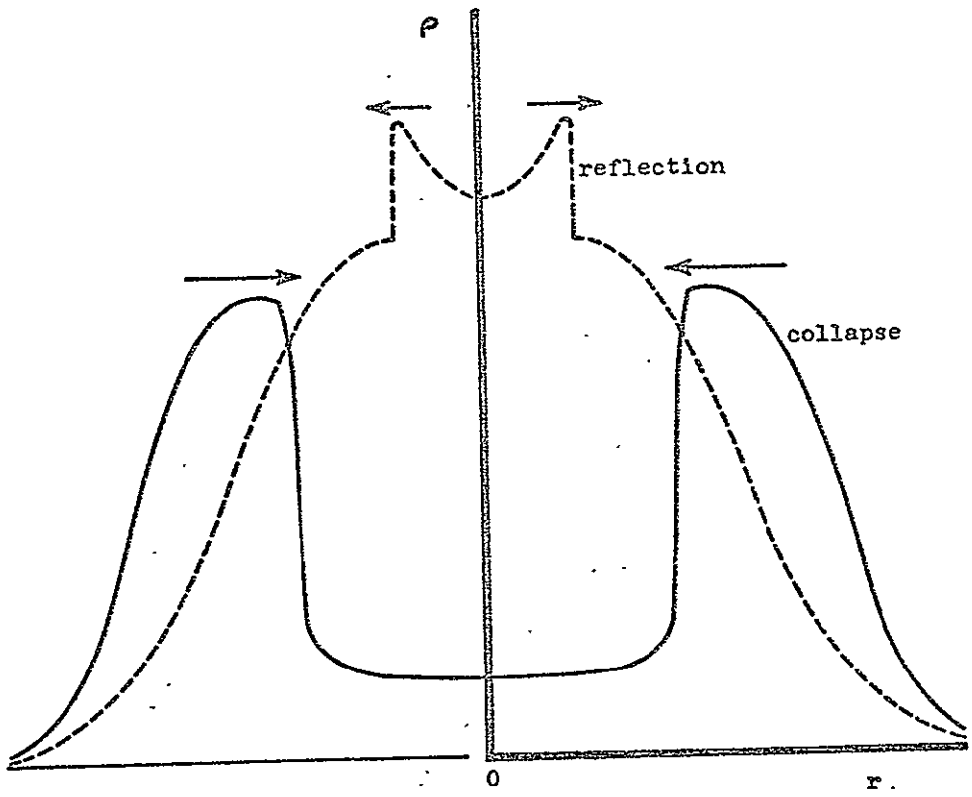

Figure 45. Favorable density profiles in the collapse and reflection phases of a θ-pinch

shorter than the lifetime of the favorable density profile.

All subsequent discussion will deal with the second approach, that of changing an unfavorable density profile into a favorable one. The basic method here might be called "selective heating" whereby the region near the axis is heated with a small laser, the "pre-laser". The added energy would produce a pressure imbalance causing redistribution of the plasma and possibly a favorable density profile for trapping the beam from the main laser.

This approach offers a great deal of flexibility in achieving the desired result. The pulse lengths, the wave lengths, and the energy of each pulse can be treated as independent parameters. For example, suppose the intent is to prepare a plasma for heating by a powerful CO_2 laser. Then the plasma length would correspond roughly to the absorption length of 10.6μ radiation at 10 KeV. But the absorption length at, say, 100 eV is only 1/1000 of its value at 10 KeV. Hence, a CO_2 pre-laser could not be used to heat the plasma longitudinally. Only a small fraction of the lengt would get heated. But a Nd^+ glass laser which has a longer absorption length may be used.

Another advantage of using a shorter wavelength for the pre-laser is the refractive improvement. Figure 37 shows that if the initial plasma column has $n_{e\ x} = 5 \times 10^{18}\ /cm^3$ and $\Gamma = 0.10$, then for a CO_2 gas laser, one half the laser beam would have left the column in three plasma radii. However if $\lambda_o = 1.06\mu$ corresponding to a Nd^+ glass laser, then $x_{\frac{1}{2}}/b \tilde{=} 100$.

Figure 46 (which is the same as figure 38 except $\lambda_o = 1.06\mu$, Nd^+ glass laser) shows that if $b = 1$ cm, 80% of the energy would be absorbed.

A second consideration is that the pre-laser preparation of a favorable density profile need not be a high efficiency process. For example, if the initial temperature is 100 eV, then this represents only 1% of the energy required to achieve 10 KeV. If the heating from 100 eV to 200 eV were done in a way that produces a favorable density profile, then the remainder of the heating (to 10 KeV) could be done very efficiently, since there would be no refraction losses. Inefficiencies in the heating to 200 eV could be tolerated since this represents only 1% of the total energy required.

It is also interesting to note that once a favorable density profile has been produced the additional energy absorption due to an incident Gaussian laser beam will continue to push mass towards the outer edge of the beam. This problem is very similar to the thermal blooming problem[31,32] which is experienced in the propagation of a laser beam through the atmosphere. The fundamental and convenient difference is that in the case of a fully ionized plasma the laser beam is trapped because $\tilde{n} - 1 \simeq -n_e$.

2. Governing Parameters

Before considering the methods of density tailoring, it is necessary to calculate the various parameters that govern the dynamics. Rather than set up the full equation, it is sufficient at this point to examine the scale of the parameters.

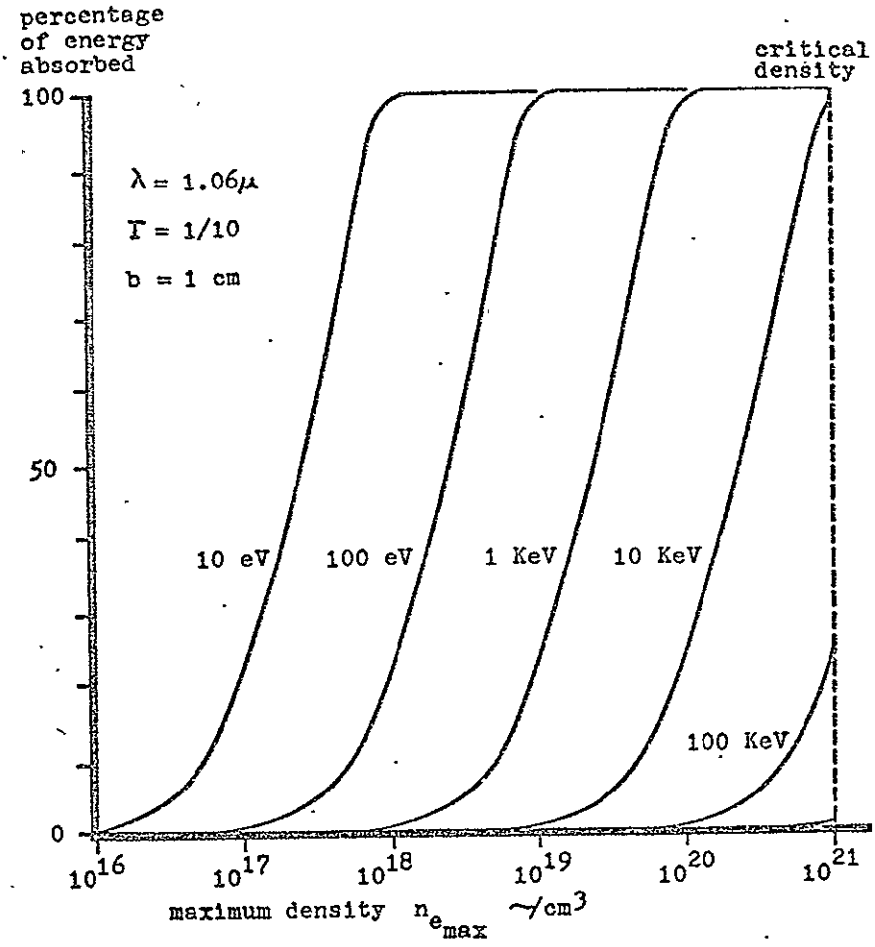

Figure 46. Energy absorbed in a parabolic density profile at a given temperature

The length scale is $2r_b$ where r_b is the radius of the laser beam entering the plasma. r_b will be less than or equal to the plasma radius, b. The density and temperature scales are the maximum density and temperature respectively in the unheated plasma column.

There are several time scales of interest. There is the heating time scale t_h which is the time in which the temperature would double if the plasma were held stationary. Then

$$t_h = \frac{T}{dT/dt} = T / \frac{1}{C_v} \frac{K_\nu}{\rho} \frac{W}{\pi r_b^2} \quad ,$$

where T is the initial temperature, C_v is the constant volume specific heat, K_ν is the absorption coefficient, ρ is the density, and W is the laser power. Then t_h becomes

$$t_h = 7.40 \times 10^{17} r_b^2 T^{5/2} / W\lambda_o^2 n_e \text{ sec} \quad . \tag{3-19}$$

where r_b is in cm, T in eV, λ_o in microns, W in watts, and n_e in cm^{-3}.

The acoustic time scale t_a is defined in the usual way as the quotient of the length scale and the acoustic speed. Then

$$t_a = 1.80 \times 10^{-6} r_b T^{-1/2} \text{ sec} \tag{3-20}$$

The thermal conduction time t_{th} is defined as the time for significant thermal conduction to traverse a distance $2r_b$,

$$t_{th} = \rho C_v (2r_b)^2 / K_e \quad ,$$

where K_e is the electron thermal conduction coefficient. Then

$$t_{th} = 1.29 \times 10^{-20} r_b^2 n_e T^{-5/2} \text{ sec} \qquad (3\text{-}21)$$

Figures 47 and 48 compare the acoustic and thermal conduction time scales to the heating time for $\lambda_o = 1.06\mu$ and 10.6μ, respectively. Figure 49 compares the acoustic time to the thermal conduction time. The interpretation of the various limits will depend on the particular method of density tailoring, but a general comment can be made. If the thermal conduction time is shorter than the characteristic time of the particular method, then thermal conduction will tend to wipe out any favorable density profile that might be generated. This conducting regime poses a major difficulty. A nonconducting regime occurs if the thermal conduction time is longer than the characteristic time of the particular method, then favorable density profiles generated will endure at least for that characteristic time. Several schemes for density tailoring are presented below for both conducting and nonconducting regimes.

One more time scale must be introduced, the magnetic diffusion time, which will be important in determining the characteristics of the conducting regime. The magnetic diffusion time, t_B, is the time in which a significant amount of the magnetic field diffuses through one characteristic length. It is found by an examination of Maxwell's equations,

$$t_B \cong \mu\sigma(2r_b)^2$$

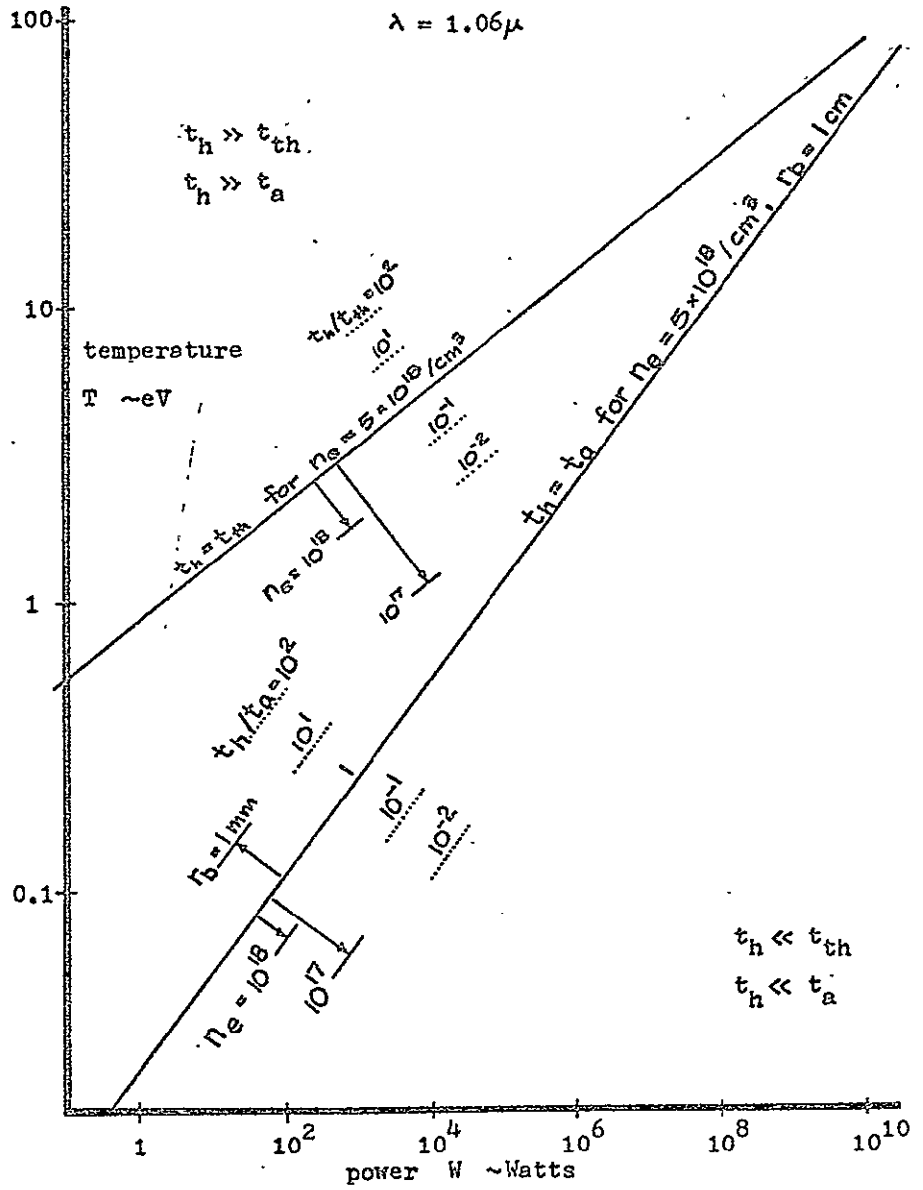

Figure 47. Comparison of acoustic and thermal conduction time scales with the heating time scale for a Nd^+ glass laser

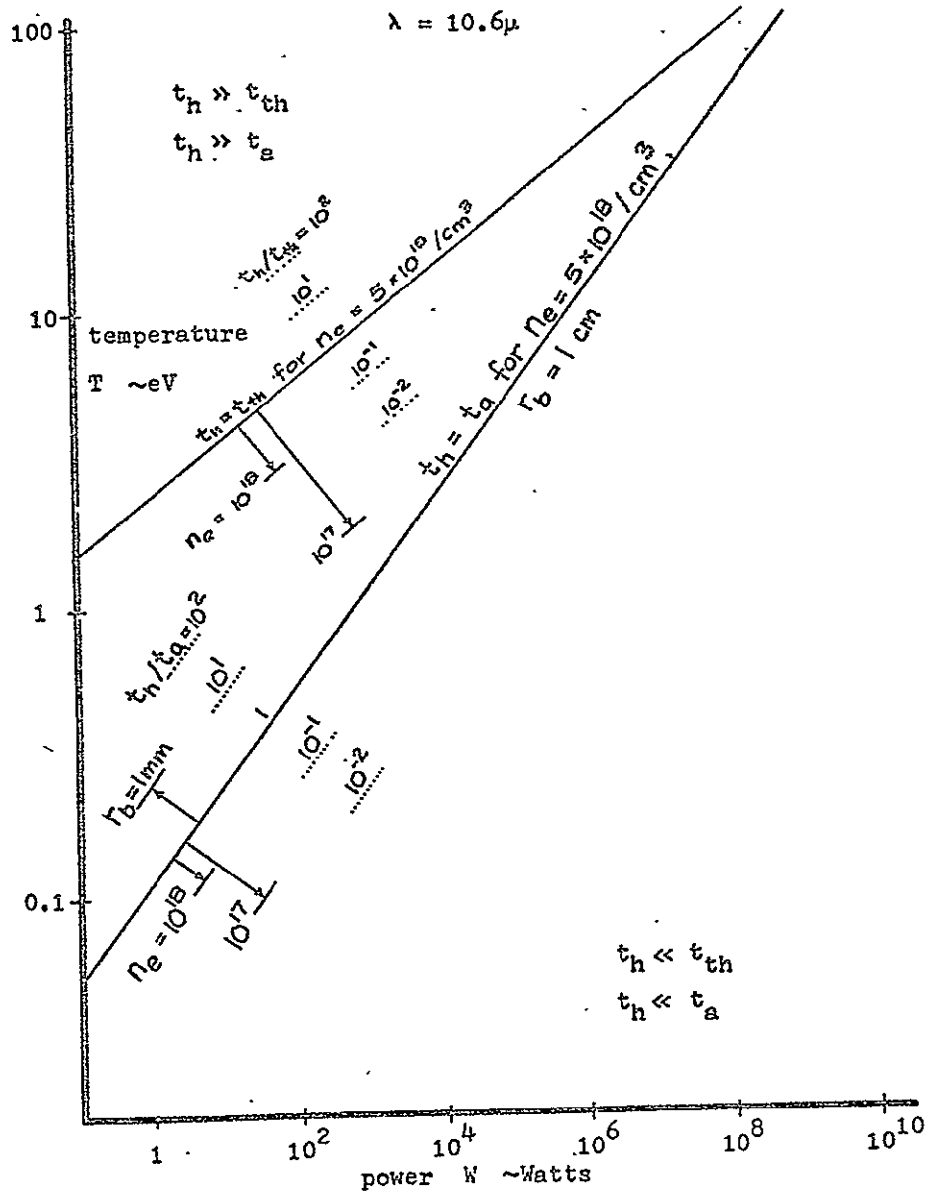

Figure 48. Comparison of acoustic and thermal conduction time scales with the heating time scale for a CO_2 gas laser

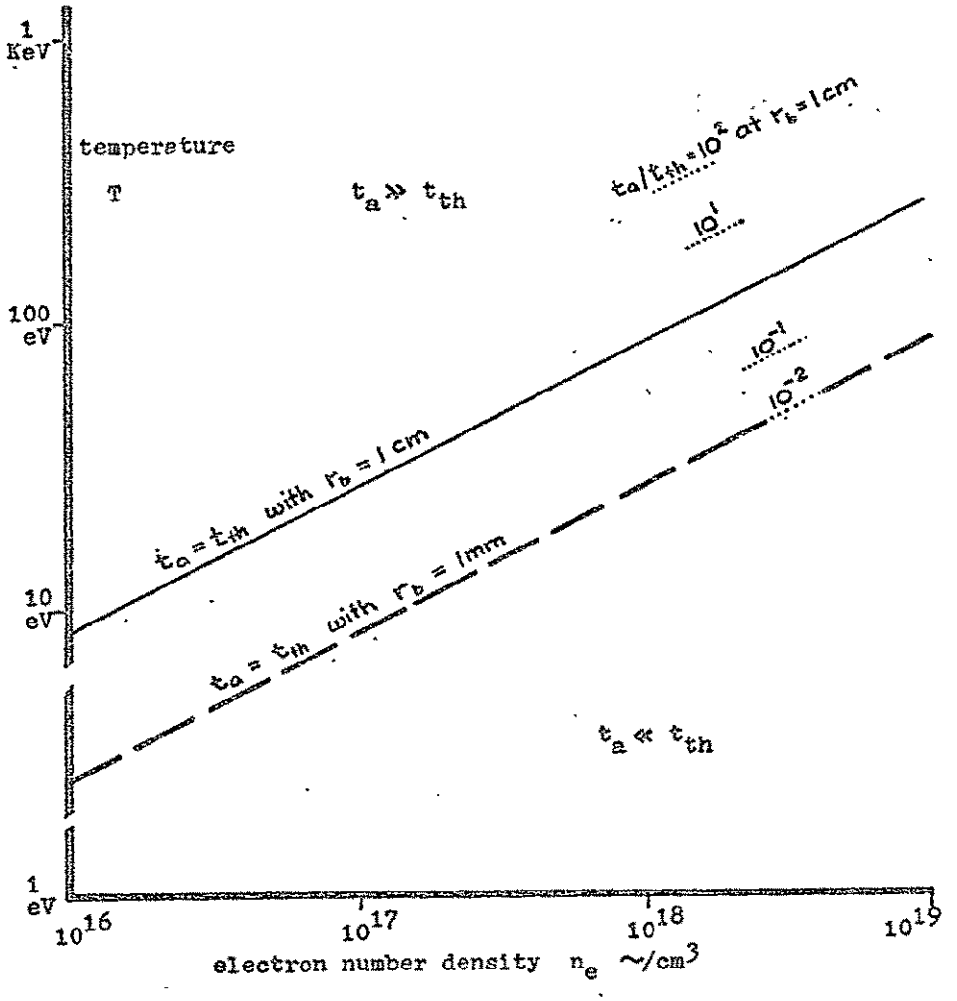

Figure 49. Comparison of acoustic and thermal conduction time scales

where μ is the permeability, and σ is the electrical conductivity. Using electrical conductivity from Spitzer,[14] t_B becomes

$$t_B \cong 7 \times 10^{-5} T^{3/2} r_b^2 \quad \text{sec} \qquad (3\text{-}22)$$

for temperatures in the eV range. The magnetic diffusion time is plotted versus temperature in figure 50.

3. Density Tailoring in the Nonconducting Regime

If t_{th} is much longer than the characteristic time of the process, no thermal conduction occurs. In this regime it is relatively easy to change an unfavorable density profile to a favorable one. The central part of the plasma is heated, it expands and the density drops to a relative minimum on the axis. There is no thermal conduction to smooth out the temperature profile and consequently the density. Moreover, fairly modest energies are required to make a significant density minimum in a plasma.

The simplest estimate of the behavior can be made using the work of Raizer[33] on laser focusing and defocusing in atmospheric air. This can be applied exactly to weak laser heating of an unconfined nonconducting plasma slab so long as the correct absorption length is used. Applying Raizer's results, it can be shown that for laser pulses longer than the time for an acoustic wave to traverse the beam, the density change is given by,

$$\frac{\delta\rho}{\rho_o} = 1.73 \times 10^5 \frac{J_o/A}{T_e^{5/2}} \frac{\zeta}{\sqrt{1-\zeta}} \left(-\frac{I(r)}{I_{max}}\right)$$

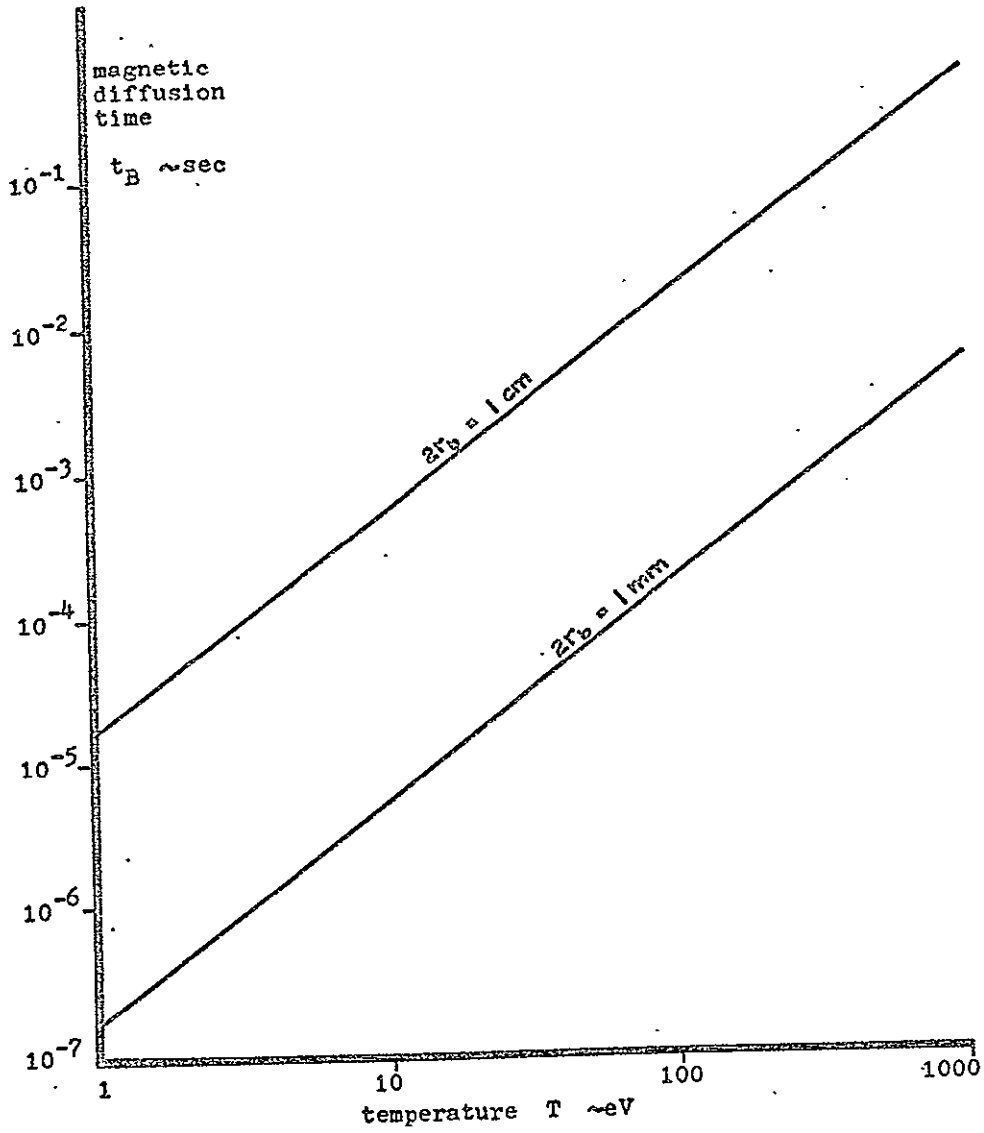

Figure 50. Magnetic diffusion time in a fully ionized plasma

where $I(r)$ is the beam intensity profile, and I_{max} is the maximum intensity. Here it has been assumed that the absorption length is long compared to the radius of the beam, and linearized fluid mechanics is used to evaluate the motion. Physically, it is seen that the heating produces a "hollow" in the density with the same shape as the beam intensity profile. As an example, the density profile that would be produced by a laser beam with a parabolic intensity profile is shown in figure 51. For practical values, e.g., $J_o = 20$ Joules at 1.06μ, $A = 3\ mm^2$, $\zeta = 1/2$, and $T_e = 10^2$ eV; then $\delta\rho/\rho_o = O(1)$. This calculation is valuable only as an order of magnitude estimate but it does indicate that a sizeable density hollow can be produced by a modest laser pulse.

a. Longitudinal Boring

Suppose the pre-laser is fired down the length of the plasma, then the technique might be called "longitudinal boring" since a hollow is being "bored" into the column in a longitudinal manner.

There are basically two ways that a plasma can be bored longitudinally. The first way could be used if the plasma length is comparable to the absorption length of an available pre-laser. The laser beam could be made very narrow by a couple of lenses (beam shrinking). In this case the entire length of the plasma could be heated simultaneously with a very short pulse. The subsequent motion of the plasma would produce a density minimum along the axis where most of the radiation had passed. For this method the characteristic time is not the pulse length, but the acoustic time---

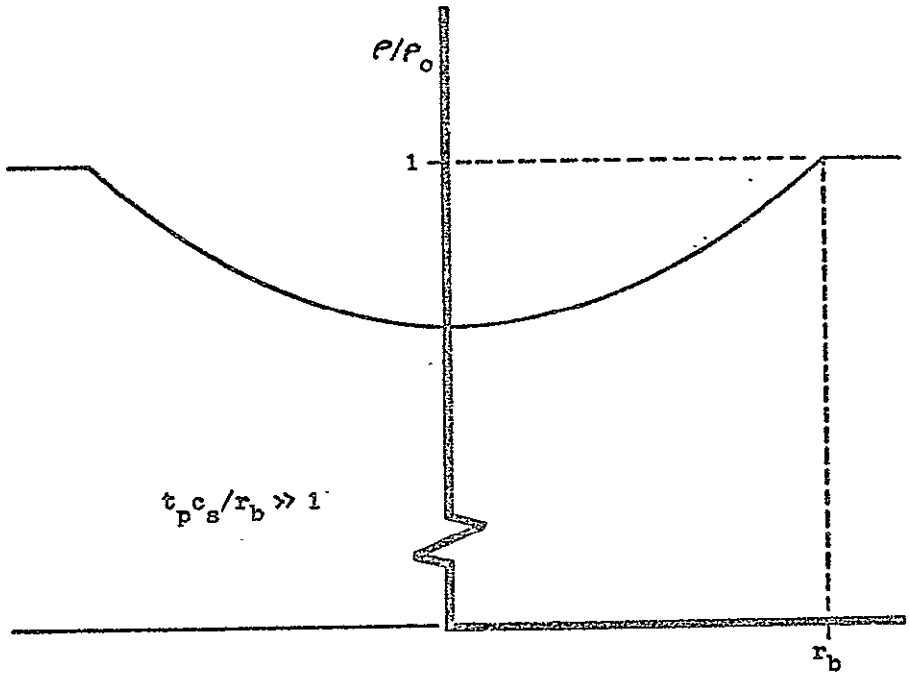

Figure 51. Density produced by weak laser heating of a uniform plasma

which is the time in which the dynamics will produce a favorable density profile. Then to be in the nonconducting regime one must be below the correct $t_a = t_{th}$ line in figure 49. This corresponds to lower plasma temperatures or higher plasma densities.

Beam shrinking corresponds to a reduction in the parameter Γ ; $\Gamma = (r_b/b)^2$. Small values of Γ allow the beam to be trapped for much longer lengths as seen from figures 37 and 40. Of course the smallness of the beam is limited by diffraction effects so that there is a limit on the length that a beam can be contained by beam shrinking. The diffraction limit for a Nd^+ glass laser is shown in figure 52 where the focused laser results of figure 40 are also plotted. For example, at $n_e = 10^{18}/cm^3$ ($\zeta_m = 0.001$) with $b = 1$ cm and $r_b/b = .25$, a column of plasma ~ 10 meters long can be irradiated. The absorption length at 100 eV of 7.2 m is comparable. So an Nd^+ glass laser could be used to prepare such a plasma for later heating by the main laser.

A second approach to longitudinal boring uses the favorable effects of plasma motion that arise during longer laser pulses. The physical process that will ensue is described briefly. When the laser pulse begins, the beam is refracted out of the column in a few diameters. But the absorption and the higher intensity in the center of the beam tends to heat the central portion more strongly. It expands and a very weak density hollow is formed right at the end of the column. As soon as it is formed, the refraction losses cease at the

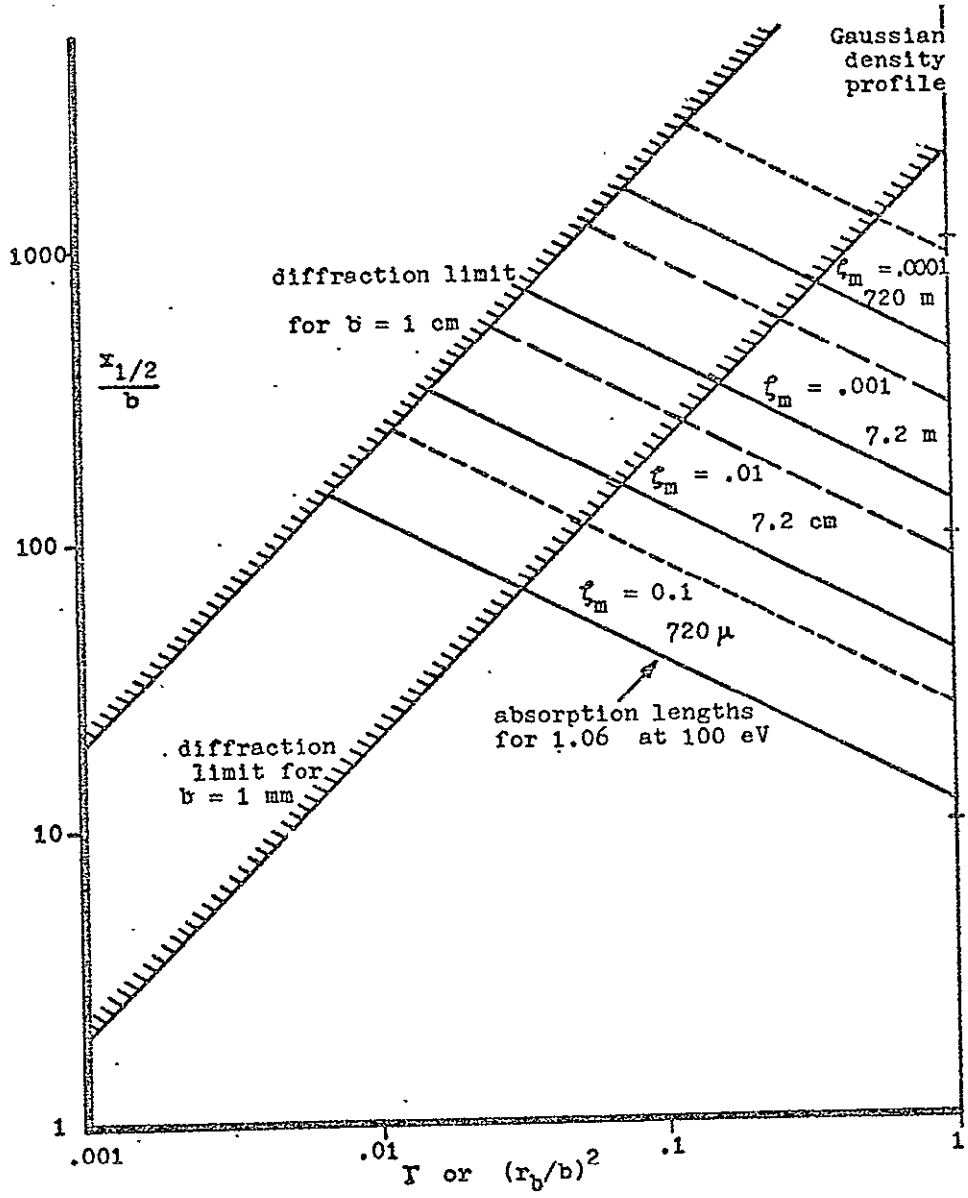

Figure 52. Diffraction limit for a 1.06μ Nd^+ glass laser with a focused laser beam

hollow, so the beam can travel a few more diameters down the column before being refracted out. Stronger heating of the central region of the plasma beyond the density hollow occurs. It then expands and extends the hollow farther down the column. The process continues with the hollow-formation region moving on down the plasma column much like a wave. Behind the hollow-formation region is a trapped beam in a favorable density profile. Ahead of the follow-formation region is a rapidly diverging beam in an unfavorable density profile. The "laser drill" as it might be called is shown schematically in figure 53. So then a curious coupling of the refraction and the dynamics produces a phenomenon whereby the laser actually "drills" out a density hollow in the plasma column. The column is then prepared for the main laser whose beam will propagate down the column without refraction loss.

It is clear that the laser drill will work in the nonconducting regime. But it is not certain that it will work when thermal conduction effects become important--for they tend to prevent the formation of density hollows. The possibility of a laser drill in the isothermal regime is discussed in section B 4.

The velocity of the laser drill is an interesting calculation to make. This cannot be calculated exactly without solving the complete problem in which dynamics and refraction are coupled, but a suitable estimate can be made.

The length of the hollow-formation region is roughly the length in which the beam is refracted out of the unfavorable density region, i.e., $x_{\frac{1}{2}}$. Then the velocity of the drill

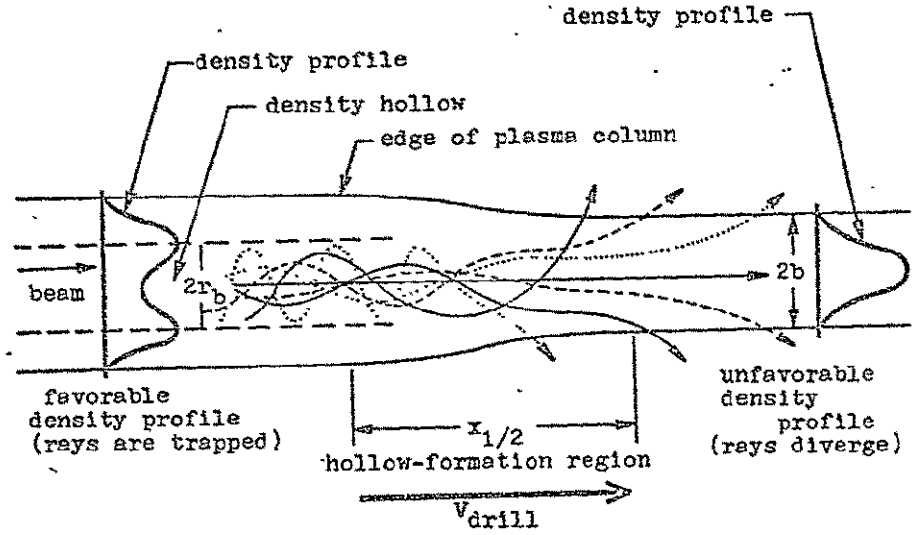

Figure 53. The laser drill

must be on the order of $x_{\frac{1}{2}}$ divided by the acoustic time. Otherwise the drill would be moving faster than the plasma can move to establish a favorable profile--which is impossible. Hence the governing condition is

$$v_{drill} \tilde{=} x_{\frac{1}{2}} / t_a = \frac{x_{\frac{1}{2}}}{2r_b} a$$

where a is the acoustic speed in the plasma. So the drill velocity exceeds the acoustic speed by a factor of $x_{\frac{1}{2}}/2r_b$. This condition is necessary for another reason. If the drill velocity does not significantly exceed the acoustic speed, then the plasma will squirt out the ends of the column before the drill gets moving.

b. Lateral Boring

There is another technique whereby a plasma column may be selectively heated from the sides to produce a favorable density profile. If a laser were fired into the column from the side, then the denser parts of the plasma would absorb more energy. But in an unfavorable profile, the highest density is in the center. Hence, if one is in the nonconducting regime, the hotter center region will expand to produce a density minimum, a favorable profile. The requirement for this regime is simply $t_a < t_{th}$, i.e. below the appropriate line in figure 49, except now the characteristic distance is $2b$ instead of $2r_b$. This merely involves identifying the lines in figure 49 with b instead of r_b. A possible geometry for lateral boring is shown in figure 54.

4

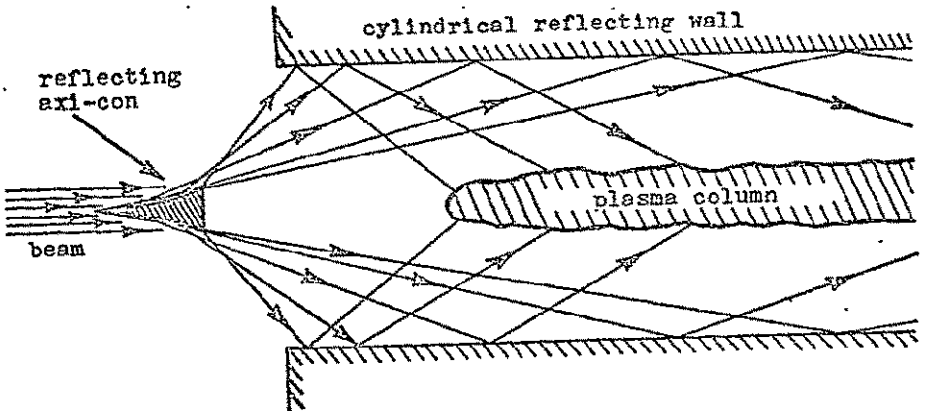

Figure 54. Lateral boring of a plasma column

4. Density Tailoring in the Conducting Regime

The conducting regime is dominated by thermal conduction so that temperature nonuniformities are small. This is a major problem in a plasma with an unfavorable density profile since there must be a higher relative temperature near the axis to achieve a density minimum.

a. Unconfined Plasmas

The problem can be amply illustrated by solving a simple case--weak laser irradiation of an infinite plasma slab in the isothermal regime. Assume small perturbations in temperature $T/T_o = 1 + \theta'$, with $\theta' \ll 1$, where T_o is the temperature of the unheated plasma. Let the dimensionless distance and time be $R = r/r_b$, and $\tau = t/t_p$, respectively. Suppose the heating is slow enough that pressure equilibrium is maintained, i.e., $t_a \ll t_p$. Then the energy equation is

$$\frac{\gamma+1}{\gamma} \frac{\partial \theta'}{\partial \tau} - \eta' \frac{1}{R} \frac{\partial}{\partial R} \left(R \frac{\partial \theta'}{\partial R} \right) = \alpha' \, i(R)$$

where γ is the ratio of specific heats. The thermal conduction parameter, $\eta' = t_p/t_{th}$ is large in the isothermal regime. The absorption parameter $\alpha' = t_p/t_h$ is small for weak heating. The density is assumed to be less than the critical density. The dimensionless intensity profile $i(R)$ is the quotient of the intensity at a point in the beam and maximum intensity.

This equation can be solved using Hankel transforms and has the solution,

$$\theta'(R,\tau) = \frac{\gamma\alpha'}{\gamma+1}\left[i(R) - \int_0^\infty \frac{}{i(s)}\left(e^{-s^2\frac{\gamma\eta'}{\gamma+1}\tau}\right) sJ_o(sR)ds\right], \tag{3-23}$$

where $i(s)$ is the Hankel transform of $i(R)$ and J_o is the Bessel function of order zero. Since the pressure is constant, the density perturbation $\zeta' = (\rho - \rho_o)/\rho_o$ is related to the temperature by $\zeta' = -\theta'$. Examination of (3-23) reveals that the initially uniform density profile decays in roughly the time $\eta'\tau = 1$ ($t_{decay} \tilde{=} t_{th}$) to a steady state profile with a hollow the exact shape of the intensity profile. Thus,

$$\zeta'(R,\tau) = -\frac{\gamma}{\gamma+1}\alpha' i(R) + O(\frac{1}{\eta'\tau}) \tag{3-24}$$

for $\eta'\tau \gg 1$. The resulting density profile resembles that shown 31. The depth of the density hollow is

$$-\Delta\rho/\rho_o|_{R=0} = \gamma t_p/(\gamma+1)\, t_h$$

Thus, it would seem that even in an isothermal plasma, density hollows can be produced. But, as soon as the pulse ends, thermal conduction will fill in the hollow in a time of order t_{th}, so one cannot delay firing the main laser into the favorable density profile.

b. Magnetically Confined Plasmas

The conclusion is a bit optimistic when the reality of a nonuniform initial density profile is faced. Instead of making a density hollow in a uniform density profile, one must make a density hollow out of what begins as a density "hump". This is

a more difficult problem. Complicating the problem is the fact that the magnetic field is nondiffusive as seen from figure 50. The magnetic diffusion time is very slow compared to times of interest, so the magnetic lines of flux remain fixed to the fluid particles. The disadvantage of this is that the plasma has a "memory", it remembers its initial density profile and is inclined to retain a profile of similar shape. Thus, as soon as the laser pulse ends, the nonuniform temperature decays away in a time t_{th} and a density profile resembling the original one is assumed.

A discussion of the problem of heating an isothermal plasma column contained by a nondiffusive magnetic field is given in appendix two. There it is seen that it is impossible to change a density hump to a density hollow in an isothermal plasma contained by a nondiffusive magnetic field.

Thus, the question of making a favorable profile out of an unfavorable one is simply a matter of making the hollow of (3-24) deep enough to over power at least the center of the hump in the density profile. An approximate expression for the net density profile would be simply the sum of (3-24) and the initial profile. This is reasonably accurate under the assumptions of (3-24). It disregards the effect that the overall temperature of the plasma will increase slightly due to the heating.

It becomes even easier to make a density hollow if the radius of the laser beam is somewhat less than the radius of the column. Then the adverse curvature of the density profile

will seem much flatter relative to the narrower beam. This effect is demonstrated in figure 55 for a parabolic density profile and a laser pulse of 22 joules, a column radius $b = 1$ cm, $n_e = 5 \times 10^{18}/cm^3$, $\lambda_o = 1.06\mu$, for various beam radii. It is seen that the smaller beam radii produce deeper but narrower density hollows. The larger beam radii produce no density hollows at all.

Then it is possible to generate a favorable density profile in a conducting plasma. It is done by continuous energy addition to a localized region in the center of the column. This is made possible by the fact that when there is continuous energy addition, the temperature really isn't spatially uniform but may have a density hollow. Therefore there is a possibility of having a laser drill in an isothermal plasma column, if the absorption length is less than the length of the column. It is also possible to use the beam shrinking approach in the conducting regime, except the pulse must be long enough for the ensuing dynamics to create a density hollow.

5. Summary

There are many varied approaches to achieving a plasma column with a favorable density profile. One is to catch the plasma during its formation when it may have a favorable profile due to collapsing or reflecting shock waves. The other is to operate on the quasi-steady plasma column in such a way as to produce a favorable profile.

The laser which is used in the operation need not have the same wave length as the main laser. In fact the low temperatures

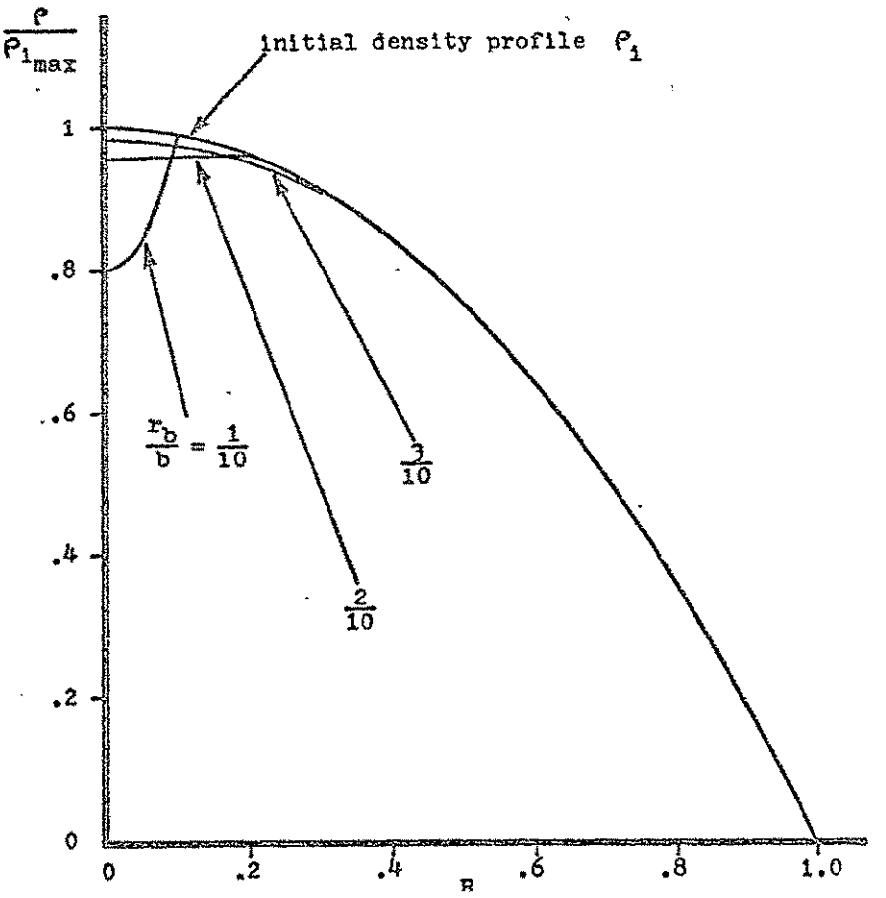

Figure 55. Density hollow boring in an isothermal plasma column

seem to demand a shorter wave length for the pre-laser.

Laser irradiation of a plasma column falls generally into one of two regimes. The nonconducting regime has no thermal conduction and will arise for lower temperatures. The conducting regime is dominated by thermal conduction and occurs for higher temperatures.

If the plasma column is about as long as the absorption length of the pre-laser, then the whole column can be bored out in the center by beam shrinking, making the laser beam narrow enough to travel the entire length without being refracted out. If beam-shrinking doesn't work, then the laser drill can be used whereby the shape of the intensity profile actually drills out a density hollow along the axis. The plasma column can also be bored by heating from the side (in the nonconducting regime).

There are certain peculiarities of the conducting regime. It is possible to generate a density hollow but it persists only as long as the laser pulse. After the pulse ends, the "memory" of the nondiffusive magnetic field returns the plasma to an unfavorable profile much like it had in the beginning.

C. APPENDICES

Appendix 1

Behavior Near the Axis and Near Caustics

Applying directly the results of geometrical optics leads to infinite electric fields at both caustics and at the axis. They arise at caustics since the rays envelope. They arise at the axis simply due to the cylindrical symmetry, a wave collapsing to the axis will generate a singularity in the intensity (at least in the linear case). But singularities in electric fields do not occur in nature and thus there must be an effect that limits the magnitude of the electric field. The failure of geometrical optics can reasonably be expected--one cannot apply it to phenomena occuring in lengths shorter than a wave length.

The study of these singularities begins with an examination of the full linear equations. Eliminating the magnetic field intensity from Maxwell's equations, an equation for the electric field can be found,

$$0 = \nabla\times(\nabla\times\vec{E}) + \mu\frac{\partial\vec{J}}{\partial t} + \frac{1}{c_o^2}\frac{\partial^2\vec{E}}{\partial t^2} \quad , \tag{3-25}$$

where $\vec{E}$ is the electric field intensity and $\vec{J}$ is the current density. Consider only the current due to electrons, $\vec{J} = -en_e\vec{v}_e$ where $\vec{v}_e$ is the mean electron velocity which is governed by an electron momentum equation,

$$m_e \frac{\partial \vec{v}_e}{\partial t} = -e\vec{E} - \frac{m_e \vec{v}_e}{\tau_{ei}} \qquad (3\text{-}26)$$

The last term in (3-26) is the electron-ion collision term. It assumes the electrons lose their ordered oscillatory motion to random motion due to collisions in a time τ_{ei} . τ_{ei} is the electron-ion collision time. Considering only oscillatory fields, $\vec{E} = \vec{E}(r,z)e^{-i\omega t}$, then all time derivatives can be replaced by the factor $-i\omega$. Then (3-25) and (3-26) combine to yield

$$\nabla^2\vec{E} - \nabla(\nabla\cdot\vec{E}) + k^2\vec{E} = 0 \quad , \qquad (3\text{-}27)$$

where k is the magnitude of the wave vector

$$k^2(r) = \frac{\omega^2}{c_o^2}\left[1 - \frac{\omega_p^2}{\omega^2+1/\tau_e^2}(1-i/\omega\tau)\right]$$

which depends only on r .

If attention is confined to the case where the electric field is in the azimuthal direction, then (3-27) becomes

$$\frac{\partial^2 E}{\partial z^2} + \frac{1}{r}\frac{\partial}{\partial r}\left(r\frac{\partial E}{\partial r}\right) + k^2 E = 0 \quad . \qquad (3\text{-}28)$$

Suppose now that in addition to k being independent of z , that E is also independent of z except for periodic spatial oscillations. This assumption is not exactly true in a real plasma column irradiated from the end by a laser. In that case, rays entering the column at different points will trace somewhat different shaped paths. This model has all rays tracing

the same paths--so will only be locally valid. In other words, the behavior of a particular ray in the real case is being simulated by a solution in which all rays trace the same shaped path as that particular ray.

Then one can take $E = F(r)\exp[\pm k(r)\sin\theta(r)\, z]$ where $\theta(r)$ is the angle between the wave vector and the r axis. Then (3-28) becomes, eliminating the dependence on z :

$$\frac{1}{r}\frac{d}{dr}\left(r\frac{dF}{dr}\right) + [k^2(r) - k_o^2\sin^2\theta(r)]F = 0 \quad , \tag{3-29}$$

and

$$k(r)\sin\theta(r) = k_o\sin\theta_o \quad , \tag{3-30}$$

where k_o is the wave vector at $r = 0$ and θ_o is its angle with the r axis at $r = 0$. (3-30) is the condition that must be satisfied to eliminate the dependence of F on z . (3-30) also gives the angle of the rays at a particular r and gives the "turning point" where a ray is reflected. Figure 56 plots the radial position of the turning point versus the angle of the ray as it emanates from the axis for the case of the parabolic density profile (3-14) with $\zeta_m = 0.1$.

The turning point in this approximate model corresponds to the point where a ray borders the caustic in the real problem. In the real problem the ray touches the caustic a short distance after achieving the maximum distance from the axis--not right at the maximum point.

Applying (3-29) to a parabolic density profile (3-14) yields,

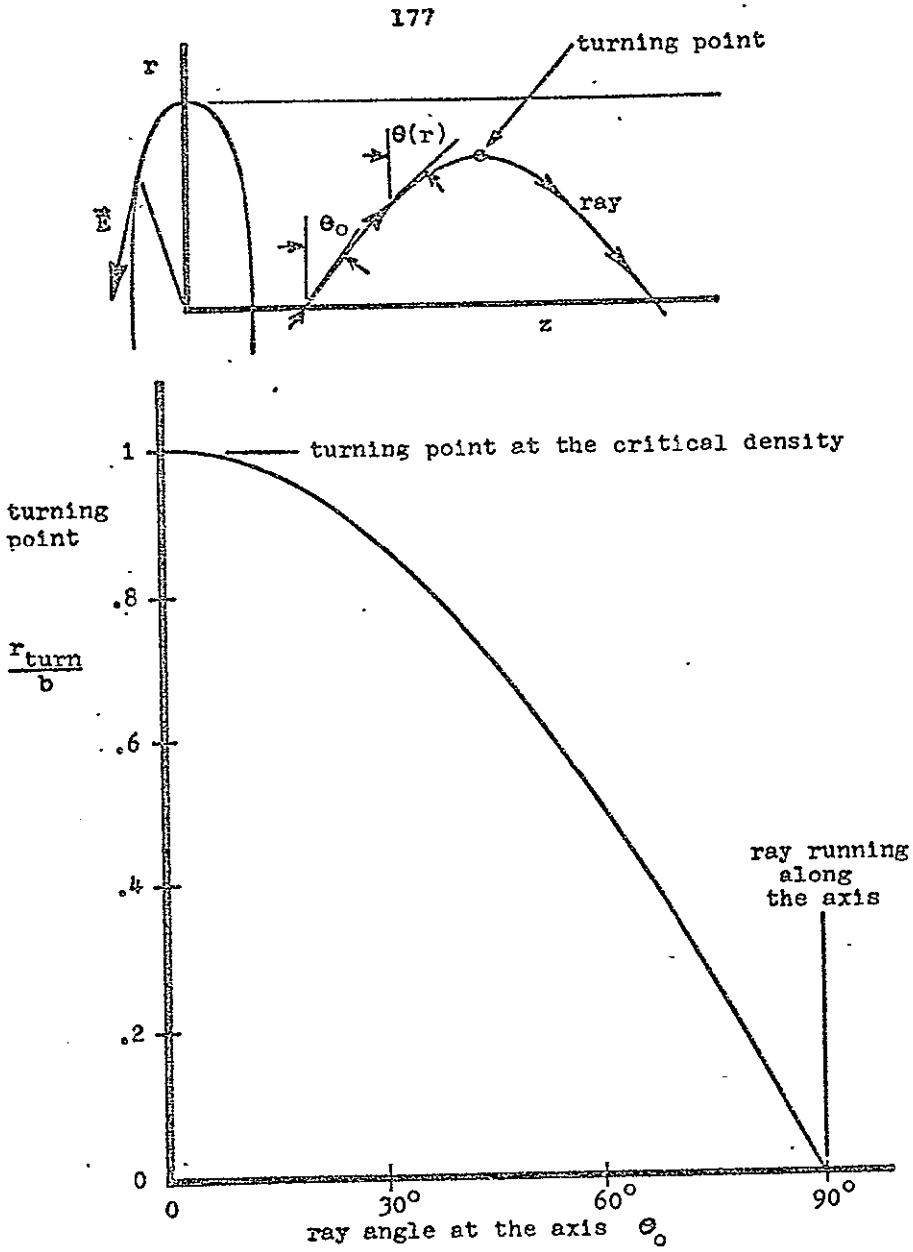

Figure 56. Turning point of a ray in a parabolic density profile

$$r\frac{d}{dr}\left(r\frac{dF}{dr}\right) + r^2\frac{\omega^2}{c_o^2}(1-\zeta_m)\left[\cos^2\theta_o - \frac{r^2}{a^2} + O\left(\frac{1}{\omega\tau_{ei}}\right)\right]F = 0 \quad . \qquad (3\text{-}31)$$

It is seen that the coefficient of F in (3-31) becomes small at two places; at $r = 0$ it actually vanishes, and near $r = b \cos\theta_o$ (the turning point) where the coefficient becomes small (of order $1/\omega\tau$). Near the turning point, $r = b\cos\theta_o$, the solutions are Bessel functions of one third order,

$$F \approx \text{const}\; y^{1/3}\left(J_{1/3}(y) + J_{-1/3}(y)\right) \quad ,$$

with

$$y = \frac{b\omega}{c_o}\frac{2(1-\zeta_m)\cos\theta_o}{\cos^2\theta_o+\zeta_m\sin^2\theta_o}\left[(\cos\theta_o - \frac{r}{b})\frac{2(1-\zeta_m)\cos\theta_o}{\cos^2\theta_o+\zeta_m\sin^2\theta_o} - \frac{i}{\omega\tau}\right]^{3/2}$$

where $b\cos\theta_o - r \ll b$.

This type of solution has been discussed by Ginzburg.[21] Physically it represents a standing wave pattern near the turning point due to the superposition of the incoming and reflected rays. There is not a real singularity since $y^{1/3}J_{-1/3}(y)$ approaches a constant value as $y \to 0$. The electric field intensity near the turning point will exceed that in nonsingular regions by a factor on the order of $(b\omega/c_o)^{1/6}$.

Near the axis, $r = 0$, (3-31) approaches Bessel's equation of zero order so that the solution will be for $r \ll b$,

$$F \approx \text{const}\; J_o\left(\frac{\omega r}{c_o}\sqrt{1-\zeta_m}\right) + \text{const}\; Y_o\left(\frac{\omega r}{c_o}\sqrt{1-\zeta_m}\right)$$

where J_o and Y_o are the Bessel functions of zero order of the first and second kinds respectively. It is Y_o that has an actual singularity. Geometrical optics predicts a $1/r$ singularity in the intensity or a $1/r^{\frac{1}{2}}$ singularity in the electric field. For large values of the argument of Y_o,

$$Y_o\left(\frac{\omega r}{c_o}\sqrt{1-\zeta_m}\right) \approx \left(\frac{2c_o}{\pi\omega r\sqrt{1-\zeta_m}}\right)^{1/2} \sin\left(\frac{\omega r}{c_o}\sqrt{1-\zeta_m} - \frac{5\pi}{12}\right) ,$$

which (aside from the oscillatory part) varies like $1/r^{\frac{1}{2}}$ and agrees with geometrical optics. But geometrical optics fails for distances smaller than a wave length, $r < c/\omega$, i.e., when the argument of Y_o becomes small. Then,

$$Y_o\left(\frac{\omega r}{c_o}\sqrt{1-\zeta_m}\right) \approx \frac{2}{\pi} \log\left(\frac{\omega r}{c_o}\sqrt{1-\zeta_m}\right)$$

which is a much weaker singularity--though nonetheless still present. Physically this means that most of the wave is reflected within a wave length of the axis and only a small part ever converges all the way to the axis to generate a singularity.

Of course the axial singularity is not a real one. Nonlinear effects will stop the singularity at some point. Moreover the significance of the singularity is doubtful anyway. Only for small distances much less than a wave length) will the electric field be very large. But the electron mean free path (for collisions with ions)is never much less than the laser wavelength for thermonuclear plasmas. There can be no

heating without electron-ion collisions, hence the temperature couldn't have a singularity even if the electric field did.

There is another effect that has been observed along the axis of a laser beam. That is the collapse of part of the beam into an intense filament.[34] This has been attributed to nonlinear effects of intensity on the index of refraction.[35,36] This effect--which is not well understood--may hold possibilities for the trapping of very narrow laser beams.

Appendix 2

Heating of Conducting Plasmas Contained by Nondiffusive Magnetic Fields

A solution has been found for the heating and expansion of a plasma column which is in the conducting regime. The heating is slow enough that pressure equilibrium is maintained, $t_a \ll t_h$, and the heating is conducting, $t_{th} \ll t_a$. This requires a plasma temperature above the line $t_h = t_a$ in figure 47 and above the line $t_a = t_{th}$ in figure 49.

In a cylindrical magnetic field, the magnetic field, B, is related to the magnetic flux, Φ_B, by

$$B = \frac{1}{2\pi r} \frac{\partial \Phi_B}{\partial r}$$

Since the field is nondiffusive, Φ_B is fixed to the fluid particles and moves with them. The displacement function for a particle is $r = X(r_o, t)$, where X is the location at time t of the particle that was at r_o when $t = 0$. Then Φ_B

is a function of r_o alone, so that

$$B = \frac{d\Phi_B/dr_o}{X \frac{\partial X}{\partial r_o}}$$

Then the magnetic pressure $p_B = B^2/2\mu$ becomes

$$p_B = p_{B_o} r_o^2/X \frac{\partial X}{\partial r_o} \qquad (3\text{-}32)$$

where $p_{B_o}(r_o)$ is the magnetic pressure profile before the heating; $t = 0$.

Nondimensionalizing the variables, the pressure scale is the total pressure before the heating. The temperature scale is the initial temperature which is spatially uniform like the pressure. The density scale is the maximum initial density which is on the axis. Then the equation of state is the pressure, Π , equals the sum of the magnetic pressure Π_B and the thermodynamic pressure $\zeta\theta$,

$$\Pi = \zeta\theta + \Pi_B \quad . \qquad (3\text{-}33)$$

Initially, the equation of state is,

$$1 = \zeta_o + \Pi_{B_o} \qquad (3\text{-}34)$$

The Lagrangian continuity equation relates the density to its initial value using the displacement function,

$$\zeta X \frac{\partial X}{\partial r_o} = \zeta_o r_o \qquad (3\text{-}35)$$

where $\zeta_o(r_o)$ is the initial density profile (at $t = 0$). Then, combining (3-32, 33, 34, 35), an equation for X results,

$$\Pi\left(X\frac{\partial X}{\partial r_o}\right)^2 - \theta r_o \zeta_o \left(X\frac{\partial X}{\partial r_o}\right) - (1-\zeta_o) r_o^2 = 0 \qquad (3\text{-}36)$$

Since Π and θ are spatially uniform and depend only on time, (3-36) can be integrated exactly and has the solution

$$X^2 = \frac{\theta}{\Pi}\int_0^{r_o} \left[\zeta_o + \sqrt{\zeta_o^2 + \frac{4}{\Pi}(1-\zeta_o)}\right] r_o dr_o \qquad (3\text{-}37)$$

The density profile ζ can be written using (3-35) and (3-36),

$$\zeta = \frac{\frac{2\Pi}{\theta}}{1 + \sqrt{1 + \frac{4\Pi}{\theta^2}\frac{1-\zeta_o}{\zeta_o^2}}} \qquad (3\text{-}38)$$

The pressure, Π, and temperature, θ, are functions of time which depend on the laser power and on the character of the confining magnetic field.

Unfortunately, (3-38) gives ζ as a function of r_o, but one is interested in $\zeta(r)$. It is then necessary to invert the displacement function found in (3-37); $r_o = X^{-1}(r,t)$, which probably cannot be found explicitly in most examples of interest. But at least the solution is available in quadrature form.

The solution has been calculated for the case of a parabolic initial density profile, $\zeta_o = 1 - (r_o/b)^2$. The displacement function using dimensionless variables, $y = r/b = X/b$ and $x = r_o/b$, is

$$y^2 = \frac{\theta}{2\Pi}\left[x^2 - \frac{1}{2}x^4 + \frac{2x^2+\Lambda}{4}\sqrt{1+\Lambda x^2+x^4} - \frac{\Lambda}{4} + \frac{4-\Lambda^2}{8}\log\frac{2x^2+\Lambda+2\sqrt{1+\Lambda x^2+x^4}}{\Lambda+2}\right], \qquad (3\text{-}3$$

where $\Lambda = \frac{4}{\Pi} - 2$.

An approximate expression for the density profile near the axis is

$$\zeta = \frac{\Pi}{\theta}\left(1 - \frac{\Pi^2}{\theta^3}y^2 + O(y^4)\right) \qquad (3\text{-}40)$$

It is seen that it is impossible in an isothermal plasma to change an unfavorable density profile to a favorable one. (3-40) shows that it is still unfavorable with maximum ζ on the axis. The only way then to get a favorable profile is to have continuous localized laser heating as described in section B 4. Then a small density hollow can be maintained as long as the laser pulse lasts.

Chapter Four

DIFFUSION WAVE PHENOMENA

A. THE BLEACHING WAVE

One of the really interesting results of chapter II on laser heating of a stationary plasma was the appearance of the so called bleaching wave. This phenomenon differs significantly from the usual linear absorption. In the linear absorption problem, light is attenuated by a substance whose absorption coefficient is a constant. The result is that the intensity decays in simple exponential fashion.

In the case of laser plasma heating, the absorption coefficient is not a constant but decreases with increasing electron temperature ($K_\nu \sim T_e^{-3/2}$) . Generally, K_ν is quite large in the unheated plasma so that the radiation is attenuated in a very short distance, i.e., the plasma is opaque to the radiation. If the absorption coefficient is large, then all the laser energy is added to a very thin layer of plasma. The energy addition causes the temperature to increase rapidly, so that K_ν decreases--even more rapidly. Thus, the layer becomes successively more transparent as time proceeds.

Then the overall behavior is characterized by the propagation of a bleaching wave into the plasma. Successive layers absorb the radiation and become transparent. In essence, the radiation bores its way into the plasma. Behind the wave, the plasma is highly excited and nearly transparent, so that the radiation is only weakly attenuated. In the front

of the wave is a region of rapid attenuation of the radiation and consequently rapid "heating". Ahead of the wave is a weak exponentially damped beam in a "cold" plasma, closely resembling a linear absorption problem.

The term bleaching wave is an appropriate name for this phenomenon. As the wave moves, it bleaches the opaque plasma, making it transparent to the laser radiation.

It seems intuitive that any material having an absorption coefficient that decreases under continuous radiation--will exhibit a bleaching wave behavior. This is indeed true and several illustrative examples are discussed. However, first a presentation of a general example is given to demonstrate the bleaching wave.

The radiative transfer equation for radiation propagating in the +x-direction and neglecting thermal radiation is

$$0 = \frac{\partial I_\nu}{\partial x} + K_\nu I_\nu \quad , \tag{4-1}$$

where I_ν is the radiation intensity. The absorption coefficient is some function of the temperature and the density, ρ, $K_\nu = K_\nu(\rho, x)$. The energy equation for a stationary substance is

$$\rho(x) C_v \frac{\partial T}{\partial t} = - \frac{\partial I_\nu}{\partial x} \tag{4-2}$$

where the right member represents the divergence of the energy flux (intensity), C_v is the constant volume specific heat,

and $\rho(x)$ is the density. The initial condition is the spatial temperature distribution at time $t = 0$; $T(x,0) = T_o(x)$. The boundary condition is the intensity entering the substance at its edge ($x = 0$); $I_\nu(0,t) = I_{\nu_0}(t)$ which is the intensity delivered by the laser.

Combining (4-1) and (4-2) yields a second order partial differential equation

$$0 = \frac{\partial}{\partial x}\left[\frac{1}{K_\nu}\frac{\partial}{\partial t}(\rho T)\right] + \frac{\partial}{\partial t}(\rho T) \qquad (4\text{-}3)$$

In general, the absorption coefficient is a function of ρ and T : $K_\nu = K_\nu(\rho,T)$. This can also be expressed as a function of ρ , and ρT : $K_\nu = K_\nu^*(\rho,\rho T)$. Over any given range of the variable ρT , the anti-derivative of $1/K_\nu^*$ with respect to ρT exists such that

$$\frac{\partial L(\rho,\rho T)}{\partial(\rho T)} = \frac{1}{K_\nu^*(\rho,\rho T)} \qquad (4\text{-}4)$$

L being the anti-derivative. The anti-derivative is not unique because if any function of ρ is added, (4-4) is still satisfied. Then one can say that $L(\rho,\rho T) = L_o(\rho,\rho T) + F(\rho)$, where L_o is chosen as the principle anti-derivative and $F(\rho)$ is an arbitrary function.

Based on the existence of the anti-derivative, and the independence of ρ on time, (4-3) can be rearranged to give,

$$0 = \frac{\partial}{\partial t}\left[\frac{\partial}{\partial x}\,(L_o + F) + \rho T\right] \qquad (4\text{-}5)$$

Using the initial condition $T(x,0) = T_o(x)$, (4-5) can be integrated with respect to time to yield,

$$0 = \frac{\partial}{\partial x}\left[L_o(\rho,\rho T) - L_o(\rho,\rho T_o)\right] + \rho T - \rho T_o \qquad (4\text{-}6)$$

Notice that the arbitrary function $F(\rho)$ has disappeared in the application of the initial conditions.

The boundary condition can be written as

$$I_{\nu_o}(t) = \frac{C_v}{K_\nu}\frac{\partial(\rho T)}{\partial t}\Big|_{x=0}$$

which in turn can be integrated, applying the initial condition to yield

$$\left[L_o(\rho,\rho T) - L_o(\rho,\rho T_o)\right]\Big|_{x=0} = \frac{1}{C_v}\int_o^t I_{\nu_o}(t')dt' \,. \qquad (4\text{-}7)$$

The first order partial differential equation (4-6) together with the boundary condition (4-7) comprise a well posed problem. These are the general equations governing temperature in a one-dimensional medium irradiated by a laser.

If the absorption happens to be linear (K_ν independent of ρT), then L_o is just $\rho T/K_\nu$. Then the familiar exponential decay temperature profile will appear. For

example, if the initial temperature is zero, density, laser intensity, and absorption coefficient are constant, then the temperature profiles are

$$T = \frac{K_\nu I_{\nu o}}{\rho C_\nu} t\, e^{-K_\nu x}$$

The temperature is exponentially damped as one moves into the plasma, and rises with a uniform time factor as time moves on. This illustrates the basic character of linear absorption.

There are two types of nonlinear absorption; K_ν decreasing or increasing with temperature. The former rarely occurs in nature and does not produce a bleaching wave except in the case of a focused beam. The latter leads to the bleaching wave.

(4-6) cannot be integrated in general. Three physical examples are presented for which solutions to (4-6) have been found. Laser heating of a stationary plasma was presented in chapter II. Laser irradiation of a resonant two level substance, and the laser induced breakdown wave are presented in this section.

1. Laser Irradiation of a Two Level Substance

Generally an atom or molecule has many discrete energy levels in its internal structure. A molecule has one or more vibrational modes, each with its own set of energy levels and the corresponding quantum numbers. An atom also has a complex set of energy levels and corresponding quantum numbers.

Transitions by individual particles from one energy level to another are made by several means. For example, a particle in a lower energy state of energy E_1 can be raised to a higher energy state E_2 by the absorption of a photon of of exactly the right energy; $h\nu = E_2-E_1$. Or, a particle in the higher energy state when bombarded by the same photon, will drop to the lower energy state, emitting a photon of the same energy--so that two identical photons result, which is called stimulated emission.

Consider a substance that has more particles in the lower energy state that is being irradiated by a laser of exactly the right wave length so that $h_\nu = E_2-E_1$. Then, on the statistical average more photons are being absorbed than are being emitted by stimulated emission. This is simply because more particles are in the "absorbing" state than are in the "emitting" state. But, as the beam is absorbed, more and more of the particles are raised to the upper level, so that the number in the upper level approaches the number in the lower level. Now, the absorption is much weaker since the ratio of absorbed to emitted photons is reduced to near one. Eventually, the numbers in the two levels will be equal so that there is no absorption at all, because the number being emitted is equal to the number being absorbed.

It is immediately seen that this is exactly the same phenomenon that occurs in the laser heating of a plasma. The local absorption coefficient diminished with time under continous irradiation.

This sort of phenomena is known as saturable absorption, a type of nonlinear absorption. It has been studied extensively since it is this sort of substance that makes a laser or a laser amplifier. The only difference is that for a laser, there are more particles in the upper energy state than the lower so that a beam of the right wave length is amplified rather than being attenuated.

The solution to this problem was first worked out independently by Bellman, et. al.,[37] by Frantz and Nodvik,[38] and by Schultz-Dubois.[39] Each worked out the general time dependent solution in a two level substance. These papers neglected spontaneous emission and thermal relaxation from the upper energy level which is appropriate for short time scales. Bellman, et. al., pointed out the appearance of a phenomena whereby the radiation "bores" its way through the substance with a certain velocity which is simply a bleaching wave. Later, Siegmann[40] worked out the solution neglecting the transient term in the radiative transfer equation. He obtained the same results as in the original studies but in a much easier manner with more lucid results according to his claim.

Presented below is a simple solution of laser irradiation of a two level substance. This calculation is similar to the approach of Siegmann but it is instructive in that it clearly demonstrates the bleaching wave.

The radiative transfer equation has the usual form (4-1). For this problem the energy equation takes a slightly different form,

$$h\nu \frac{\partial n_u}{\partial t} = - \frac{\partial I_\nu}{\partial x} \qquad (4\text{-}8)$$

where n_u is the number density of particles in the upper state and is analogous to the temperature in (4-2). h is Planck's constant and ν is the frequency of the radiation. Of course the sum of the number densities in the upper (n_u) and lower (n_ℓ) states in a constant (n) .

In a two level substance, the absorption coefficient is

$$K_\nu = \sigma_\nu (n_\ell - n_u) \qquad (4\text{-}9)$$

where σ_ν is the absorption cross section of the radiation. The initial condition is

$$n_u(x,0) = n_{uo}(x) \qquad (4\text{-}10)$$

The boundary condition is $I_\nu(0,t) = I_{\nu o}(t)$. (4-8) and (4-9) combine to yield,

$$0 = \frac{\partial}{\partial x}\left(\frac{1}{K_\nu} \frac{\partial n_u}{\partial t} \right) + \frac{\partial n_u}{\partial t} \qquad (4\text{-}11)$$

$1/K_\nu^*$ has as its principle anti-derivative, $-(1/2\sigma_\nu)\log(n-2n_u)$ so that (4-11) can be integrated with time. Performing the integration and applying the initial condition yields,

$$0 = -\frac{1}{2\sigma_\nu} \frac{\partial}{\partial x} [\log(n-2n_u) - \log(n-2n_{u_o})] + n_u - n_{u_o} \qquad (4\text{-}12)$$

This is in the same form as (4-6) with ρT replaced by n_u. The boundary condition is

$$-\frac{h\nu}{2\sigma_\nu}\left[\log(n-2n_u)-\log(n-2n_{uo})\right]\Big|_{x=0} = \int_o^t I_{\nu_o}(t')dt' \qquad (4\text{-}13)$$

which is analogous to (4-7).

A particularly simple solution is available for the case n_{uo} = const. Solving (4-12) for this case gives the solution,

$$\eta = \eta_o + \tfrac{1}{2}(1-\eta_o)\{1+\tanh[(1-\eta_o)(\xi_w-\xi)]\} \quad , \qquad (4\text{-}14)$$

where $\eta = 2n_u/n$ is the dimensionless measure of n_u. $\xi = x/\Delta x$, and $\tau = t/\Delta t$ are dimensionless distance and time respectively. The length scale is $\Delta x = 2/\sigma_\nu n$ and the time scale is $\Delta t = h\nu/2\sigma_\nu \bar{I}_o$, $\bar{I}_o$ being the average incident intensity. The position of the wave as a function of time is given by

$$\xi_w(\tau) = \frac{1}{2(1-\eta_o)}\int_o^\tau \tilde{I}_o d\tau' + \log\{1-\exp[-\int_o^\tau \tilde{I}_o d\tau']\}$$

where $\tilde{I}_o = I_{\nu_o}/\bar{I}_o$. The number density is seen to be a hyperbolic tangent function. It raises η from η_o ahead of the bleaching wave ($\xi \gg \xi_w(\tau)$) to 1 behind the wave ($\xi \ll \xi_w(\tau)$). When $\eta = 1$, the substance is said to be "saturated".

The expression for $\xi_w(\tau)$ is composed of a steady state term and a transient term. Considering only the steady state term, the velocity of the bleaching wave is given by

$$V_w = \frac{\tilde{I}_o(\tau)}{2(1-\eta_o)} \frac{\Delta x}{\Delta t}$$

The velocity of the bleaching wave can also be found by using the conservation of energy. This is done by requiring that the energy flux delivered by the laser (energy per unit time per unit area) must be equal to the energy required per unit volume to bleach the substance times the velocity of the bleaching wave. The calculation is made possible by the fact that essentially all of the laser energy is added to a thin region, the "front" of the bleaching wave. However, the conservation of energy cannot be used to calculate the velocity of the bleaching wave in a plasma. For this case the energy continues to be added to the plasma far behind the actual front of the bleaching wave. A plasma never saturates completely as does a two level substance since an infinite plasma temperature is required for perfect transparency.

The thickness of the bleaching wave is roughly the distance in which the argument of the hyperbolic tangent makes a change of one, so that

$$\Delta x_w \sim \frac{\Delta x}{1-\eta_o}$$

For the particular example of $\eta_o = 0$ (no molecules initially

in the upper state) and a uniform laser pulse, $\tilde{I}_o = 1$, the solution becomes

$$\eta = \tfrac{1}{2}[1 + \tanh(\xi_w - \xi)] ,$$

$$\xi_w = \tfrac{1}{2}\tau + \ln(1-e^{-\tau})$$

$$V_w = \tfrac{1}{2}\frac{\Delta x}{\Delta t}$$

This example is shown graphically in figure 57. Also shown in the same figure are temperature profiles for the heating of a uniform stationary plasma by a uniform laser pulse. While certain features differ between the two phenomena, a bleaching wave is seen to appear in both. Ahead of the wave there is apparently little radiation since the variable (η or θ_e) changes slowly. In the front of the wave, the variable rises rapidly, due to strong irradiation and large absorption coefficient. Behind the wave, the variable rises much more slowly due to bleaching as the absorption coefficient goes to zero.

2. Laser Induced Breakdown Wave

For many conditions, an un-ionized gas such as air is essentially transparent to laser radiation. At least the absorption lengths are quite long compared to absorption lengths that arise in partially and fully ionized gases, or from resonant line absorption (section A 1). Nevertheless, an extremely intense laser beam can cause breakdown of the gas. This phenomenon was first observed experimentally by

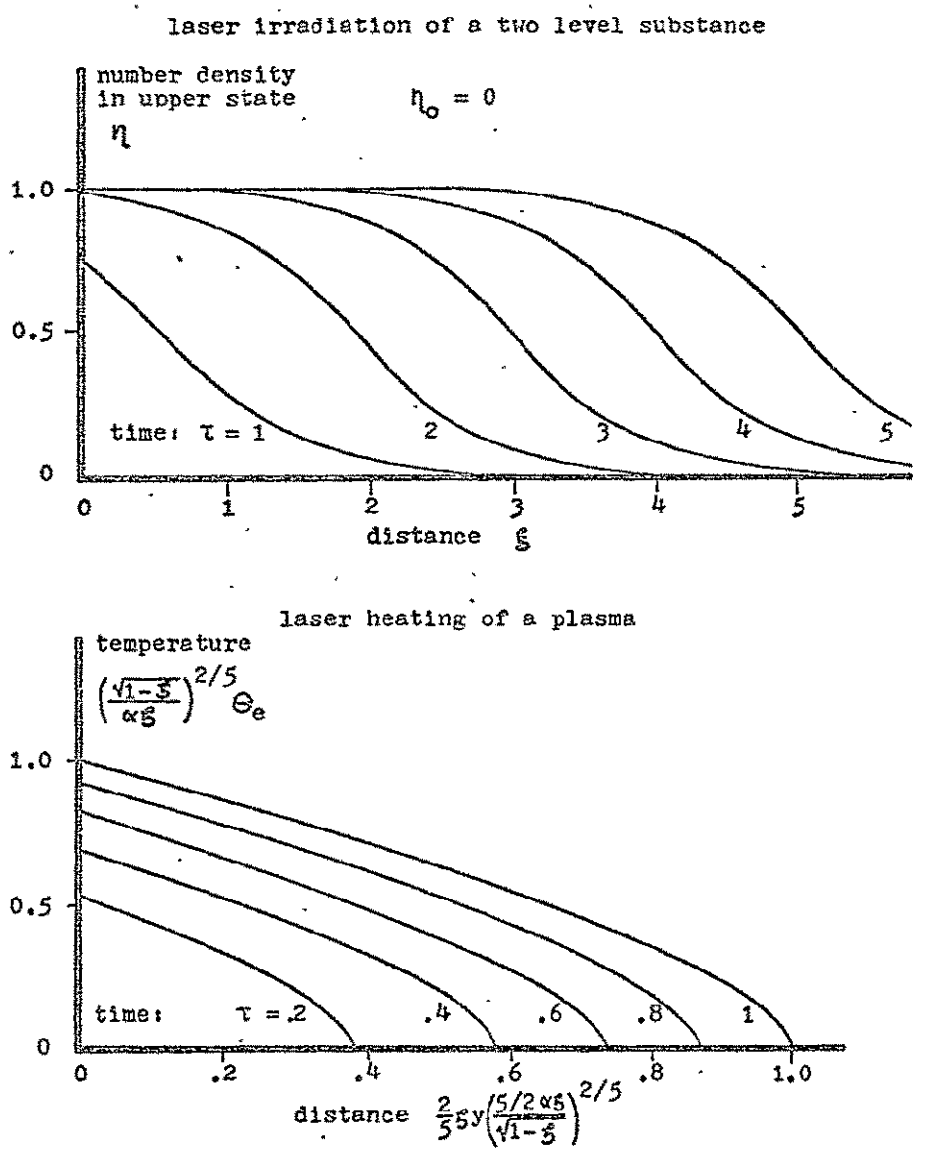

Figure 57. Comparison of bleaching waves

Damon and Tomlinson[41] and by Meyerand and Haught.[42]

Studies of the mechanism of laser induced breakdown show that the breakdown begins with either stray free electrons in the gas, or with electrons produced by the multiphoton effect. The multiphoton effect is due to the simultaneous bombardment of an atom by several quanta of light, with enough total energy to free an electron. Once an electron is free, the large oscillating electric field causes the electron to collide with atoms and free more electrons. The cascading process produces a large number of electrons in a very short time. A clearly defined threshold intensity characterizes this breakdown. Several theoretical investigations of the breakdown phenomena followed the experimental discovery.[43,44,45,46,47]

The dynamical behavior following the initial breakdown was seen to exhibit unusual effects. The expansion of the ionized region was not uniform in all directions. Rather, it moves much more rapidly in the cone of the focused laser beam. This phenomena was first explained by Ramsden and Savic[48] and was shown to be a radiative detonation wave, that is a detonation wave whose fuel is the energy absorbed from the laser beam.

If the intensity of the laser beam appreciably exceeds the threshold intensity for breakdown at the focus, then another phenomena can occur. In this case the intensity will also exceed the threshold over a certain length of the beam and breakdown will occur at these points also. The gas in

the breakdown region is stationary and the wave like propagation of the region towards the laser source is due to the breakdown limit being reached at successively longer times for points closer to the source. The speed of this "breakdown wave" may exceed the speed of all of the possible gas dynamical processes. The breakdown wave was studied by Raizer[49] and its speed was calculated by a phenomenological model.

It is shown here that the breakdown wave is governed by equations which give the bleaching wave solution. The only variation is due to the non-one-dimensional geometry which causes the wave to move backwards, i.e., moving towards the laser source as contrasted to the usual sense of a bleaching wave moving away from the source. Otherwise one sees all the usual features of a bleaching wave. On one side of the wave (behind) is an opaque plasma. On the other side (ahead) is a transparent un-ionized gas. The heating of the gas is done by absorption of the laser radiation--most of which occurs very rapidly at the front of the wave.

The nature of the breakdown wave as a bleaching wave is seen by considering a solution to a simple breakdown model. The radiative transfer equation is given in terms of the power , W ,

$$\frac{\partial W}{\partial x} - KW = 0 \qquad (4\text{-}15)$$

The opposite sign from the usual equation arises since the

beam is assumed to travel in the -x direction as shown in figure 58. Figure 58 also shows the geometry of the focal region. At any point the intensity is related to the power by $I = W/A(x)$, where $A(x)$ is the cross sectional area of the beam.

The energy equation is

$$\rho A(x) C_v \frac{\partial T}{\partial t} = \frac{\partial W}{\partial x} \tag{4-16}$$

where $\rho A(x)$ is analogous to the density in (4-2) and the power W is analogous to the intensity. Combining (4-15) and (4-16) yields,

$$0 = \frac{\partial}{\partial x}\left(\frac{A(x)}{K}\frac{\partial T}{\partial t}\right) - A(x)\frac{\partial T}{\partial t}$$

which is clearly analogous to (4-3).

This problem can be easily solved with the following two assumptions. First the absorption coefficient is given by

$$K = \frac{I}{\ell} H(n_e - n_{et}) \tag{4-17}$$

where ℓ is a short absorption length, n_{et} is the electron number density for breakdown, and $H(\ )$ is the Heaviside function. Thus there is no absorption for electron densities below the threshold, and strong absorption above the threshold.

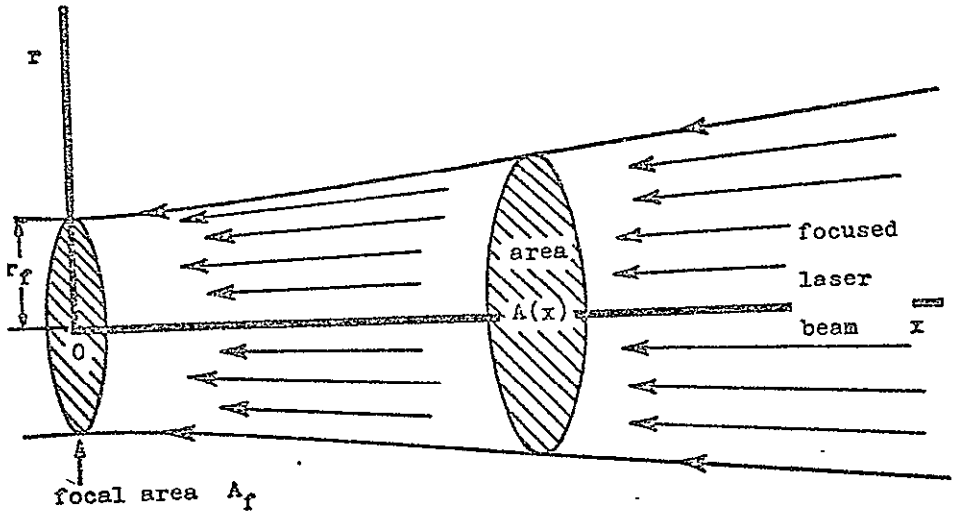

Figure 58. Geometry of the focal region

Following Raizer,[49] the second assumption is that the electron number density grows at a rate proportional to the intensity times the number density,

$$\frac{\partial n_e}{\partial t} = \left(\frac{A_f}{t^* W_{max}} \right) \frac{n_e W}{A(x)} \tag{4-18}$$

where A_f is the focal area, W_{max} is the maximum power and t^* is the characteristic time of breakdown at the focal area.

Since the absorption coefficient depends on the electron density, it is easier to solve the problem in terms of n_e and then find the temperature.

Solving (4-18) for W and applying to (4-15) to eliminate W yields

$$0 = \frac{1}{K} \frac{\partial}{\partial x} \left(\frac{A(x)}{n_e} \frac{\partial n_e}{\partial t} \right) - \frac{A(x)}{n_e} \frac{\partial n_e}{\partial t} \quad . \tag{4-19}$$

Applying the absorption coefficient (4-17) to (4-19) yields

$$0 = \frac{\partial^2}{\partial t \partial x} (A(x) \log n_e) - \frac{1}{\ell} H(n_e - n_{et}) \frac{\partial}{\partial t} (A(x) \log n_e) \tag{4-20}$$

The initial conditions are

$$n_e(x,0) = n_{eo} \tag{4-21}$$

$$T(x,0) = T_o$$

where n_{eo} is a small residual electron density due to chance free electrons in the gas, or due to electrons produced by the multiphoton effect.[49] The boundary condition is

$$W(\infty,t) = W_L(t) \quad , \tag{4-22}$$

where $W_L(t)$ is the time history of the laser power. (4-20), (4-21), (4-22), plus (4-18) relating n_e and W form a well posed problem. (4-20) can be solved in two parts; for $n_e < n_{et}$ and for $n_e > n_{et}$, and these two parts can be matched. First solve for $n_e < n_{et}$ so that the Heaviside function is zero. Then (4-20) becomes $\partial^2(A(x)n_e)/\partial x\partial t = 0$, for which the solution is

$$A(x) \log n_e = a_1(t) + b_1(x) \quad , \tag{4-23}$$

where a_1 and b_1 are arbitrary functions in t and x respectively. Applying the initial condition (4-21) yields $0 = a_1(0) + b_1(x)$. But this can only be true if $b_1(x)$ is a constant. Without loss of generality, this constant can be taken as zero so that $b_1(x) = 0 = a_1(0)$.

Applying the boundary condition requires a little intuitive thinking. Consider that for $n_e < n_{et}$ there is no absorption. Consider also that the successive points of breakdown (where $n_e = n_{et}$) will have to move in the $+x$ direction as time proceeds. Then, if at some point in time, breakdown has not occurred at a point x, then it surely has not occurred at any place between x and the laser.

Then the intensity at x must be the undiminished intensity delivered by the laser. So then the boundary condition (4-22) actually becomes

$$W(x,t) = W_L(t) \quad , \quad \text{for} \quad n_e < n_{et} \, .$$

Applying this to (4-18) using the solution (4-23) yields

$$\frac{da_1}{dt} = \left(\frac{n_{et} A_f}{t^* W_{max}} \right) W_L(t)$$

which integrated using $a_1(0) = 0$ becomes

$$a_1 = \left(\frac{A_f}{t^* W_{max}} \right) \int_o^t W_L(t')dt' \quad . \qquad (4-24)$$

Then the electron number density is

$$\frac{n_e}{n_{e_o}} = \exp \left\{ \frac{A_f}{t^* W_{max}} \frac{1}{A(x)} \int_o^t W_L(t')dt' \right\} \quad \text{for} \quad n_e < n_{et} \qquad (4-25)$$

Since the absorption coefficient is zero for $n_e < n_{et}$, the temperature will not rise at all, but remains at T_o in this region.

The location of the breakdown wave $x_w(t)$ is at the point where $n_e = n_{et}$ which using (4-25) is given implicitly by

$$\frac{1}{A_f} W_{max} \, t^* \log \frac{n_{et}}{n_{eo}} = \frac{1}{A(x_w(t))} \int_o^t W_L(t')dt' \qquad (2-26)$$

Of course this is precisely the point where the solution (4-25) becomes valid.

Now the solution for $n_e > n_{et}$ must be constructed. Then (4-20) becomes

$$0 = \frac{\partial^2}{\partial t \partial x} (A(x) \log n_e) - \frac{\partial}{\partial t} \left(\frac{1}{\ell} A(x) \log n_e\right)$$

This equation can immediately be integrated with respect to time, resulting in a first order linear differential equation in x for $(A(x) \log n_e)$. Solving this equation yields

$$\log n_e = a_2(t) \frac{1}{A(x)} e^{x/\ell} + b_2(x) \qquad (4\text{-}27)$$

At this point it is possible to go directly to an equation for the temperature behind the wave rather than solving for n_e. Using (4-18) and (4-27), the laser power at a point behind the wave is

$$W = \left(\frac{t^* W_{max}}{A_f}\right) a_2'(t) \; e^{x/\ell}$$

The boundary condition is $W(x_w(t), t) = W_L(t)$ so that

$$a_2'(t) = \left(\frac{A_f}{t^* W_{max}}\right) W_L(t) \; e^{-x_w(t)/\ell}$$

and

$$W = W_L(t) \exp[\tfrac{1}{\ell} (x-x_w(t))] \qquad (4\text{-}28)$$

Then the temperature can be found by applying (4-28) to the energy equation (4-16) and integrating with respect to time,

$$T = \frac{1}{\rho \ell C_v A(x)} \int_o^t W_L(t') \exp[\tfrac{1}{\ell} (x-x_w(t'))]dt' + \text{const}$$

The constant is found by applying the condition that $T(x_w(t),t) = T_o$. Evaluating the constant, the equation for the temperature can be written,

$$T = T_o + \frac{1}{\rho \ell C_v A(x)} \int_o^t H(x_w(t')-x) W_L(t') \exp[\tfrac{1}{\ell} (x-x_w(t'))]dt' \qquad (4\text{-}29)$$

where $x_w(t)$ is given implicitly by (4-26).

Another form of (4-29) which is more amenable to calculation involves the inverse of the function $x_w(t)$,

$$T = T_o + \frac{1}{\rho \ell C_v A(x)} \int_{t_w(x)}^t W_L(t') \exp[\tfrac{1}{\ell} (x-x_w(t'))]dt' \quad , \qquad (4\text{-}30)$$

where $t_w(x)$ is given implicitly by

$$\frac{1}{A_f} W_{max} \, t^* \log \frac{n_{et}}{n_{eo}} = \frac{1}{A(x)} \int_o^{t_w(x)} W_L(t')dt' \, . \qquad (4\text{-}31)$$

The wave motion is clearly seen in (4-29) where the Heaviside function in the integral implies there is no heating until the wave arrives, at which time the temperature rises.

The velocity of the breakdown wave can be found by taking the time derivative of (4-26),

$$V_w = \frac{A_f}{t^* \left.\frac{dA}{dx}\right|_{x=x_w(t)} \log \frac{n_{et}}{n_{eo}}} \frac{W_L(t)}{W_{max}}$$

This velocity could also be calculated by applying conservation of energy.

The wave is more clearly seen by calculating an example. Consider a uniform laser pulse so that $W = W_o H(t)$, $T_o = 0$, and a focal region where $A(x) = A_f(1 + \beta\frac{x}{r_f})^2$, i.e., a conical beam shape, where r_f is the radius of the focal area. For this case the solution is

$$T = \frac{W_{max}\beta t^*}{\rho r_f A_f C_v} \frac{2}{(1 + \beta\frac{x}{r_f})^2} \left[(1 + \beta\frac{x}{r_f}) - (1 + \beta\frac{x_w'}{r_f}(t))e^{-\frac{1}{\ell}(x_w(t)-x)}\right.$$

$$\left. + \frac{\beta\ell}{r_f}\left[1 - e^{-\frac{1}{\ell}(x_w(t)-x)}\right]\right]$$

These temperature profiles are plotted in figure 59. for various times. The temperature profiles have the same wave character as the laser heated plasma and the laser irradiation of a two level substance. The only major difference is that the bleaching wave moves backwards. This is due to the geometry--the focusing effect on the laser intensity.

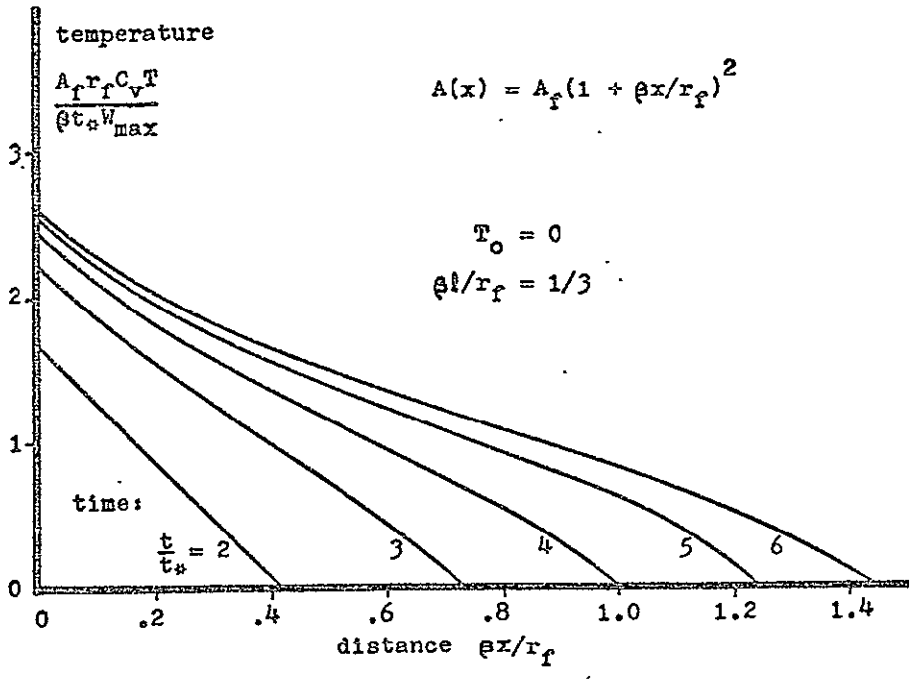

Figure 59. Breakdown wave

Thus three examples of the bleaching wave have been presented which bear similar characteristics. In the first two, laser irradiation of a layer of substance in time produced a significant decrease in the absorption coefficient. The result was a boring effect of the laser beam into the substance. In the third example, laser irradiation produced in time a sharp increase in the absorption coefficient. This, together with the focused geometry caused a reversed boring effect to appear. The penetration of the beam diminished with time. All three of these phenomena show similar profiles in the dependent variable, as seen in figures 57 and 59. In the next section, another phenomenon will demonstrate this same wave like behavior.

B. THE THERMAL WAVE

There is another class of phenomena which seems to have a different physical base than the bleaching wave but whose solutions exhibit a very similar behavior. There are several manifestations of this in physics as will be discussed in section D, but in this section, the discussion will be confined to one example, thermal waves in media with nonlinear thermal conduction.

In thermal conduction problems, one usually assumes a constant coefficient of thermal conductivity. This is motivated by a desire to make the equations tractable--linear in this case so that superposition and all the other techniques associated with linear equations can be used. Yet, there is no substance found in nature which has a constant thermal conduction coefficient: it always depends on the temperature. Only for small changes in temperature will linear analysis apply--and then only approximately.

Most real diffusion problems are nonlinear and numerous examples have been cited by Cole.[50] Some of these examples will be mentioned in section D. A thorough review of the mathematics of nonlinear diffusion has been given by Crank.[51] The numerical approach to nonlinear diffusion problems has been discussed by Richtmeyer.[52]

A typical nonlinear thermal conduction problem is governed by an equation of the form,

$$\rho C_v \frac{\partial T}{\partial t} - \frac{\partial}{\partial x}\left(K(T) \frac{\partial T}{\partial x} \right) = Q \qquad (4\text{-}32)$$

where T is temperature, $K(T)$ is the coefficient of thermal conduction, and Q is a source term if needed. Suppose that at the edge of a substance, energy is being added. Then thermal conduction will transport the energy from the edge to deeper layers of the substance. At any point in time, the temperature profile will be monotonically decreasing with increasing distance into the substance. If the thermal conduction coefficient were constant (linear diffusion) then any temperature profile would be an exponentially damped curve.

However, if the thermal conduction coefficient is greater for higher temperature, then heat will conduct more easily in hotter regions, i.e., nearer the edge. Thus the hotter regions will require smaller temperature gradients to conduct a certain amount of heat than cooler regions. Hence the temperature profiles will exhibit the humped shape seen in the laser heated plasma of figure 57.

This is clearly seen if a particular example is worked out, that of a fully ionized plasma. In a fully ionized plasma, the thermal conduction coefficient is proportional to $T_e^{5/2}$.[53] Suppose the source term in (4-32) corresponds to a constant heat addition rate at the edge of the plasma, $Q = Q_0 \, \delta(x) \, H(t)$, where $\delta(x)$ is the delta function. If the initial condition is $T(x,0) = 0$, and the boundary condition is $T(\infty,t) = 0$, then (4-32) can be written as an ordinary differential equation using similarity methods. The similarity variable is $\eta = \tilde{x} / \tilde{t}^{7/9}$, where $\tilde{x}$ and $\tilde{t}$

are suitably chosen dimensionless distance and time, respectively. The dimensionless temperature is $\tilde{T} = \tilde{t}^{2/9} f(\eta)$. $f(\eta)$ is governed by

$$0 = \tilde{K} \frac{d^2 f^{7/2}}{d\eta^2} + \frac{7}{2} \eta \frac{df}{d\eta} - f \quad ,$$

where $\tilde{K}$ is the dimensionless parameter representing the thermal conductivity. The boundary conditions are $f(\infty) = 0$ and $\frac{df^{7/2}}{d\eta} (0) = -1$. Then for length and time scales for which the conductivity parameter is large, $K \gg 1$, an approximate solution can be calculated,

$$f(\eta) \tilde{=} (\eta_o - \eta)^{2/7}$$

This solution becomes invalid for $|\eta - \eta_o| \ll 1$. For $\eta > \eta_o$ the solution is $f = 0$. Near $\eta = \eta_o$, a boundary layer approach is necessary to give the details of the solution. η_o is a constant which can be evaluated by integrating over $\tilde{x}$ to get the total energy added, and equating this to the time integral of the source term. Conducting the integrations yields $\eta_o = (9/7)^{7/9}$. Then the temperature profiles are

$$T \tilde{=} (\eta_o \tilde{t}^{7/9} - \tilde{x})^{2/7}$$

Several of these profiles are plotted in figure 60 for a fully ionized plasma. The "boundary layer" at the front of the wave is not shown.

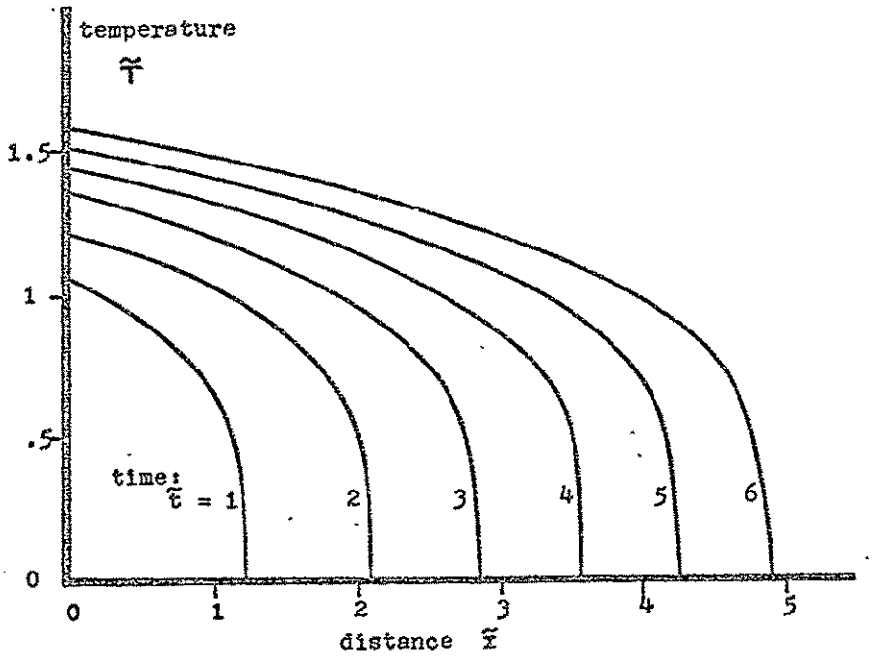

Figure 60. Nonlinear thermal conduction in a uniform plasma slab.

The presence of wave like behavior is clearly seen. This has been appropriately called a thermal wave by Zel'dovich and Raizer.[54] The resemblance is even more striking due to the differing character of the governing equations. The thermal wave is governed by an equation of the form of (4-32) which is parabolic. The bleaching wave is governed by an equation of the form of (4-3) which is hyperbolic. This resemblance is carried over to the linear case where laser irradiation and thermal conduction both produce exponential decays in the temperatures produced.

The resemblance of the thermal wave to the bleaching wave is not presented as a mere curiosity. Nor is it presented to introduce a coincidental resemblance between two physical phenomena. Rather, the goal is to demonstrate that these two phenomena--which arise out of widely differing equations--actually are due to two opposite limits of a physical process, i.e., they both fit into a general class of "diffusion waves". There are many physical phenomena which exhibt these diffusion waves. This contention is presented and supported in the next section.

C. DIFFUSION WAVES

The bleaching wave and the thermal wave actually belong to a single class of diffusion waves. These diffusion waves appear since the rate of diffusion varies with the magnitude of the property that is being diffused. Specifically, diffusion proceeds more rapidly for higher values of the property being diffused. This process can be understood by examining the character of diffusion processes.

A diffusion process is a transport process. Therefore two things are required: something must be transported and there must be a transporter. There are several examples of things that can be transported: energy which may be measured by temperature, momentum which is essentially measured by velocity, and mass such as the mass of a particular species which is measured by concentration. There are four things that can perform the transporting. This first three fall into one group and are atoms, molecules and macroscopic particles. This group is simply referred to as "particles". The last are massless particles, photons.

Hence, one sees a curious wedding of two opposite viewpoints, the continuum viewpoint and the particle viewpoint. Discrete particles transport--by their motion--continuum properties. For example, electrons move and have a certain energy. The continuum viewpoint measures the average energy of the electrons in terms of temperature, a continuum concept. The random motion of the electrons transport energy

and the process is called thermal conduction.

Actually, any system always has both particles and photons present. Thus both photon and particle transport will always be present; however, one or the other may dominate.

1. Equilibrium

A system will always attempt to reach an equilibrium state. That is, the tendency is to smooth out any macroscopic nonuniformities that might exist. Macroscopic nonuniformities are smoothed out by either macroscopic or microscopic motion or both. If by macroscopic motion, then a dynamical process ensues. If by microscopic motion, then a diffusion process ensues.

Thus a diffusion process is unidirectional, it always proceeds toward equilibrium. This is just another statement of the second law of thermodynamics which says that on the average, a system of particles will always approach a more random disorganized state.

a. Types of Equilibrium

There are four types of equilibrium that must be established by diffusion or a dynamical process. The most obvious is <u>spatial</u> equilibrium of a macroscopic property. For example, diffusion processes attempt to smooth nonuniformities in the temperature.

The second kind is interspecies equilibrium. If there is more than one kind of particle in a system, then there will be an exchange between the two groups of particles to establish equilibrium. For example a fully ionized plasma is a mixture of electrons and ions. If the electrons and ions each have a different temperature, then the system will seek to equalize the two temperatures. Another example, any system is a mixture of particles and photons. If there is an imbalance of energy between the photons and particles, then adjustments will be made to create the correct balance between the two systems.

The third kind is intraspecies equilibrium. There is a certain kind of equilibrium that must be established between the members of a certain species. For example, suppose all of the members of a certain species were moving at the same speed. This is certainly not a equilibrium situation. Such a system would approach a state where all speeds are represented. A few particles would be moving fast, and a few very slow and most would be somewhere in between, i.e., in equilibrium a "distribution" of speeds exists. An equilibrium system is characterized by a certain statistical distribution of its members. For example, there is a certain statistical distribution of energies for a system of particles which is called the Boltzmann distribution. This distribution function gives the probability of a particle having a certain energy in a

system with intraspecies equilibrium. For particles in the classical limit it is the Boltzmann distribution that a particular particle species will approach within itself. Another example: there is a certain statistical distribution function characterizing photons which is the Planck function. It gives the probability of a photon having a certain energy in an equilibrium system.

The fourth kind is directional equilibrium. A system of particles will tend toward a state in which there is an equal number of particles moving in all directions with speeds independent of direction. This is the random component of velocity since macroscopic velocity always has a single direction with a certain velocity. This equilibrium state is called isotropy of particle velocities. Thus four types of equilibrium are simultaneously being approached by the particles in a system. Of course, the rates of approach to the various kinds of equilibrium are all different--but this is one of the things that makes diffusion processes so interesting.

b. Approach to Equilibrium

If the particles of a system did not interact, then there would be no means by which to approach an equilibrium state; the particles would continue in their initial state forever. But particles do interact by means of collisions. There are four types of collisions that may occur between particles:
1) collisions between particles in which energy or momentum

is shared; 2) collisions between a particle and a photon in which the photon is deflected (Compton scattering); 3) collisions between a particle and a photon in which the photon is extinguished (absorption); and 4) collisions between particles in which a photon is emitted (emission).

In each type of collision, the quantity that is being transported is shared between the colliding particles. On the statistical average therefore, collisions tend to move the system toward equilibrium. For example: 1) collisions between particles tend to share energy and to promote isotropy of particle motion; 2) collisions between particles and photons promote isotropy of photon motion; 3) absorption and emission share particle and photon energy.

2. Degrees of Equilibrium

Of the four kinds of equilibrium, the degree of intra-species and directional equilibrium are important in discussing thermal and bleaching waves.

The tendency of a group of particles is to approach a certain energy distribution function. A system with such an equilibrium distribution can be said to be in energetic equilibrium. The most extreme nonequilibrium situation is when all the particles have exactly the same energy. This state is called isoenergetic for particles and monochromatic for photons. An example of a system in energetic equilibrium is the interior of a perfect black body. An example of an isoenergetic state

is an electron beam, and an example of a monochromatic state is a laser beam.

A group of particles will approach directional equilibrium. Such an equilibrium is called isotropy. The extreme directional nonequilibrium state is when all particles are moving in exactly the same direction. This is called coherence. There is a directional state that is somewhere in between these two that might be called quasi-coherence. This is where all of the particles have a positive velocity component in say, the x direction, i.e., tend to be moving through the y z plane in the same direction. The particles are not moving in exactly the same direction, but in the same general direction. An example of a coherent state is a laser beam, or an electron beam. An example of a quasi-coherent state is the diffusion of particles from a very hot substance into an adjoining cold substance (such as the hot region behind a shock adjoining the cold region ahead of it). Here, the vast majority of the transport is crossing from the hot to the cold region.

3. Bleaching and Thermal Waves as Diffusion Processes

Both thermal conduction and laser irradiation are diffusion processes. Clearly, thermal conduction is a diffusion process. The transporters are the particles themselves (primarily electrons in the case of a plasma). The quantity being transported is energy, as measured by temperature. Diffusion takes place as particles migrate and collide with

other particles, thereby sharing their energy. Thermal conduction is usually characterized by a thermal conduction coefficient K and assuming that the energy flux vector is given by the Fourier heat conduction law,

$$\vec{q} = - K \nabla T$$

This law was derived assuming quasi-equilibrium in the energy both spatially and locally. A typical derivation is given by Vincenti and Kruger.[55] It is only valid when the spatial variation in the temperature is small in a mean free path, and when there is nearly an equilibrium distribution function. Thus, thermal conduction when governed by the Fourier law is diffusion in the equilibrium limit.

Laser irradiation is also a diffusion process. The transporters are photons. The quantity being transported is energy which may be measured by temperature, or by the number of molecules in the upper state of a two level system. Diffusion takes place as the photons migrate, are absorbed, and stimulate the emission of other photons, thereby transporting energy into the system. This type of behavior which has not been identified as diffusion is governed by a radiative transfer equation,

$$\frac{\partial I}{\partial x} + K_\nu I = 0$$

Where the absorption coefficient K_ν includes the net effect

of absorption and stimulated emission. Then, laser irradiation is diffusion in the extreme nonequilibrium limit, i.e., monochromatic particles moving in coherent fashion.

Hence, laser irradiation and thermal conduction are both diffusion processes, which are merely at opposite ends of the equilibrium spectrum. Then the fact that both exhibit similar characteristics (bleaching waves and thermal waves) is not surprising. The character of equilibrium and coherent diffusion operating side by side is demonstrated in the next section.

4. An Illustration of a Single Diffusion Process in the Equilibrium and Coherent Limits

Consider the example of thermal radiation in a medium as discussed by Zel'dovich and Raizer.[56] The radiative transfer equation in the steady state case for a particular direction can be written as

$$\frac{dI_\nu}{ds} + K_\nu I_\nu = K_\nu I_{\nu p} \quad , \tag{4-33}$$

where I_ν is the spectral intensity, K_ν is the absorption coefficient (taking into account stimulated emission). $I_{\nu p}$ is the spectral intensity for radiative equilibrium and s is the coordinate in the direction of interest. The solution of (4-33) is

$$I_\nu(s) = \int_{-}^{s} K_\nu I_{\nu p} \exp\left[-\int_{s'}^{s} K_\nu ds''\right] ds' + I_{\nu o} \exp\left[-\int_{s_o}^{s} K_\nu ds'\right], \tag{4-34}$$

where $I_{\nu o}$ is the constant of integration, and s_o is the value of s at the edge of the system. The interpretation of (4-34) reveals both equilibrium and coherent diffusion. The first term is the radiation due to equilibrium processes. This term is due to incoherent radiation, which is generated and absorbed within the system. The second term describes the coherent radiation coming from outside the system. If the direction being considered is the same as the laser radiation, then $I_{\nu o}$ is the laser intensity entering the system. In any other direction, $I_{\nu o}$ is zero.

A quasi-coherent case would arise if the system was bounded by a much hotter black body. Then $I_{\nu o}$ would represent the spectral intensity corresponding to the temperature of the hot black body. $I_{\nu o}$ would be nonzero for all directions that pass through the boundary into the system.

Examination of the governing equations in both the equilibrium and coherent limits shows that they are similar in character even though they seemed quite different in section B. In either limit, the energy equation is

$$\rho c_v \frac{\partial T}{\partial t} = - \nabla \cdot \vec{q} \quad . \tag{4-35}$$

In the coherent limit, the intensity is given by

$$I = I_o \exp\left[-\int_{s_o}^{s} K \, ds'\right] \tag{4-36}$$

The energy flux is the radiation intensity; $\vec{q} = I \vec{e}_s$ where $\vec{e}_s$ is a unit vector in the direction of the laser beam.

In the equilibrium limit, the energy equation is the same as (4-35) but the energy flux vector is different. The spectral energy flux vector $\vec{S}_\nu$ is given by

$$\vec{S}_\nu = - \frac{\ell_\nu c}{3} \nabla U_{\nu p} \quad , \tag{4-37}$$

where ℓ_ν is the absorption length at frequency ν, and $U_{\nu p}$ is the equilibrium spectral radiant energy density (the Planck function). This equation, called the diffusion approximation comes from assuming quasi equilibrium locally and spatially.[57] But the total energy flux is needed and this requires an integral of (4-37) over all frequencies ν. The integration yields the energy flux for the equilibrium limit,

$$\vec{S} = - \frac{\ell c}{3} \nabla U_p = - \frac{16}{3} \ell \sigma T^3 \nabla T \tag{4-38}$$

ℓ is the Rosseland mean free path, an averaged value of ℓ_ν (with proper weighting).[58] U_p is the radiant energy density and is given by $U_p = 4\sigma T^4/c$ where σ is the Stefan Boltzmann

constant. So then, in the equilibrium limit, the radiation and absorption mechanism actually behaves like thermal energy, diffusing with a conduction coefficient,

$$K = \frac{16}{3} \ell \sigma T^3 \qquad (4\text{-}39)$$

This radiation process has been identified as a diffusion phenomenon and shown to result in thermal waves by Zel'dovich and Raizer.[54]

The similarity of the energy flux in the coherent (4-34) and the equilibrium (4-38) limits is easily seen. In the equilibrium limit consider a hot body bordering a cold body at $x = 0$. The radiation from the hot body diffuses into the cold body. As the temperature of the cold body increases, the coefficient of radiation thermal conduction (proportional to T^3 as seen in (4-39)) increases greatly. So a thermal wave phenomenon will occur similar to that in section B.

In the coherent limit, consider a laser beam which enters the cold body at $x = 0$. If the absorption coefficient K_ν decreases with increasing temperature (as with inverse bremstrahlung or any other bleachable type absorption), then the bleaching wave phenomenon will arise.

Thus, these two limits of the same physical phenomenon produce similar results. Granted, the details of the processes may vary somewhat but the general character is the same. The next section discusses a number of physical phenomena that are governed by nonlinear diffusion. Among them are examples in both the equilibrium and coherent limits.

D. EXAMPLES OF DIFFUSION WAVE PHENOMENA

There are many physical examples of nonlinear diffusion phenomena, and almost without exception the nonlinearity is of the bleachable variety so that diffusion waves appear. Several physical examples are discussed below. A chart summarizing these phenomena is given in figure 61.

1. Particle Diffusion

a. Diffusion of Mass or Species

The diffusion of a plasma through a magnetic field is discussed by Kaufman.[59] The property being diffused is mass as measured by the number density of the particles. The diffusion coefficient is proportional to the number density, so this is bleachable diffusion. Kaufman presents a similarity solution that clearly demonstrates the diffusion wave. This diffusion is the "equilibrium" variety since it is characterized by a diffusion coefficient.

The diffusion of lead chloride in solid silver chloride is studied by Wagner.[60] The quantity being diffused is the molecules of a certain species and is measured as concentration. The diffusion coefficient is proportional to the concentration, so then it is governed by the same equation as the diffusion of a plasma in a magnetic field.

The diffusion of H_2O in swelling membranes was studied by Fatt and Goldstick.[61] In this instance the diffusion coefficient decreases with increasing concentration so that

phenomenon	transported property	transporter	directional equilibrium	energetic equilibrium	nature
diffusion of a plasma in a magnetic field	mass: (number density)	atoms	isotropy	equilibrium	wave
diffusion of PbCl in solid AgCl	mass: (concentration)	molecules	isotropy	equilibrium	wave
diffusion of H_2O in swelling membranes	mass: (concentration)	molecules	isotropy	equilibrium	exponential decay
thermal conduction in a plasma	energy: (temperature)	electrons	isotropy	equilibrium	wave
preheating by thermal conduction in front of a strong shock	energy: (temperature)	electrons	isotropy	equilibrium	wave (steady)
electron beam heating	energy: (temperature)	electrons	coherent	isoenergetic	wave
laser heating of a plasma by inverse bremsstrahlung	energy: (temperature	photons	coherent	monochromatic	wave
laser irradiation of a two level substance	energy: (number density in upper state)	photons	coherent	monochromatic	wave
laser induced breakdown wave	energy: (temperature)	photons	coherent	monochromatic	reverse wave
atomic fireball	energy: (temperature)	photons	isotropy	equilibrium	wave

Figure 61. Examples of diffusion phenomena

the diffusion is not the bleachable variety. Then no diffusion wave appears. This was the only instance found of a nonbleachable diffusion mechanism although there are probably other examples. This is diffusion in the equilibrium limit since a diffusion coefficient is used.

b. Diffusion of Energy

The diffusion of thermal energy by nonlinear thermal conduction has been demonstrated in the numerical studies of Shearer,[62] and in the analytic studies of Babuel-Peyrissac, et. al.[63] The phenomenon arose with the rapid laser heating of an overdense plasma. The laser radiation only penetrates to the critical density, hence only heats the underdense region directly. But the hot underdense region acts like an energy source and rapidly conducts energy to the overdense region. The thermal conduction coefficient is proportional to the five halves power of temperature, so is bleachable. Thus, a diffusion wave moves into the overdense material. Interestingly enough, in the calculation of Babuel-Peyrissac, et. al., the thermal wave moved very fast at first then slowed down, and was succeeded by a shock wave propagating into the material. This illustrates that diffusion waves can move faster than dynamical processes in some cases.

The preheating by thermal conduction in front of a strong shock wave is discussed by Zel'dovich and Raizer.[54] This is a steady state diffusion phenomena so the temperature profiles

produced are stationary relative to the shock wave. Nevertheless, the familiar humped shape in the temperature profile arises due to the bleachable diffusion. If the thermal conduction were constant, then only the exponentially decaying profile would be observed.

Heating by an electron beam is suggested to be an example of coherent diffusion. This is conceptually the same as the heating by a coherent monochromatic beam of photons, i.e., a laser. Some details may differ since electron beams generate streaming effects leading to the two stream instability, something that may not have an analogy in photon beams.

2. Photon Diffusion: Diffusion of Energy

The laser heating of a stationary plasma has been studied in chapter II. This is an example of coherent diffusion. The diffusion is bleachable so the familiar bleaching wave appears. Laser irradiation of a two level substance has also been discussed in section A 1. It is obviously a bleachable diffusion phenomenon so the bleaching wave appears. Any other bleachable absorption mechanism, such as bound free absorption, will also result in a bleaching wave.

The breakdown wave, an example of a backwards moving bleaching wave (or an unbleaching wave) was also discussed in section A 2. This is also coherent diffusion. The reverse nature of the wave is due to the converging geometry of a focused laser beam.

The initial expanding fireball in an atomic explosion has been explained by Marshak[64] as the diffusion of equilibrium radiation. In this example, the radiation diffuses rapidly at first, then slows down and is succeeded by a shock wave--in the same manner as in the study of Babuel-Peyrissac, et. al. However in this instance it is equilibrium radiation that is diffusing. So this is an example of equilibrium diffusion by photons. The equations governing this problem were mentioned in section C 4: (4-33) and (4-36).

These are a few examples of nonlinear diffusion and doubtless there are others. But it is clear that many physical phenomena-- especially those characterized by high temperatures-- are characterized by the diffusion wave.

FOOTNOTES

1. S. Glasstone and R. H. Lovberg, Controlled Thermonuclear Reactions (Van Nostrand: Princeton, 1960), Chapter I.

2. J. L. Tuck, AIAA Bull., 7, 338(1970).

3. J. D. Lawson, Proc. Phys. Soc., B70, 6(1957).

4. J. L. Tuck and G. B. Lubkin, Phys. Today, 22, 55(1969).

5. N. G. Basov and O. N. Krokhin, Proceedings of the Third International Congress on Quantum Electrons (Columbia University Press: New York, 1963), p. 1373.

6. J. M. Dawson, Phys. Fluids, 7, 981(1964).

7. J. W. Daiber, A. Hertzberg, and C. E. Wittliff, Phys. Fluids, 9, 617(1966).

8. F. L. Ribe, private communication.

9. W. J. Fader, Phys. Fluids, 11, 2200(1968).

10. R. E. Kidder, Nucl. Fusion, 8, 3(1968).

11. J. Dawson, P. Kaw, and B. Green, Phys. Fluids, 12, 875 (1969).

12. R. G. Rehm, Phys. Fluids, 13, 919(1970).

13. M. Lubin, Bull. Am. Phys. Soc., 13, 320(1968).

14. L. Spitzer, Jr., Physics of Fully Ionized Gases (Interscience: New York, 1962), Chapter V.

15. J. D. Cole, Perturbation Methods in Applied Mathematics (Blaisdell: Waltham, Massachusetts, 1968).

16. W. L. Kruer, P. K. Kaw, J. M. Dawson, and C. Oberman, Phys. Rev. Letters, 24, 987(1970).

17. I. R. Gekker and O. V. Sizukhin, Soviet Phys. JETP Letters, 9, 243(1969).

18. H. Hora, Phys. Fluids, 12, 182(1969).

19. H. Hora, Garching Report IPP3/87, March 1969.

20. J. Lindl and P. Kaw, Phys. Fluids, (to be published).

21. V. L. Ginzburg, The Propagation of Electromagnetic Waves in Plasmas (Pergamon Press: New York, 1964), pp. 180-187.

22. J. Dawson, private communication.

23. J. M. Dawson, R. E. Kidder, and A. Hertzberg, The Use of Long Wave Length High Powered Lasers for Controlled Thermonuclear Fusion, AEC Research and Development Report No. MATT-782, 1970.

24. A. E. Hill, Appl. Phys. Letters, 12, 324(1968).

25. A. J. Beaulieu, Appl. Phys. Letters, 16, 504(1970).

26. W. D. McKnight and G. J. Dezenberg, Proceedings of the Conference on the Laser in Science and Technology, (1970).

27. J. M. Dawson and C. R. Oberman, Phys. Fluids, 5, 517 (1962), 6, 394(1963).

28. H. Hora, Garching Report 6/23(1964), 6/27.

29. P. K. Kaw and J. M. Dawson, Phys. Fluids, 12, 2586(1969).

30. G. C. Vlases and H. G. Ahlstrom, Amer. Phys. Soc. Bull., 14, 1023(1969).

31. S. A. Akhmanov, D. P. Krindach, A. V. Migulin, A. P. Sukhorukov, and R. V. Khokhlov, IEEE J. Quant. El., QE-4, 568(1968).

32. F. G. Gebhardt and D. C. Smith, Appl. Phys. Letters, 14, 52(1969).

33. Yu. P. Raizer, Soviet Phys. JETP, 25, 208(1967).

34. S. Saikan and H. Takuma, IEEE J. Quant. El., QE-4, 618 (1968).

35. R. Y. Chiao, E. Garmire, and C. H. Townes, Phys. Rev. Letters, 13, 479(1964).

36. M. T. Loy and Y. R. Shen, International Quantum Electronics Conference (Miami, 1968), 5E-6, 15.

37. R. Bellman, G. Birnbaum, and W. G. Wagner, J. Appl. Phys., 34, 780(1963).

38. L. M. Frantz and J. S. Nodvik, J. Appl. Phys., 34, 2346 (1963).

39. E. O. Schultz-Dubois, Bell Syst. Techn. J., 43, 625(1964).

40. A. E. Siegmann, J. Appl. Phys., 35, 460(1964).

41. E. K. Damon and R. G. Tomlinson, Appl. Opt., 2, 546 (1963).

42. R. G. Meyerand, Jr. and A. F. Haught, Phys. Rev. Letters, 11, 401(1963).

43. J. K. Wright, Proc. Phys. Soc. (London), 84, 41(1964).

44. Ya. B. Zel'dovich and Yu.P. Raizer, Soviet Phys. JETP, 20, 772(1965).

45. L. V. Keldysh, Soviet Phys. JETP, 20, 1307(1965).

46. D. D. Ryutov, Soviet Phys. JETP, 20, 1472(1965).

47. G. A. Askar'yan and M. S. Rabinovich, Soviet Phys. JETP, 21, 190(1965).

48. S. A. Ramsden and P. Savic, Nature, 203, 1217(1964).

49. Yu. P. Raizer, Soviet Phys. JETP, 21, 1009(1965), and Soviet Phys. Usp., 8, 650(1966).

50. J. D. Cole, private communication.

51. J. Crank, Mathematics of Diffusion (Oxford: London, 1956), Chapter IX.

52. R. D. Richtmeyer, Difference Methods for Initial Value Problems (Interscience: New York, 1957), pp. 104-108.

53. L. Spitzer, Jr., op. cit., pp. 143-147.

54. Ya. B. Zel'dovich and Yu. P. Raizer, Physics of Shock Waves and High Temperature Hydrodynamic Phenomena (Academic: New York, 1966), Vol. II, Chapter X.

55. W. G. Vincenti and C. H. Kruger, Introduction to Physical Gas Dynamics (Wiley: New York, 1965), pp. 15-17.

56. Ya. B. Zel'dovich and Yu. P. Raizer, Physics of Shock Waves and High Temperature Hydrodynamic Phenomena (Academic: New York, 1966), Vol. I, pp. 128-133.

57. Ibid., pp. 144-149.

58. Ibid., pp. 151-154.

59. A. Kaufman, "Dissipative Effects", in Plasma Physics in Theory and Application, W. Kunkel, ed. (McGraw-Hill: New York, 1966), Chapter IV.

60. C. Wagner, J. Chem. Phys., 18, 1227(1950).

61. J. Patt and T. K. Goldstick, J. Coll. Interf. Sci., 20, 962(1965).

62. J. W. Shearer, Lawrence Radiation Laboratory, Livermore UCRL-72028 (1969).

63. J. P. Babuel-Peyrissac, C. Pauquignon, and F. Floux, Action d'Impulsions Laser Très Brèves sur une Cible Solide, CEA Internal Report.

64. R. E. Marshak, Phys. Fluids, 1, 24(1958).

BIOGRAPHICAL NOTE

for

Loren Clifford Steinhauer

Loren Clifford Steinhauer was born in [redacted] on [redacted] to Mr. and Mrs. Kenneth W. Steinhauer. He attended North Eugene high school where he graduated in 1962. He then attended the University of Washington where he received the degrees of Bachelor of Science in 1966, and Master of Science in 1967.